

AMERICAN UNIVERSITY OF BEIRUT

THE IMPACT OF DIETARY INTERVENTIONS ON  
CARDIOVASCULAR DYSFUNCTION AND ADIPOSE  
TISSUE INFLAMMATION IN NON-OBESE PREDIABETIC  
RATS

by  
HANEEN SALEM DWAIB

A dissertation  
submitted in partial fulfillment of the requirements  
for the degree of Doctor of Philosophy  
to the Department of Nutrition and Food Sciences  
of the Faculty of Agricultural and Food Sciences  
and  
to the Department of Pharmacology and Toxicology  
of the Faculty of Medicine  
at the American University of Beirut







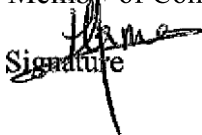
Beirut, Lebanon  
December 2021

AMERICAN UNIVERSITY OF BEIRUT

THE IMPACT OF FIETARY INTERVENTION ON  
CARDIOVASCULAR DYSFUNCTION AND ADIPOSE  
TISSUE INFLAMMATION IN NON-OBESE PREDIABETIC  
RATS

by  
HANEEN SALEM DWAIB

Approved by:

	Signature
Dr. Omar Obeid Department of Nutrition and Food Sciences American University of Beirut	Advisor  Signature
Dr. Ahmed El Yazbi Professor of Pharmacology and Therapeutics Almnein International University	Advisor  Signature
Dr. Nadine Darwiche	Member of Committee  Signature
Dr. Elena Martin Garcia	Member of Committee  Signature
Dr. Ramzi Sabra	Member of Committee  Signature
Dr. Elie-Jaques Fares	Member of Committee  Signature
Dr. Hania Al nakkash	Member of Committee  Signature

Date of dissertation defense: December 10, 2021



## ACKNOWLEDGEMENTS

To my sun and moon Mom (Huda) and Dad (Salem),  
To my siblings; Mhemed, Majed, Hiba, Hind and Ahmed, their kids, and spouses,  
To my family in Lebanon; Rayan Danker, Rosa Mashtoub, Dina Maaliki (to her mom for all the great food she made with love), Zeina Radwan and her family , Batoul Darwiche and her family, Batoul Dia, Mark Doumit, Amro Baasiri, Mariam Miari and her family and Ghina Ajouz,  
To my Advisors; Prof. Ahmed El Yazbi and Prof. Omar Obeid,  
To all the Yazbi lab members; especially Nahid Mogharbil,  
To Obeid's lab members; especially Carla Mallah,  
To my PhD partner, friend and sister, Rana Alaeddine,  
To AUB,  
Thank you all for the amazing adventures and for making these five years of my life worth every laughter and tear, I will be forever grateful.  
Above all thank you for making Lebanon a second home to me.

Last and foremost, to my eternal home Palestine from the river to the sea,

# ABSTRACT OF THE DISSERTATION OF

Haneen Salem Dwaib

for

Doctor of Philosophy

Major: Biomedical Sciences

Title: The Impact of Dietary Interventions on Cardiovascular Dysfunction and Adipose Tissue Inflammation in Non-Obese Prediabetic Rats

Cardiovascular diseases are the most common and serious complications of type 2 diabetes mellitus (T2DM). Recent evidence suggested that CVDs start at the earliest point of metabolic derangement in the prognosis of diabetes, the prediabetes stage. However, this early onset of CVDs at this subclinical phase makes it harder to diagnose and treat, as according to the international diabetes federation half of prediabetic patients are undiagnosed. In our Sprague-dawley male rats, hypercaloric (HC) feeding for 12-24 weeks exerted signs of metabolic impairment mimicking prediabetes in humans: hyperinsulinemia and insulin resistance with normoglycemia. In addition to increased adiposity with normal body weight. They also presented signs of early cardiovascular insults, endothelial dysfunction, and cardiac autonomic imbalance (the subclinical phase of cardiac autonomic neuropathy). Interestingly, these early cardiovascular events were associated with negative adipose remodeling in a very confined and small pool, the thoracic perivascular pad was observed. Perivascular adipose dysfunction was consistently characterized by hypertrophied adipocytes accompanied with elevated expression of uncoupling protein 1 (UCP1) and the inevitable hypoxia and proinflammatory markers. Our previous work showed that hyperinsulinemia alongside this hypoxia machinery in PVAT were responsible for fueling its inflammation and further exaggerating the observed early cardiovascular impairments. Hence, in this work we try to target different components of this hypoxia machinery using safe and translational dietary interventions, inorganic phosphate supplementation and therapeutic fasting (TF). Moreover, our previous data was based on male rats, so we will try to establish sex differences in the etiology and prognosis of early cardiovascular insults related to early metabolic derangements and adipose inflammation. Indeed, as expected estrogen in ovulating and estrogen treated ovariectomized female rats seemed to protect from HC-induced early metabolic and cardiovascular insults, by improving insulin sensitivity and interrupting the hypoxia machinery in PVAT. Certainly, the loss of endogenous estrogen seemed to exacerbate the outcomes of HC feeding leading to obese prediabetic phenotype, with cardiovascular dysfunction. However, 12 weeks of TF was able to reverse this non-obese prediabetic phenotype in males, and the obese prediabetic one in ovariectomized females, resetting the hypoxia machinery in PVAT and preventing the subsequent

cardiovascular dysfunction. Lastly, using inorganic phosphate supplementation was able to interfere with UCP1 activity and expression, disrupting the hypoxia machinery in PVAT, correcting hyperinsulinemia, and eventually preventing early cardiovascular insults.

# TABLE OF CONTENTS

ACKNOWLEDGEMENTS .....	1
ABSTRACT.....	2
ILLUSTRATIONS.....	7
TABLES .....	10
ABBREVIATIONS.....	11
INTRODUCTION.....	16
A. Cardiovascular dysfunction in early metabolic impairment.....	16
1. Diet Induced Adipose Tissue Inflammation, Insulin Resistance and Cardiovascular Dysfunction.....	17
2. Diet Induced Perivascular Adipose Tissue remodeling and metabolic provoked cardiovascular impairment.....	26
B. Sexual Dimorphism in Metabolic Induced Cardiovascular Dysfunction. ....	30
1. Sexual Dimorphism and Adipose Tissue Dysfunction .....	32
2. Sex Differential Involvement of Perivascular Adipose Tissue in Cardiovascular Dysfunction.....	40
C. Dietary Intervention Targeting Adipose Tissue Inflammation in Early Cardiometabolic Dysfunction. ....	43
1. Therapeutic Fasting and Diet Induced Adipose Dysfunction.....	43
2. Inorganic Phosphate Supplementation and Cardiovascular Diseases.....	51
SPECIFIC AIMS.....	55
A. Animal Model.....	60

1.	Ethical approval and experimental design.....	60
2.	Diet.....	63
B.	<i>In-vivo</i> and <i>ex-vivo</i> techniques .....	64
1.	Noninvasive blood pressure measurement .....	64
2.	Echocardiography.....	65
3.	Pressure myography.....	65
5.	Blood chemistry parameters.....	66
6.	Invasive hemodynamic recordings .....	66
C.	Molecular and <i>in-vitro</i> techniques .....	67
1.	Histopathology and immunohistochemistry.....	67
2.	Western blotting.....	68
3.	Fluorescence activated cell sorting (FACS).....	69
3.	In-vitro experiments.....	70
<b>RESULTS .....</b>		<b>73</b>
A.	Sexual Dimorphism of Metabolic and Cardiovascular Dysfunction in Prediabetic Rat Model.....	73
1.	Metabolic and gross hemodynamic outcomes after 24 weeks of HC feeding in male and female rats .....	73
2.	Sexual dimorphism in HC-induced adipose tissue negative remodeling. ....	75
3.	Sex differences in HC diet induced Cardiovascular dysfunction in vivo and in ex-vivo settings.....	77
4.	The role of estrogen in HC-feeding induced PVAT inflammation and consequent cardiovascular dysfunction. ....	80
B.	Therapeutic fasting impact on early cardiovascular dysfunction in HC fed rats.	84
1.	The impact of 12 weeks of therapeutic fasting on metabolic and gross hemodynamic outcomes in prediabetic male rats.....	84
2.	Effect of therapeutic fasting on markers of adipose tissue inflammation in HC-fed rats.....	86
3.	Therapeutic fasting impact on HC induced Cardiovascular dysfunction in vivo and in ex-vivo settings .....	88



4. Therapeutic fasting alleviates signs of cardiovascular deterioration. ....	91
5. The role of TF in PVAT inflammation induced cardiovascular dysfunction in HC fed ovariectomized rats.....	92
C. The impact of Inorganic Phosphate as a UCP1 inhibitor on PVAT Induced Cardiovascular Dysfunction.....	96
1. Metabolic and gross hemodynamic impact of HC feeding with different levels of phosphorus .....	96
2. Impact of phosphorus supplementation on markers of adipose tissue inflammation in HC-fed rats and in vitro in cultured adipocytes .....	100
3. Phosphorus supplementation ameliorates HC-induced alteration of PVAT macrophage polarization. ....	103
5. Phosphorus supplementation reverses cardiac autonomic neuropathy in HC-fed rats.....	106
6. Phosphorus supplementation alleviates signs of cardiovascular deterioration. ....	108
7. Phosphorus supplementation ameliorates HC-diet induced cerebrovascular dysfunction and the associated brainstem changes.....	110
8. Hypercaloric intake, rather than phosphorus deficiency, precipitates PVAT, metabolic, and cardiovascular alterations, which can be reversed upon reinstating dietary phosphorus.....	111
9. Dietary interventions with different phosphorus levels do not appear to induce renal structural alterations .....	116
<b>DISCUSSION</b> .....	<b>118</b>
A. Sexual Dimorphism of Adipose Tissue Remodeling and Cardiovascular Dysfunction in Prediabetes .....	118
B. Sex Dependent Effect of Therapeutic Fasting on Prediabetic Adipose and Cardiovascular Dysfunction.....	122
C. Inorganic Phosphate Supplementation and Adipose Mediated Cardiovascular Dysfunction. ....	126
D. Conclusions and Future Directions.....	136
<b>REFERENCES</b> .....	<b>140</b>

## ILLUSTRATIONS

### Figure

1. The emerging ameliorative role of intermittent fasting on perivascular adipose tissue inflammation and thermogenesis .....	49
2. Summary of previous data on PVAT dysfunction after twelve weeks of HC feeding in male rats .....	56
3. Graphical presentation of the hypothesis .....	58
4. Sprague-dawley male rats fed for twelve weeks on either control or hypercaloric diet with different levels of inorganic phosphate (mg of Pi/Cal). .....	61
5. Male and Female Sprague-dawley rats assigned for twenty-four weeks on control diet, hypercaloric diet and hypercaloric diet and therapeutic fasting. ....	62
6. Female Sprague-dawley rats with bilateral ovariectomy fed for twenty-four weeks fed on normal chow or hypercaloric diet with or without 17 beta-estradiol (E2) treatment .....	63
7. Metabolic and gross hemodynamic impact of 24 weeks HC feeding in male and female rats .....	74
8. Sex differences of the impact of twenty-four weeks of HC feeding on adipocytes size of different depots .....	76
9. Sex differential molecular manifestations of twenty-four weeks of HC feeding on adipose tissue remodeling .....	77
10. Cardiac autonomic modulation by HC feeding in male rats .....	78
11. Cardiac autonomic modulation by HC feeding in female rats .....	79
12. Ex vivo evaluation of the impact of twenty-four weeks NC or HC feeding in male and female rats on endothelial function .....	80
13. Metabolic and gross hemodynamic impact of 12 weeks Estradiol treatment in HC and NC fed ovariectomized female rats .....	82
14. Impact of E2 treatment on PVAT of HC fed ovariectomized rats .....	83
15. Cardiac autonomic modulation by ovariectomy and E2 treatment in female rats	84
16. Metabolic and gross hemodynamic impact of therapeutic fasting and HC feeding in male rats for twelve weeks .....	85

17. The impact of twelve weeks of fasting on adipocytes size of different depots. .....	87
18. Sex differential molecular manifestations of twenty-four weeks of HC feeding on adipose tissue remodeling.....	88
19. Therapeutic Fasting restores parasympathetic cardiac autonomic function. .....	90
20. Ex vivo evaluation of the impact of therapeutic fasting on HC mediated impaired endothelial function.....	91
21. Impact of 12 weeks therapeutic fasting on histopathological and molecular signs of cardiac and aortic impairment induced by hypercaloric feeding.....	92
22. Metabolic and gross hemodynamic impact of 12 weeks fasting in HC fed ovariectomized female rats.....	93
23. The impact of twelve weeks of fasting on adipocytes size of ovariectomized female rats .....	94
24. Impact of therapeutic fasting on PVAT of HC fed ovariectomized rats.....	95
25. Cardiac autonomic modulation by therapeutic fasting in ovariectomized female rats.....	96
26. Metabolic and gross hemodynamic impact of inorganic phosphorus supplementation of hypercaloric diet.....	98
27. Phosphorus supplementation does not affect serum Pi, calcium, or magnesium concentrations.....	99
28. Impact of 8 weeks of inorganic phosphorus supplementation of hypercaloric diet on metabolic and gross hemodynamic parameters as well as Pi, calcium, and magnesium concentration.....	100
29. Manifestations of PVAT inflammation in HC-fed rat compared to changes in a visceral WAT and BAT pools and the ameliorative effect of inorganic phosphorus supplementation .....	102
30. Adipocytes differentiated from human bone marrow-derived mesenchymal stem cells respond to stress by 40 mIU/L insulin and 1.6 mM palmitic acid by an inflamed phenotype.....	103
31. Phosphorus supplementation restores PVAT macrophage polarization in rats fed a hypercaloric diet.....	104
32. Phosphorus supplementation restores metabolic efficiency without affecting protein metabolism .....	106
33. Phosphorus supplementation of hypercaloric diet restores parasympathetic cardiac autonomic function .....	107

34. Impact of inorganic phosphorus supplementation on histopathological and molecular signs of cardiac impairment induced by hypercaloric feeding.	108
35. Impact of inorganic phosphorus supplementation on histopathological and molecular signs of vascular impairment induced by hypercaloric feeding. .....	109
36. Inorganic phosphorus supplementation reverses cerebrovascular hypercontractility and brainstem inflammation induced by hypercaloric feeding.	110
37. Gross metabolic and functional parameters following low phosphorus control diet feeding or phosphorus reinstatement after a ten-week high calorie phosphorus deficient diet feeding. ....	113
38. Serum Pi, calcium and magnesium following low phosphorus control diet feeding or phosphorus reinstatement after a ten-week high calorie phosphorus deficient diet feeding.....	114
39. Impact of low phosphorus control diet feeding or phosphorus reinstatement after a ten-week high calorie phosphorus deficient diet feeding on parasympathetic cardiac autonomic function and brainstem inflammation. .....	115
40. Impact of different phosphate and fat levels in diet on renal microscopical structure and calcium deposition .....	117

## TABLES

### Table

1. Table 1. Diet composition analysis of control and hypercaloric diet, presented in calorie percentage .....64

## ABBREVIATIONS

ACs - Adipocytes

Akt – Protein kinase B

AIM – Adipogenic induction medium

AIN – American Institute of Nutrition

AMPK – AMP-activated protein kinase

AT – Adipose tissue

ATMs – Adipose tissue macrophages

AT2-R – Angiotensin 2 receptor

BAT– Brown adipose tissue

BMI – Body mass index

BMMSCs – Bone marrow-derived mesenchymal stem cells

BP – Blood pressure

BRS – Baroreceptor sensitivity

BUN – Blood Urea Nitrogen

CaSR – Calcium sensing receptor

CVD – Cardiovascular disease

DHE – Dihydroethidium

DIO – Diet-induced obesity

DMEM-LG –Dulbecco’s Modified Eagle’s Medium- low glucose

DRP-1 – Dynamin-Related Protein-1

dP/dt max – change in pressure to change in time ratio

E2 – 17 $\beta$ -estradiol

eNOS – Endothelial nitric oxide synthase

ER $\beta$  – Estrogen receptor- $\beta$

FACS – Fluorescence-activated cell sorting

FFA – Free fatty acids

FGF23 – Fibroblast growth factor-23

GAT– Gonadal adipose tissue

GPR – G-protein coupled receptor

HC – Hypercaloric diet

HDL – High density lipoprotein

H&E – Hematoxylin & Eosin

HF – Heart failure

HFD – High-fat diet

HIF-1  $\alpha$  – Hypoxia-inducible factor-1  $\alpha$

HOMA-IR – Homeostatic model assessment-Insulin resistance

HR – Heart Rate

HTN – Hypertension

IBMX – 3-isobutyl-1-methylxanthine

I $\kappa$ B $\alpha$  – Nuclear factor of kappa light polypeptide gene enhancer in B-cells inhibitor  $\alpha$

IL – Interleukin

iNOS – Inducible nitric oxide synthase

IRS-1 – Insulin receptor substrate 1

LDL-c – Low density lipoprotein cholesterol

LPL – Lipoprotein lipase

MAP – Mean arterial pressure

NADPH oxidase – NOX

NC – Normal chow

NF- $\kappa$ B – Nuclear factor kappa-light-chain-enhancer of activated B cells

NMR – Nuclear Magnetic Resonance

PAS – Periodic acid Schiff

PE – Phenylephrine

Pi – Inorganic phosphate

p-IKK $\beta$  – phosphor-IK kinase  $\beta$

P/Kcal – Diluted inorganic phosphate to energy ratio.

PGC-1  $\alpha$  – PPAR $\gamma$  gamma coactivator-1  $\alpha$



PLC – Phospholipase C

PPAR $\gamma$  – Peroxisome proliferating activated receptor  $\gamma$

PTEN – Phosphatase and tensin homolog

PTH – Parathyroid hormone

PUFA – Polyunsaturated fatty acids

PVAT – Perivascular adipose tissue

ROS – Reactive oxygen species

SEM – Standard error of mean

SFA – Saturated fatty acids

SNP – Sodium nitroprusside

SREBP -1 – Sterol response element binding protein-1

SVF - Stromal vascular fraction

sWAT– Subcutaneous adipose tissue

T1DM – Type 1 diabetes mellitus

T2DM – Type 2 diabetes mellitus

TBS – Tris buffered saline

TBST – Tris buffered saline-tween

TNF $\alpha$  – Tumor necrosis factor  $\alpha$

Tregs – Regulatory T cells

UCP1– Uncoupling protein 1

VAT– Visceral Adipose tissue

VSMC – Vascular smooth muscle cell

# CHAPTER I

## INTRODUCTION

### **A. Cardiovascular dysfunction in early metabolic impairment.**

According to the world health organization cardiovascular diseases (CVDs) accounted for more than one third of annual deaths worldwide [1], of which 80% are recorded in low and middle income countries[2]. Most of CVDs are driven by modifiable risk factors such as obesity, poor dietary behaviors, and sedentary lifestyle among many others[1]. Excessive energy intake, especially the one obtained from fat and sugar, makes up the basis of metabolic imbalance risk factors, which fuel CVDs [1]. This association is certainly evident in type 2 diabetes mellitus (T2DM) patients[3-5]. Currently, it is well accepted that cardiovascular (CV) dysfunction commences at the earliest stages of metabolic impairment occurring during the pathogenesis of diabetes [6, 7]. This stage is referred to as the compensatory stage in T2DM prognosis, where the pancreas overproduces insulin, to overcome the increase in blood glucose in response to insulin resistance [5]. This highly prevalent stage is accompanied with early metabolic distress and related to overweight and obesity [8]. Moreover, these metabolic anomalies are correlated to adiposity and fat percentage rather than body weight. This is referred to as a metabolically obese phenotype [9], which masks the apparent face of early prediabetes [9, 10]. In the following sections, CVDs will be reviewed in the context of diet induced early metabolic dysfunction including insulin resistance and negative adipose tissue remodeling, sex differences, in addition to the dietary interventions tested in this thesis, namely intermittent fasting and inorganic phosphate supplementation.

## ***1. Diet Induced Adipose Tissue Inflammation, Insulin Resistance and Cardiovascular Dysfunction***

Based on scientific consensus on the role of the metabolic state in the development of CVDs, there has been a reorientation in research towards the involvement of adipose tissue (AT) in early metabolic challenges, T2DM and correlated CVDs. AT is considered a dynamic organ rather than an energy reservoir. It is accepted that AT affects cardiovascular health through paracrine and endocrine interactions with cardiovascular tissues [11, 12]. AT is classified based on the differences in depots' morphologies and localization into white AT (WAT), brown AT (BAT) or beige AT. On the one hand, WAT is considered the largest of all in terms of quantity, as it accounts for up to 80% of all adipose pools and is distributed all over the body mainly in the subcutaneous (sWAT), visceral (VAT) and gonadal (GAT) depots. Its main building block is the unilocular adipocyte (AC), which has one large lipid droplet with few mitochondria. It also has the stromal vascular fraction (SVF) which contains other cell types. The main function of WAT is energy storage; nonetheless, it is the major source of adipokines and hormones such as leptin [13-15]. On the other hand, BAT can be considered the opposite of WAT, as it is only found in confined places, such as cervical and subscapular depots, with ACs showing multilocular morphology, containing large number of small lipid droplet with a high count of mitochondria (MT), giving it the brownish color, where the name comes from [16, 17]. These MT are highly rich in uncoupling protein 1 (UCP1) that gives BAT its special function of thermogenesis [18, 19]. The role of UCP1 in AT inflammation and dysfunction will be further discussed in later sections. Moving to the third class of AT, beige or bright AT has a singular morphology that combines both BAT and WAT, as it has more lipid droplets than WAT but fewer and bigger than the ones in BAT. MT count is

intermediate between BAT and WAT, and UCP1 expression and function depends on the site of this special depots, the most important example is perivascular AT (PVAT), which is a naturally occurring beige AT that surrounds the blood vessels and has a major role in regulating the vascular tone [20-22]. PVAT is considered a vital organ in CV dysfunction and prognosis [20, 21]. Its role and function will be reviewed in detail in the upcoming parts.

Since each class of AT has unique characteristics, energy induced response is expected to be particular in each pool [11, 23-25]. However, high fat diet (HFD) and positive energy intake will definitely induce pathological changes in all depots, which is found to be linked to CVDs [26]. Significantly, excessive calorie intake, diet induced obesity (DIO) and T2DM are correlated with a wide range of CVDs while sharing a background of low-grade AT inflammation [23, 27]. Particularly, HFD is known to produce an extensive set of pathological changes in AT, which can be referred to as AT negative remodeling[24, 28, 29].

Indeed, positive energy intake induces hypertrophy of ACs, which is considered a failure of ACs to proliferate normally [30], resulting in malfunctioning ACs that are typically accompanied with cardio-metabolic derangements [11, 31], like hyperinsulinemia, hyperlipidemia, hypertension and atherosclerosis [32]. For example, subjects diagnosed with T2DM or dyslipidemia were found to have larger subcutaneous ACs than their control counterparts [11]. The failure of recruitment and differentiation of fat progenitor cells in obesity and prediabetes occurs due to a combination of factors including AT insulin resistance that is observed in obese and prediabetic individuals, which provokes the expansion of existing ACs [32]. As insulin inhibits lipolysis, insulin resistance lead to increased circulating free fatty acids (FFA), which in turn fuels

and exaggerates the insulin resistance tightly correlated with hypertension and CVDs [31]. In this context, nutrient excess triggers an increased demand for protein and lipid synthesis leading to endoplasmic reticulum stress, which in turn activates nuclear factor- $\kappa$ B (NF- $\kappa$ B). The latter pathway impairs the action of insulin by promoting the inhibitory phosphorylation of insulin receptor substrate 1 (IRS-1). As well, it could be plausible that compensatory hyperinsulinemia in obesity or HFD intake may augment AC glucose uptake eventually leading to abnormally hypertrophied ACs [31] in a self-reinforcing vicious cycle. The vital role of insulin in white AC hypertrophy was confirmed in several animal models. A mouse model of AT insulin receptor knockout showed a significant reduction in total fat mass, age related obesity, and other metabolic abnormalities [30]. Moreover, a knockout rat model of insulin receptor in AT was found to be resistant to diet induced hypertrophy compared to their wild type littermates [33].

The oxygenation status of the AT is considered one of the most essential parameters in AT pathophysiology in obesity, and considered the upstream regulator of AT inflammatory cascade leading to increased proinflammatory cytokines like TNF- $\alpha$  and macrophage infiltration and other cytotoxic cells like (CD4+) in obese animal models, as well as AT fibrosis and insulin resistance [34-37]. Caloric intake-induced hyperinsulinemia drives AC hypertrophy promoting its diametric expansion beyond the diffusion potential of oxygen [38]. Importantly, this occurs in the absence of compensatory AT vascularization creating a local hypoxic state that is associated with an increased expression of HIF-1 $\alpha$  [36, 39, 40]. An extensive crosstalk between signaling pathways involving HIF-1 $\alpha$  and other transcription factors implicated in the AT hypoxic response such as NF- $\kappa$ B occurs, where NF- $\kappa$ B was shown to regulate HIF-1 $\alpha$  transcription [39, 41, 42]. Additionally, it was shown that hypoxia-triggered

expression of HIF-1 $\alpha$  induces NF- $\kappa$ B-mediated cytokine production including IL-1 $\beta$ , which results in subsequent recruitment and accumulation of distinct populations of immune cells giving rise to a state of chronic AT inflammation [43-46]. Importantly, the dysfunction of adipose depots implicated in the pathogenesis of cardiovascular dysfunction, such as epicardial, perivascular, and perirenal adipose depots, is associated with a perturbed immune cell landscape and adipokine profiles in different states of metabolic dysfunction [47].

Adipose tissue macrophages (ATMs) exhibit remarkable polarization-dependent transcriptomic heterogeneity that is highly dependent on microenvironmental factors [48, 49]. AT-resident or infiltrating macrophages can either adopt a classical, pro-inflammatory M1 polarization, or an anti-inflammatory M2 polarization. ATMs in lean AT are predominantly of M2 polarized [50, 51], while M1 macrophage infiltration into inflamed ATs as well as the phenotypic switch of resident M2 macrophages to M1 macrophages occur in response to HFD consumption [52, 53]. As such, these macrophages associate with crown-like structures, which represent macrophages actively phagocytosing apoptotic adipocytes with the concurrent increased production of proinflammatory cytokines and chemokines as well as reactive oxygen species (ROS) [51, 54-58]. Moreover, it was suggested that ATMs represent the primary source of the proinflammatory cytokines TNF $\alpha$ , IL-1, IL-6 and iNOS [57, 59]. Noteworthy, it was suggested that WAT preadipocytes can undergo a phenotypic switch, by which they transdifferentiate into macrophages *in vivo* in response to HFD under a contact-dependent macrophage-mediated stimulation [59, 60]. Nevertheless, *in vitro* studies suggest that AC-macrophage crosstalk is mainly mediated by FFA and TNF $\alpha$ . Indeed, TNF $\alpha$  was shown to drive AT inflammation and to reduce adiponectin expression,

while FFAs were found to increase macrophage cytokines production [61]. This crosstalk was found to be exaggerated upon the use of hypertrophied or obese ACs [61]. Accumulating evidence suggests a role for  $TNF\alpha$  in inhibiting peroxisome proliferator activated receptor  $\gamma$  (PPAR $\gamma$ ) activity through several pathways [62], among which is the activation of the classical NF- $\kappa$ B pathway, which prevents PPAR $\gamma$  binding to its response element, and hence blocks its downstream effect [63]. As PPAR $\gamma$  represents a major promoter of adipogenesis, it is thought that  $TNF\alpha$ -mediated suppression of PPAR $\gamma$  signaling would increase levels of circulating FFAs and subsequently enhancing the proinflammatory polarization of ATMs [64]. This is supported by evidence from PPAR $\gamma$  receptor agonist treated HFD-fed mice, which exhibited an enhanced overall insulin sensitivity and an increased M2 count in VAT [65]. Indeed,  $TNF\alpha$  KO mice were protected from HFD-induced IR and exhibited reduced serum FFA levels [66]. Moreover, ATM-derived  $TNF\alpha$  is suggested to be the leading promoter of adipose-specific insulin resistance through various mechanisms [59, 67, 68]. It was shown that  $TNF\alpha$  downregulates the expression of IRS-1 [69, 70], and inhibits the activity of ATP-activated protein kinase (AMPK) activity [71]. In addition to AMPK energy sensing activity, and the crucial role of AMPK signaling dysfunction in the pathogenesis of IR, AMPK activation was shown to prime M2 macrophage polarization [72]. Although ATMs are considered the main contributors to HFD-induced AT inflammation [57]. However, other immunocytes were involved in promoting AT inflammation, such as dendritic cells (DCs), mast cells, eosinophils, T cells, B cells among others [55, 73, 74]. For example, metabolically dysfunctional perivascular AT (PVAT) was found to be infiltrated by macrophages, T cells, natural killer cells, and DCs that produce either pro-inflammatory or anti-inflammatory cytokines depending on PVAT adipokine profile



shifts [46]. As such, accumulating evidence implicates local alterations of resident and infiltrating immune cell populations within the SVF in AT inflammation and the pathogenesis of insulin resistance, metabolic syndrome, and diabetes [47]. Moreover, AT dysfunction is associated with an imbalanced adipokine profile that further promotes detrimental AT immune cell landscape shifts [47].

Another important player in AT function is UCP1, which is considered one of the unique hallmarks of multilocular adipocytes and found abundantly in the inner mitochondrial membrane BAT imparting its thermogenic property, as mentioned previously [19, 75]. The expression of UCP1 is mainly mediated by the downstream pathway of  $\beta$ -adrenergic receptors (AR), more specifically  $\beta_3$ -AR [76]. Moreover  $\beta_3$ -AR activation induces lipolysis, increasing free fatty acids levels further promotes the activity of UCP1 [77]. In fact, UCP1 ablation in mice inhibited shivering thermogenesis in BAT in response to sympathetic or FFA stimulation [78].

Conversely, in WAT, UCP1 mediates browning or beiging [76, 79]. Which is the process by which unilocular adipocytes start to express brown or multilocular markers, mainly UCP1, to increase energy expenditure [22, 29, 75, 80]. Browning of WAT was mostly correlated with positive health outcomes [29, 81]. While the suppression of browning or the promotion of whitening were perceived as negative ones and were correlated with detrimental consequences. For instance, when Adipocytes were challenged with macrophages activated by lipopolysaccharide (LPS) and TNF- $\alpha$ , the expression of UCP1 mRNA, UCP1 promoter and transcriptional factor binding to cAMP response element were all suppressed in WAT [82]. Similarly, other studies suggested that UCP1 is downregulated in BAT by low-grade inflammation as seen in mice chronically treated with LPS [83]. In this study, it was proposed that BAT is

immunologically naïve since *in vitro* LPS treatment was not able to induce inflammation and produce UCP1 downregulation, which was achieved by direct stimulation with IL-1 $\beta$  instead.

Interestingly and from a different perspective, murine studies reported an increase in UCP1 expression in BAT in response to high-fat diet feeding [84]. Specifically, a recent study showed that AC browning and increased expression of UCP1, among other BAT markers, were observed in several WAT depots in rats receiving a high-fat diet [85].

One of the possible pathways for IL-1 $\beta$ -evoked UCP1 downregulation was proposed to be via stimulating the endogenous protein deleted in breast cancer -1 being natural inhibitor of Human silent information regulator Type -1/ Sirtuin-1 (SIRT1). SIRT1 was shown to stimulate UCP1 expression [83]. In this regard, SIRT1 plays a crucial role in the AT, as it acts as a natural suppressor for PPAR $\gamma$  in ACs thus decreasing fat accumulation [86]. This is associated with an increase in lipolysis by inducing mitochondrial fatty acid oxidation, through the activation of the transcriptional coactivator; PPAR $\gamma$  gamma coactivator-1  $\alpha$  (PGC-1  $\alpha$ ) [87]. Significantly, a lack of increase in UCP1-mediated energy dissipation in response to high-fat feeding triggered BAT changes reminiscent of AT hypertrophy typically seen in WAT depots. Indeed, UCP1 knockout mice receiving high-fat diet showed a whitening of BAT, with increased adipocyte size and macrophage infiltration [88]. As well, reduced mitochondrial biogenesis, increased endoplasmic reticulum stress, and disrupted glucose tolerance were more pronounced in these mice upon high-fat feeding. However, these mice did not show any sign of change in visceral adiposity, body weight, energy intake or expenditure [88]. Another important factor is the sympathetic overactivation that is usually triggered by cold exposure. Sympathetic stimulation

induces proliferation of BAT through the activity of PPAR $\gamma$ , which in turn increases the expression of UCP1 and mitochondrial biogenesis. This was shown in an *in vivo* study comparing innervated and denervated BAT and demonstrating that PPAR $\gamma$ -mediated UCP1 activation was dependent on the sympathetic nervous system (SNS) [89]. This is in contrast to *in vitro* research findings, where treating BAT cells with Rosiglitazone, a selective PPAR $\gamma$  agonist [90], was enough to increase UCP1 and mitochondrial biogenesis in manner that does not involve sympathetic activation [91]. Significantly, it has long been recognized that hyperinsulinemia in early metabolic dysfunction in humans and animals, triggers increased sympathetic activity [92, 93].

On the other hand, increased oxygen consumption associated with browning of white ACs differentiated from human adipose-derived stem cells was correlated with increased mitochondria fission indicated by increase in Dynamin-Related Protein-1 (DRP-1) phosphorylation on serine 616 (ser616) [94]. Moreover, other triggers leading to sub-cutaneous white AC browning were also associated with increased Erk-mediated ser616-DRP1 phosphorylation and mitochondrial fission [95]. Indeed, DRP1-mediated mitochondrial fission was shown to be utilized by BAT adipocytes in response to sympathetic stimulation to increase energy dissipation and involved protein kinase A-evoked DRP1 phosphorylation at the same site [96]. The exact molecular relationship between increased UCP1 expression and mitochondrial fission remains unclear. However, increased mitochondrial fission observed under these circumstances has recently been proposed to act as a feedback mechanism increasing the metabolic resilience and protecting against the deleterious effect of increased caloric intake [17]. Yet, in the above situations, mitochondrial changes were seen under circumstances not perceived to contribute to adipose pathologies. Interestingly, WAT inflammation in

diabetic mice was associated with increased ser616-DRP1 phosphorylation. Both observations were reversed when animals received treatments increasing AMPK activity. However, this study did not examine the status of UCP1 expression [97]. Nevertheless, the deletion of either the  $\alpha$  or  $\beta$  subunits of AMPK resulted in an impaired WAT being with a resistance to  $\beta$ -AR stimulation [98, 99]. In another study, AMPK gain of function mutation induced sWAT browning [100].

Ultimately, energy induced AT negative remodeling including hypertrophy, hypoxia, inflammation and altered UCP1 expression among many others will mount metabolic imbalance and cardiovascular dysfunction, eventually leading to CVDs in clinical and subclinical stages. One example is the increase of proinflammatory macrophages, cytokines, and ROS in epicardial AT in patients with coronary artery diseases [101-103]. In fact, obese patients with insulin resistance had systemic arterial dysfunction concurrent with high M1 ATMs and TNF $\alpha$  mRNA in SAT and elevated serum C reactive protein (CRP), indicating a proinflammatory state [104]. Indeed, in our work AT inflammation was related to autonomic imbalance, the preclinical stage of cardiac autonomic neuropathy (CAN) [6]. and endothelial dysfunction (ED) [105], both considered major risk factors predisposing to CVD associated with diet induced metabolic impairment and prediabetes [106].

CAN is one of the most serious and prevalent complications of diabetes, it is manifested by the impaired ability for cardiovascular autonomic control [107]. It is known to occur early during metabolic derangement exemplified by the prediabetic stage [108-110]. Indeed, subclinical CAN exhibited by autonomic imbalance, with dysfunctional parasympathetic autonomic response, were detected in early metabolic

derangements in the absence of systemic inflammation and apparent hyperglycemia, but rather with confined inflammation and AT modulation [6, 111].

ED is a major predisposing factor for CVDs[110, 112, 113], it is a term referred to the altered endothelium state, characterized by proinflammatory, prothrombic and reduced vasodilatory activity [114]. The main drivers of impaired vasodilation are reduced endothelial nitric oxide production, compromised hyperpolarization factors and increased oxidative stress[114, 115]. It is highly prevalent in early metabolic insults[116], prediabetes, diabetes, obesity, HTN and many others [104, 110, 112, 113, 115, 117, 118]. Henceforth, one of the most significant depots in mirroring the cardiovascular status is perivascular adipose tissue (PVAT) [119]. Indeed, recent studies on a prediabetic rat model showed that mildly increased caloric intake led to clear cardiovascular manifestations even in absence of overt hyperglycemia, increased body weight, or high blood pressure [6, 7, 105]. Significantly, the observed endothelial dysfunction and CAN were linked to localized PVAT inflammation with neither inflammatory changes in other adipose pool nor systemic involvement [6, 7, 105]. This further indicates the peculiar and sensitive nature of PVAT in responding to positive energy intake, and its dramatic effect on metabolic and cardiovascular state despite being a minute pool. PVAT remodeling and CVDs will be elaborately discussed in the following section.

## ***2. Diet Induced Perivascular Adipose Tissue remodeling and metabolic provoked cardiovascular impairment.***

PVAT is the adipose layer surrounding the adventitia of most large blood vessels. It is a distinct depot anatomically and functionally[22]. First, it is considered one of the few naturally occurring beige adipose pools, which has both multi and unilocular ACs,

with moderate UCP1 expression depending on the localization and the metabolic state of the subject[21, 22]. Second, it plays a major role in regulating the vasomotor tone in blood vessels, by producing various cytokines and adipokines. For example, adiponectin is considered one of the important vasorelaxant agents produced by PVAT[20]. Lastly, despite being relatively a small depot, the unique localization of PVAT engulfing blood vessels, being a dynamic and metabolically active tissue, its dysfunction will eventually incite CVDs, [21, 120-122]. For instance, PVAT ACs had higher proinflammatory and reduced adipogenic differentiation state compared to other depots, in addition to other anti-inflammatory products such as adiponectin[123]. The produced adipokines and cytokines do not only have humoral effects, but also interrupt the contractile machinery of endothelium and smooth muscle cells of blood vessels, a process referred to as adipose-vascular coupling [124], which was found to be a contributor to ED as well [116, 124-126]. Metabolic stress was found to compromise endothelial dependent vasorelaxation, nitric oxide (NO) and endothelial-dependent hyperpolarization (EDHP)[126]. As stated before, ED is known to be a strong contributor to CVDs in individual with insulin resistance in human and murine models [113, 118]. Moreover, PVAT was suggested to be responsible for aortic remodeling [127]. One study even suggested that exercise mediated endothelial protection in T2DM mice, is mediated by inducing anti-inflammatory state in PVAT[128]. According to the Framingham offspring heart study, in human subjects increased PVAT mass was tightly associated with coronary calcification, HTN and metabolic anomalies such as glucose intolerance, low HDL, even in the absence of overweight , obesity and elevated VAT[129, 130].

Moreover, inflammation of PVAT can be a confounding factor of plaque formation and stability [131]. Mechanistic pathways by which PVAT secretes a complex array of factors to modulate vascular tone have been proposed. Indeed, as early as 1991, periaortic fat was shown to exert an anti-contractile effect [132] that persisted when vessels without AT were treated with PVAT-conditioned media [133]. In this regard, PVAT adipokines are highly likely to exert direct effects on the nearby vascular tissue. Of these, adiponectin was shown to mediate the anticontractile effect via eNOS stimulation [134, 135]. Additionally, animal models of deleted PPAR $\gamma$  that lacked the PVAT depot, showed endothelial dysfunction and increased cardiovascular diseases [136] supporting the fundamental role of PVAT in modulating cardiovascular health [20, 21]. Of note, studies have shown that the anticontractile effect is lost in metabolic diseases like diabetes, as PVAT phenotype shifts into a proinflammatory state [121]. This is accompanied by significant perturbation in the adipokine profile involving several of these products including adiponectin, leptin, chemerin, resistin, and visfatin [137]. Another study indicated that upon the transplant of thoracic aortic PVAT from HFD fed mice to the carotid artery of HFD-fed ApoE<sup>-/-</sup> mice vascular injury was augmented, and it was mediated by macrophage chemotactic protein 1 (MCP1) expression [138]. It also was suggested that proinflammatory ATMs migration induces inflammation in the vascular bed and poses atherogenic effect [139]. Furthermore, it appears that PVAT is especially sensitive to hypoxia-driven inflammation [140]. Indeed, isolated PVAT inflammation, with significant implications on vascular structure and function, was observed in more than one animal model of metabolic challenge. Transplantation of inflamed PVAT from HFD-fed ApoE<sup>-/-</sup> mice increased the incidence of atherosclerosis and ED in recipient animals on a control diet [141]. Moreover,

prediabetic rats fed mild hypercaloric diet showed increases in PVAT UCP1, DRP1 as well as HIF1- $\alpha$  expression, in addition to a hypertrophied inflamed morphology that were associated with vascular dysfunction in absence of similar changes in other adipose depots [7]. One would assume that this peculiar nature, whereby several PVAT pools expressed brown adipose-specific genes [142-144], might be the cause of the observed early involvement and increased sensitivity to inflammation. In this context, an assumed exaggerated oxygen consumption triggered by increased UCP1 expression would be exacerbated by the observed adipocyte hypertrophy in a combination of events less likely to occur in other adipose depots. Importantly, another rat model on HFD showed increased UCP1 expression in PVAT, however this increase was not explained nor were its implications investigated [88]. Since sympathetic activation requires  $\beta_3$ -AR in beige ACs to induce thermogenesis and increase UCP1[145]. This can explain the increase of UCP1 in PVAT in response to excess energy intake. Likewise, spontaneously hypertensive rats had elevated UCP1 in PVAT[146]. On the other hand, HFD reduced UCP1 in WAT and VAT, supporting the hypothesis indicating that AT depots act varying in response to the same energy stimuli [88]. In the above rat model of early metabolic dysfunction, localized PVAT inflammation led to increased IL-1 $\beta$  and TGF- $\beta$ 1 production, which was associated with reduced AMPK activation, increased vascular Erk1/2 phosphorylation, medial hypertrophy, oxidative stress, increased rho-associated kinase (ROCK)-mediated calcium sensitization and a hypercontractile response [7, 147]. This isolated PVAT inflammation model was also associated with impaired endothelial relaxing function due to reduced expression/function of inward rectifier K<sup>+</sup> channels [105]. On the contrary, exercise



showed to increase PVAT UCP1 expression in diabetic mice, alongside anti-inflammatory markers and M2 polarization [128].

Furthermore, targeting the constituents of PVAT inflammation ameliorated diet induced endothelial dysfunction. As such, different animal study using *AMPK $\alpha$ 1* knockout mice assessed the impact of HFD on PVAT function. HFD in wild-type mice reduced P-AMPK and adiponectin levels, in addition to diminished anti-contractile involvement of PVAT accompanied by an infiltration of macrophage with M1 polarization, indicated by increase in iNOS and IL-1  $\beta$ . Yet in *AMPK $\alpha$ 1* KO mice, PVAT of both HFD and control fed animals showed a massive reduction in P-AMPK, adiponectin and abolished vasorelaxation [122].

All these findings further confirm the early involvement of diet induced PVAT inflammation in disposing to metabolic and cardiovascular dysfunction.

## **B. Sexual Dimorphism in Metabolic Induced Cardiovascular Dysfunction.**

Gender plays a confounding role in CVDs incidence, prevalence, and prognosis[1]. It is well established that women and female animals with circulating estrogen are less prone to develop CVDs in response to HFD compared to their male and nonovulating female opponents. As such, premenopausal women are at lower risk for developing CVDs compared to men at the same age, and odds are not in favor of women after menopause. [148-150]. Also, HFD fed female mice were protected from diastolic dysfunction and left ventricle (LV) hypertrophy, unlike their male equals [151]. Another human study showed that women had less markers of ED, vascular injury, and inflammation compared to men[152]. Plus, premenopausal women had more pronounced endothelium dependent vasorelaxation compared to men [153]. A study

exploring the impact of adiponectin level on cardiovascular health in *eNOS* KO male and female mice, showed that in response to HFD female mice were able to compensate for eNOS absence when adiponectin was overexpressed and they maintained normal cardiac function and left ventricle mass, unlike males who had compromised LV function and hypertrophy in response to HFD independent of adiponectin levels. Interestingly, adiponectin overexpression in females reduced adiposity and fat mass increase. The same study also suggested the deletion of eNOS led to an upregulation of adiponectin, and this was even more pronounced in females implying the possible role of sex hormones in modulating the compensatory upregulation of adiponectin. [154].

Even though women have higher fat mass than men at the same age, they are protected from cardiometabolic risk, which is mainly attributed to increased peripheral adiposity and lower central fat mass[149, 150, 152, 155, 156]. Women are more insulin sensitive than men , which is a fundamental contributor to the female CV privilege [150, 157]. Moreover, female mice were protected from HFD induced hyperglycemia and glucose intolerance whereas males were not [151]. Another *ex-vivo* study measuring the impact of E2 on insulin sensitivity in muscles taken from female rats showed that treatment with E2 enhanced muscles' AMPK phosphorylation rather than not glucose uptake [158]. Moreover, prediabetic women were found to have less fasting blood glucose, but scored higher in glucose tolerance test than their male counterparts[149]. However, others suggested that it is not the insulin resistance that is different between men and women, but rather the ability of women to mitigate the role of insulin resistance in CVDs development[150]. Moreover, In female rats estrogen controls vascular tone by modulating endothelial  $\beta$ -AR expression, increasing  $\beta$ 1-AR

and  $\beta_3$ -AR but not  $\beta_2$ -AR. OVX reduced  $\beta_1$ -AR and  $\beta_3$ -AR in vascular tissues, which induced a similar vascular tone to the males[159].

Hence, functional and anatomical differences such as sex hormones and adiposity patterns make women more resistant to metabolic distress[149].

### ***1. Sexual Dimorphism and Adipose Tissue Dysfunction***

Sexual dimorphism in cardiovascular status is a sum of intertwined biological and non-biological factors, however, the most prominent and dominant ones are sex hormones and adiposity [148, 152, 155, 156, 160]. Women tend to have higher sWAT with peripheral adiposity that is referred to as ‘gynoid phenotype’, while men mainly accumulate fat centrally in the viscera, referred to as ‘android phenotype’ [149]. Since each depot of AT has different characteristics and function, ectopic or VAT is more related to cardiometabolic disorders than sWAT [29, 149, 161]. ACs in the latter are larger in size yet more sensitive to insulin [149]. Furthermore, in response to positive energy balance sWAT expand in a more hyperplastic manner, while VAT respond in a more hypertrophied one[29]. Moreover, several lines of evidence coincided that in men ingested lipids are mostly stored in the visceral depot rather than subcutaneous, compared to women [162, 163]. Additionally, premenopausal women were noticed to have more active LPL in extracted sWAT from different sites (femoral, gluteal, abdominal, and epigastric) than men. While in men, they had larger depots of VAT (omental and mesenteric) without any change in LPL activity[164]. In fact, studies on transsexual human subjects indicated a clear shift in adiposity patterns, as female-male treated subjects with testosterone esters had higher VAT and lower peripheral sWAT, while male-female transgenders had higher overall sWAT and lower VAT upon

treatment with estradiol and pregestational antiandrogen [165]. As previously detailed, adipose hypertrophy is associated with a pro-inflammatory state and tissue hypoxia, which will further exaggerate the inflammation, fibrosis, and insulin resistance [29, 149, 166].

a. The Role of Estrogen and Estrogen Receptors in Diet Induced Adipose Remodeling.

Estrogen is well known to reduce energy intake and increase energy expenditure [167]. As such, premenopausal healthy women were found to have an advantage in postprandial lipid metabolism, which was compromised in premenopausal prediabetic women and in postmenopausal women [168]. On the same note, bilateral ovariectomy (OVX) in murine models increased food intake and body weight [169]. Similar conclusions regarding energy expenditure were drawn from another model of endogenous estrogen deficiency, the aromatase cytochrome P450 KO mouse model, as in both males and females it promoted hyperinsulinemia with weight gain and increased adiposity especially in the gonadal pool, these changes were not associated with hyperphagia but rather with reduced energy expenditure, reduced physical activity, reduced glucose oxidation and decreased lean body mass [170]. Leptin as well was suggested to mediate the changes in food intake correlated with menopause, as one human study following postmenopausal women for 5 years indicated an increase in circulating leptin compared to their HRT recipient peers, adiposity and fat mass increased in the control group as well[171].

Furthermore, estrogen was found to protect from GAT hypertrophy, fibrosis and inflammation in male and female mice [172]. Indeed, the absence of circulating estrogen provoked a state of proinflammatory immune response in human subjects and

animal models[173, 174]. Estrogen was found to exert these beneficial outcomes even in the presence of HFD. As female and male mice fed for 4 weeks on HFD, males had higher total body weight while females had higher fat mass, however, they had lower fasting blood glucose than males. Still, E2 treatment improved insulin sensitivity in both sexes and reduced fat mass in males, in addition to a massive reduction in WAT and plasma IL-6 and TNF- $\alpha$  levels[175]. Moreover, sWAT in HFD fed female rats was found to be protected against redox stress compared to males, increased NADPH oxidase (NOX) activity and mRNA expression, while glutathione peroxidase (GPx) and superoxide dismutase (SOD) were reduced. At the same time mRNA levels of inflammatory markers seemed to be higher in sWAT of male rats like; IL-6, TNF- $\alpha$ , IL-1  $\beta$  and CD68, a marker of macrophages[176]. Interestingly, AT specific *IL-6* KO mice had sex dependent impact upon HFD feeding, as female KO mice had lower adiposity especially in GAT and sWAT and ACs count in GAT, with weight gain and higher PGC1- $\alpha$  level than the WT, while males did not show similar patterns. These KO females were also protected against impaired insulin sensitivity and glucose tolerance[177]. Since women have more insulin sensitivity than men in AT, this might also attribute to the differential adiposity in lower sWAT than VAT compared to men [178-180].

Intriguingly, the quality of fat in the HFD affect the AT inflammation related metabolic outcomes in a sex dependent manner. As mice fed low cholesterol HFD that either contained Monounsaturated FA (using cotton and soy oils) vs Saturated FA (using lard), showed that despite the unified increased in body weight in both sexes in response to both diets. However, adiposity pattern did not, as VAT increased in response to animal FA diet rather than the vegetable based one[151]. In addition to the

prominent effect of estrogens on adiposity patterns in human subjects and animal models, it also reduced ACs hypertrophy, protected various AT depots from HFD induced inflammation and redox damage, in addition to the promotion of anti-inflammatory state.

In addition to the crucial role of estrogens in regulating metabolism and AT functions, estrogen receptors (ERs) possess fundamental roles in animal models in both genders, especially  $ER\alpha$ , since E2 has higher affinity to it than to  $ER\beta$  [181], and it's more abundant in ACs than  $ER\beta$ [182]. Moreover, HFD lead to a reduced  $ER\alpha$  in AT of both male and female mice, however the females maintained a higher level compared to the males [151]. Adipocyte specific  $ER\alpha$  KO produced an inflamed and hypertrophied GAT in mice; interestingly these pathologies were more prominent in male mice[172]. Moreover, E2 treatment after ovariectomy (OVX) in  $ER\alpha$  KO mouse model did not seem to correct the increased adiposity, weight gain and caloric intake[183]. Furthermore,  $ER\alpha$  showed an important role in AT of males  $ER\alpha$  KO model, as it increased adiposity in both hyperplastic and hypertrophic modes in WAT (inguinal, perirenal and epididymal) but not in BAT, in addition to increased body mass, which was also recorded in females KO counterparts, alongside insulin resistance and glucose intolerance. Interestingly, despite the weight gain induced by  $ER\alpha$  KO in male mice, food intake did not differ from the WT littermates, however, energy expenditure was found to be compromised, explaining the observed increased adiposity and weight gain[184]. This was also found in a human male with mutation in ER that had increased weight gain and hyperinsulinemia, impaired glucose tolerance [185].  $ER\alpha$  was found to play the upper hand in these metabolic changes induced by OVX in rats, as upon using selective agonist for  $ER\alpha$  propylpyrazole triol (PTT), it was able to reduce food intake

and weight gain, while ER $\beta$  selective agonist diarylpropionitrile ( DPN) failed to exert similar response [186, 187]. Nonetheless, using ER $\beta$  selective agonist in HFD fed OVX female mice showed the protective effect of ER $\beta$  activation in weight gain, adiposity, especially WAT mass and hypercholesterolemia. Strikingly, UCP1 in BAT was found to be upregulated by ER $\beta$  agonist, increasing thermogenesis, in addition to repressing PPAR- $\gamma$  in BAT and WAT indirectly by competing on the binding site with PGC1- $\alpha$  [188]. Knockdown (KD) of ER $\alpha$  in AC was also accompanied with upregulation of TLR4 in both sexes and TNF- $\alpha$  only in males. Furthermore, OVX induced adiposity and weight gain are ER $\alpha$  dependent, as OVX in the KD model did not induce weight gain, suggesting the possible role of ER $\alpha$  in adipose expansion in the absence of exogenous and endogenous Estrogen, it was even suggested the protective effect of ER $\alpha$  KO in OVX mice in improving AT inflammation and fibrosis. Again, in the absence of ER $\alpha$ , ER $\beta$  was found to have a protective role in AT insults [172].

Overall estrogen plays an important role in adiposity pattern, maintaining adipose tissue function and preventing its inflammation even when challenged with excessive energy intake, mainly through ER $\alpha$ .

b. Sex Differences in Adrenergic Receptors Function in Adipose Tissue Modulation.

Variation in ARs activity and expression in different adipose pools were implicated to play a major role in sex dependent catecholamines induced lipolytic differences. As concluded by one study using ACs from nonobese human subjects , both  $\beta$ -AR sensitivity and expression were higher in abdominal derived ACs than gluteal ones in both sexes, unlike  $\alpha$ 2-AR, where females abdominal ACs had significant lower sensitivity to  $\alpha$ 2-AR compared to the gluteal derived ACs, with no

major difference in expression[189]. On the other hand, a longitudinal study on women suggested the effect of aging is more prominent in catecholamines induced lipolysis rather than hormonal changes in isolated ACs from the abdominal sWAT, as they measured a decreased  $\beta$ -AR activity but maintained  $\alpha$ 2-AR activity, as well as a decrease in lipolysis linked genes and AC size regardless of the hormonal status[190]. On a different note, another study examining the role of estrogen in catecholamine induced lipolysis, reported an increase in  $\alpha$ 2-AR activity and expression in sWAT but not VAT (E2 activity was mediated thru  $E_{r\alpha}$ ) [191]. This might explain the sex dependent adiposity pattern in females, as they have more antilipolytic activity in sWAT rather than VAT, that is likely to be affected by age and hormonal status. In line with these findings, another human study on FFA release in response to epinephrine injection in men and women showed a sharp increase in FFA release in peripheral sWAT in men but not in women, but similar release of FFA from VAT in both sexes[192]. Indeed, uptake of injected radiolabeled FFA was traced in lower sWAT in women and visceral in men [193].

c. Sex-Dependent UCP1 Modulation in Adipose Tissue.

Sex related differences in UCP1 expression and activation have been inconsistent in cellular and preclinical models. For instance, women have higher fat derived resting metabolic rate, as well as increased UCP1 expression and ACs count in BAT compared to men [194]. Another *in-vitro* experiment showed that sex hormones had dose dependent effect on UCP1 expression in brown ACs, such that testosterone inhibits UCP1 expression in response to norepinephrine (NE), whereas progesterone promoted the NE mediated UCP1 expression, while estrogen had no effect on its



expression; however both female sex hormones increased the size of lipid droplets in ACs [195]. In contrast, a previous *in-vitro* experiment on brown ACs, indicated that both female sex hormones reduced NE dependent UCP1 synthesis [196]. Still, UCP1 KO female mice had a higher tendency to insulin resistance, and glucose intolerance in response to western diet (WD) [197]. Actually, in HFD fed Wistar rats, females had lower expression of  $\beta_3$ -AR in BAT, alongside impaired insulin signaling pathway, implied in the decrease of glucose transporter 4 (GLUT4) and IRS levels, which were not observed in males who had better Mt function as well[198]. In normal conditions, female rats tend to have higher sensitivity of  $\beta_3$ -AR to NE response in BAT, with elevated UCP1 and oxygen consumption and less  $\alpha_2$ -AR than males[199]. Another study reported lower expression of  $\beta_3$ -AR and  $\alpha_2$ -AR in female BAT compared to males[200, 201].

Similarly, sWAT in women also had higher gene marker for UCP1 compared to men [194]. GAT browning in response to  $\beta_3$ -AR activation in females appears to be more pronounced [202]. Additionally, increased UCP1 expression in female mice GAT was correlated with positive metabolic outcome, opposite to males where UCP1 expression was positively correlated with insulin resistance and adiposity [203]. Besides, Mt activity in subcutaneous white ACs derived from obese female subjects was higher and more effective compared to their male controls[204]. Cold induced browning in peripheral sWAT in ACs derived from women but in the ones derived from men, while VAT did not differ in UCP1 expression and oxygen consumption between both sexes[159]. Since the contribution of fat mass to the resting metabolic rate in women was found to be higher than in men, which was independent of the hormonal status of women, It was suggested to be due the increased MT density and activity, in

addition to the increase of UCP1 expression in BAT [194]. Taken all together, these findings suggest the higher sensitivity of female UCP1 in regulating metabolism.

Another important protective mechanisms of estrogen in the AT is the promotion of hypoxia inducible factor 1 (HIF1- $\alpha$ ) ubiquitination and degradation, by ER $\alpha$  activation and upregulation of prolyl hydroxylase[149]. However, it was found that E2 and PTT induced HIF-1 $\alpha$  binding to vascular endothelial growth factor (VEGF) promoter *in-vitro* in ACs[205], still this increase in hypoxia was found to be beneficial to induce angiogenesis and protect AT dysfunction. However, in mammary carcinoma endothelial cell line E2 treatment induced HIF1- $\alpha$  expression, interestingly, E2 treatment induced VEGF expression more than hypoxia did. Indicating the pathological role of E2 in promoting hypoxia vascularization of the tumor[206]. Moreover, GAT in female mice exhibited a more metabolic active pool despite HFD feeding, as they had smaller ACs, more insulin sensitive, with higher adiponectin level, UCP1 and more angiogenic markers such as VEGF [207]. Interestingly E2 and PPT were found to play a very important role in upregulating VEGF in preadipocytes cell line mediated by ER $\alpha$ , as using ER $\alpha$  antagonist or ER $\alpha$  selective Knockdown reduced VEGF expression and inhibited E2 modulation of VEGF level. Besides, *Era* KO mice had lower VEGF in GAT and inguinal pools compared to the WT[205].

Taken all together, female adipose tissue can be considered a major underlying factor of sex depend CVDs differences, as it is seems to be more resilient to diet induced irregularities such as insulin resistance, inflammation, and hypoxia[208, 209].

## ***2. Sex Differential Involvement of Perivascular Adipose Tissue in Cardiovascular Dysfunction.***

Sex differences in the role of PVAT in diet induced CVDs development has not been deeply investigated, however, several attempts were recorded. In the Framingham study postmenopausal women were found to have an increased PVAT mass by 50%, while men in the same age had 20% increase [130]. Noteworthy, PVAT in postmenopausal women was found to have a higher number of proinflammatory macrophages, compared to other depots, and it was suggested that this is associated with increased CV risk [52]. Indeed, women who had higher thoracic PVAT had lower HDL [130], making them more at risk of developing CVDs[210].

These findings were even more pronounced and detailed in animal models. HFD fed male Wistar-Kyoto rats showed hypertrophied ACs and dysfunctional PVAT that was accompanied with impaired endothelial dependent vasorelaxation. Female pigs showed an anticontractile superiority when PVAT attached arteries were challenged with vasorelaxant agents compared to male pigs, although both males and females had the same level of PVAT adiponectin. Yet, female pigs had higher sensitivity of adiponectin receptor in the coronary artery, which was confirmed by anti-adiponectin inhibition of vasorelaxation in female vessels in the presence of PVAT, but not in males[211]. Additionally, OVX in murine models produced a dysfunctional PVAT compared to their sham littermates[212]. Furthermore, HFD feeding in Dahl salt sensitive rat model showed a sex dependent PVAT dysfunction, although both sexes developed HTN, nonetheless, PVAT was more fibrotic and lost some of its anticontractile properties in males but not in females[213]. Also, in female pigs PVAT thromboxane was mainly involved in the coronary artery contraction, while in males prostaglandin F<sub>2a</sub> had the

upper hand[214], which further implies not only the anatomical differences based on sex, but also the functional differences.

Another interesting study investigated the influence of maternal HFD induced obesity on the fetal PVAT in rats: although the offspring were fed a control diet, only male offspring were hypertensive, and their PVAT suffered from an altered anti-contraction effect[215]. The same group of researchers further investigated the sex differences in the offspring, female offspring were also hypertensive and both sexes had slightly elevated serum insulin. However, endothelial dysfunction was only observed in male offspring; reduced acetylcholine dependent relaxation, and low eNOS phosphorylation, these were normal in females. Interestingly, reduced AMPK activity was found to be the main driver of PVAT dysfunction in the offspring of HFD rats, moreover, in males NO reduced bioavailability was an additional factor[216]. Contrariwise, HFD with and without high sucrose induced mesenteric PVAT dysfunction in female mice and distorted its anticontractile effect only in females. However, PVAT provoked endothelial dysfunction in high fat high sucrose diet was observed in both sexes, but earlier in females, after 3 months vs 5 months in males[217]. These findings further indicate the delicate nature of PVAT in responding to excess energy intake, as each pool of PVAT has its own characteristics, in fact, mesenteric PVAT is found to have more proliferative capacity in the adipose progenitor cells compared to the thoracic aorta PVAT. Moreover, UCP1 expression in mesenteric PVAT was lower and ACs were whiter than the aortic ones [218]. Thoracic and abdominal aortas PVAT were found to behave differently in response to the same diet as well, HFD induced hypertrophy of ACs, in addition to increased macrophage

infiltration and MCP1 in abdominal PVAT, while high sucrose diet induced the same in thoracic PVAT in addition to decrease in UCP1[219].

Another animal model of maternal intermittent hypoxia, stimulated by gestational sleep apnea, was found to induce metabolic and endothelial dysfunction in male offspring only, with increased inflammatory genetic markers and reduced adiponectin in PVAT, marking its dysfunction [220]. Interestingly, thoracic PVAT in female Sprague-Dawley control rats had higher T cells and immunocytes count compared to the one in males[221]. Undeniably, PVAT mediated vascular tone regulation and its immune responsiveness can be safely insinuated to be sex dependent.

As discussed in the previous section, dietary modulation of UCP1 is considered one of the important mechanisms underlying AT engagement in sex dependent early cardiovascular dysfunction. Nevertheless, UCP1 sex dependent differences in PVAT were merely explicitly targeted in research, and results were either inconsistent or perplexing. On one hand, *UCP1* KO female mice in response to WD had increased level of UCP1 mRNA in PVAT in the WT [197]. Interestingly, similar findings were recorded in WT male rats after 12 weeks of mild hyper caloric intake [222]. On the other hand, female Wistar rats fed on western diet were found to suffer from ED accompanied with whitening of PVAT, indicated by loss of mitochondrial density and reduced UCP1 expression and elevated redox state and ACs size[223] and inflammatory markers such as MCP1 [224]. Moreover, HFD induced increased sympathetic activation thru  $\beta$ 3-AR was more prominent in male rats compared to females [225], which can play an important factor in sex dependent differences in diet induced UCP1 expression and activity.

These findings further confirm the uncanny response of PVAT to HFD feeding, especially in a sex dependent manner, making the understanding of the key mechanisms behind such behavior a necessity, and precision interventions based on the hormonal status more plausible.

## **C. Dietary Intervention Targeting Adipose Tissue Inflammation in Early Cardiometabolic Dysfunction.**

### ***1. Therapeutic Fasting and Diet Induced Adipose Dysfunction***

Since overnutrition and positive energy balance are the key triggers of metabolic and cardiovascular dysfunction, calorie restriction became an attractive intervention as a possible way to prevent, improve and even treat diet induced cardiovascular and metabolic manifestations. Time restricted feeding regimens are referred to as intermittent fasting (IF) [226, 227], showed a strong positive impact on the metabolic state of obese and non-obese human subjects and animal models [226, 228], that is mostly mediated by provoking positive AT remodeling [229, 230]. For example, after eight weeks of treatment, 24 hours fasting 3 days a week, not only IF did improve glucose tolerance, and insulin resistance in HFD-fed mice, it also reduced adipocyte hypertrophy and markers of inflammation including macrophage infiltration [229]. Moreover, the same IF regimen and every other day (EOD) fasting for 4 weeks, both were able to evoke an increased energy expenditure and UCP1 expression in WAT tissue in diet-induced obese mice in a manner that also involved reduction of inflammatory markers [81, 231]. Yet, while IF reduced WAT fat mass in both obese mice models and obese human subjects, no UCP1 upregulation was observed in humans [81]. Nevertheless, the exact mechanism of how these fasting regimens improve the metabolic state are still not fully understood. Particularly, since isocaloric IF seems to

have a prominent effect on the metabolic health, without any caloric restriction or dietary modifications [228, 232, 233].

In murine models, HFD-induced hypertrophy was reported to be reversed by short term IF (24-72 hours) in GAT, sWAT and INAT [234]. Interestingly, the change in fat pad size was found to be triggered by IF alone, regardless of the daily caloric intake, and independent of the change in body weight as animal studies showed a decrease in size and weight of adipose depots, with mild or no change in total body weight [81, 235-237]. Certainly in our work, a calorie restricted regimen of a HFD failed to exert any corrective effect on CAN and PVAT inflammation involvement in rats [6] as opposed to isocaloric 12 hours daily IF for 12 weeks [238]. In studies involving obese human subjects, IF appeared to reduce total fat mass [239-241] and circulating markers of inflammation [240, 242], the latter effect being more marked in obese than in normal weight subjects [242]. In further confirmation of the observations in animal studies, IF regimens were more capable of reducing circulating markers of inflammation than calorie restricted regimens *per se* [242].

Nonetheless, mixed results were found in human studies. In a study examining IF during the month of Ramadan, which is the religious fasting in Islam involving fasting from sunrise till sunset for 30 days, body weight and fat percentage decreased in both men and women in absence of caloric restriction [243]. Meanwhile, others reported that the IF-induced weight loss was dependent on caloric restriction that mediated the metabolic benefit rather than the fasting regimen itself [244, 245]. Moreover, a recent clinical trial comparing the effects of 8 weeks of caloric restriction to weekly 3 non-consecutive days of IF showed a transient increase in inflammatory markers in AT after IF only, which was attributed to an AT residing macrophages response to increased

lipolysis [246]. The lack of unity and precision in the studied fasting regimes as a therapeutic intervention makes conclusions harder to acquire, still, a marked overall improvement in AT and metabolic functioning are mostly achieved.

IF might constitute an adequate intervention in the low-grade inflammatory state evoked in AT by DIO. Indeed, 8 weeks of 3 days a week IF produced the previously mentioned anti-inflammatory effects in metabolically challenged mice alongside reduction of body weight and insulin resistance [229]. Interestingly, 16 weeks of isocaloric IF (1 day fasting: 2 days of free feeding) was shown to produce the same effects and trigger alternative activation of macrophages to the M2 polarization [233]. Another study involving IF in a calorie restriction protocol showed a shift in AT macrophages to the M2 polarization that was mediated by SIRT1 activity [247]. SIRT1 is a nutrient sensitive histone deacetylase that is thought to mediate the beneficial metabolic effects of fasting and calorie restriction including improved serum glucose and lipid levels, increased insulin sensitivity and reduced body weight [248, 249]. Specifically, mild SIRT1 overexpression protected against HFD-induced inflammation by reducing NF- $\kappa$ B activation and pro-inflammatory cytokine production [250].

Pertinent to the inflammatory context in AT, SIRT1 activation was shown to mitigate hypoxic cell damage through the augmentation of autophagic flux that was mediated by AMPK activation [251]. Indeed, acute IF (15-39 hours) was found to augment AMPK phosphorylation [252]. Significantly, not only has our work shown a reduced AMPK activity in cardiovascular impairment associated with early metabolic dysfunction involving PVAT inflammation [6], our results also demonstrated autophagy suppression as a possible contributor to the observed phenotype [111, 253]. Moreover, a lack of AMPK activity was implicated in AC hypertrophy [254]. As such, IF-mediated



SIRT1 activation could offer a mechanistic link for the observed positive changes in AT remodeling. However, it is important to note that studies on human subjects reported inconsistent results where some studies showed increased SIRT1 expression in AT following fasting [255], and others have reported no change [256]. These observations could be related to a lack of consistency in the fasting regimens employed and warrant further investigation.

Remarkably, regardless of the fasting regime, IF has been shown to be a strong inducer of WAT browning and increased expression of mitochondrial UCP1, which was linked to improved metabolic state [81, 233, 247, 257]. Indeed, this could be related to SIRT1 activation that was shown to increase UCP1 expression as mentioned previously [83]. Yet, data from mouse models, showed that IF induce browning in sWAT and VAT, via eosinophils infiltration, M2 macrophage polarization and anti-inflammatory cytokines production. Genetic ablation of the effect of these cytokines (IL-4,-5 and -13) abolished AT browning along with the observed improvement of AT inflammation and metabolic parameters [247]. Significantly, another aspect of mitochondrial function involves AMPK activity. Evidence suggests that fasting-mediated AMPK activity has a role in mitochondrial metabolism and homeostasis, where chronic activation of AMPK maintains the dynamic nature of mitochondrial networks together with their ability to interact with other organelles and increase fatty acid oxidation [258]. Indeed, the increased AMPK activity is consistent with the effect of IF on adiponectin production. A localized increase in adiponectin in AT, especially WAT, was achieved by IF even in the presence of HFD. These observations were consistent in both human and animal studies [226, 227, 233, 259, 260].

a. Therapeutic Fasting in Adipose Mediated Cardiovascular Diseases.

The positive impact of IF on AT is expected to ameliorate the diet mediated cardiovascular dysfunction. Indeed, the American heart association (AHA) included IF as one of the dietary measures to prevent CVDs. Based on human studies, AHA concluded that that IF, regardless of its effect on weight, improves lipid profile, lowers LDL and cholesterol and increases HDL, in addition to improving insulin sensitivity, indicated by reduced HOMA-IR, with no change in blood glucose level [228]. As well, human and animal studies indicated that IF reduced blood pressure [261-263] and heart rate [262]. Another study found that both 40% calorie restriction and alternate day fasting in rats reduced the low frequency component in the diastolic blood pressure variability, a marker of reduced sympathetic activity, and increased high frequency component in heart rate variability, which is reflective of the parasympathetic tone, both being indicative of positive modulation of cardiovascular state [264]. Specifically, in the context of early metabolic dysfunction, preliminary data indicate that not only did IF improve parasympathetic cardiac autonomic neuropathy, this was also associated with amelioration of PVAT inflammation [238]. Ramadan IF was found to increase HRV in healthy subjects [265]. Furthermore, IF improved endothelial and non-endothelial dependent vasorelaxation in healthy men [266]. Significantly, IF exerted a similar pattern in Wistar male rats, as it showed an improved aortic endothelial dependent relaxation [267]. Moreover, IF is found to prevent atherosclerotic state by promoting an anti-inflammatory response [268]. Noteworthy, prophylactic IF was found to be protective against tissue and neurological damage caused by ischemic stroke. It works mainly on reducing inflammatory cytokines (IL-1 $\beta$ , IL-6, TNF $\alpha$  among others), inflammasome activation in the stroke side of the brain and oxidative stress, while

increasing autophagy, mitophagy and neuroprotective proteins like; neurotrophic factors (BDNF and bFGF), heme oxygenase-1 (HO-1), UCP-2 and UCP-4 [269]. In this context, it was also found the fasting mediates its beneficial effects by increasing neuronal and glial SIRT-1 and P-AMPK [269].

The previous lines of evidence reaffirm the peculiar nature of adipose depots in responding to energy imbalance. Nevertheless, all of the above observations were reported in large WAT pools including subcutaneous, gonadal, and other visceral depots. To the best of our knowledge, there is no direct investigation of the effect of IF on PVAT in situations of metabolic dysfunction. As such, a systematic examination of the impact of IF on PVAT remodeling and inflammation in early metabolic dysfunction and its impact on cardiovascular impairment is warranted. While several parallels among that responses of different WAT pools to IF can be drawn, one must be cautious in extrapolating these findings to PVAT given the peculiar nature of this adipose pool. In this context, prolonged periods of reduced caloric intake, as in case of IF, might, in addition to the previously observed effects in other AT depots, exert further benefit by relieving the UCP1-mediated exacerbation of oxygen deficiency, and hence ameliorate the early inflammatory response [28].

Calorie restriction and weight loss reported positive results regarding diet induced PVAT dysfunction. As such, calorie restriction in rats and mice alleviated PVAT inflammation, ACs hypertrophy and restored its function [270, 271]. Significantly, structured efforts to investigate whether IF regimes positive cardio and metabolic outcomes are mediated by PVAT remodeling independent of other metabolic

factors are essential. Figure 1 summarizes the potential impact of IF on PVAT remodeling.

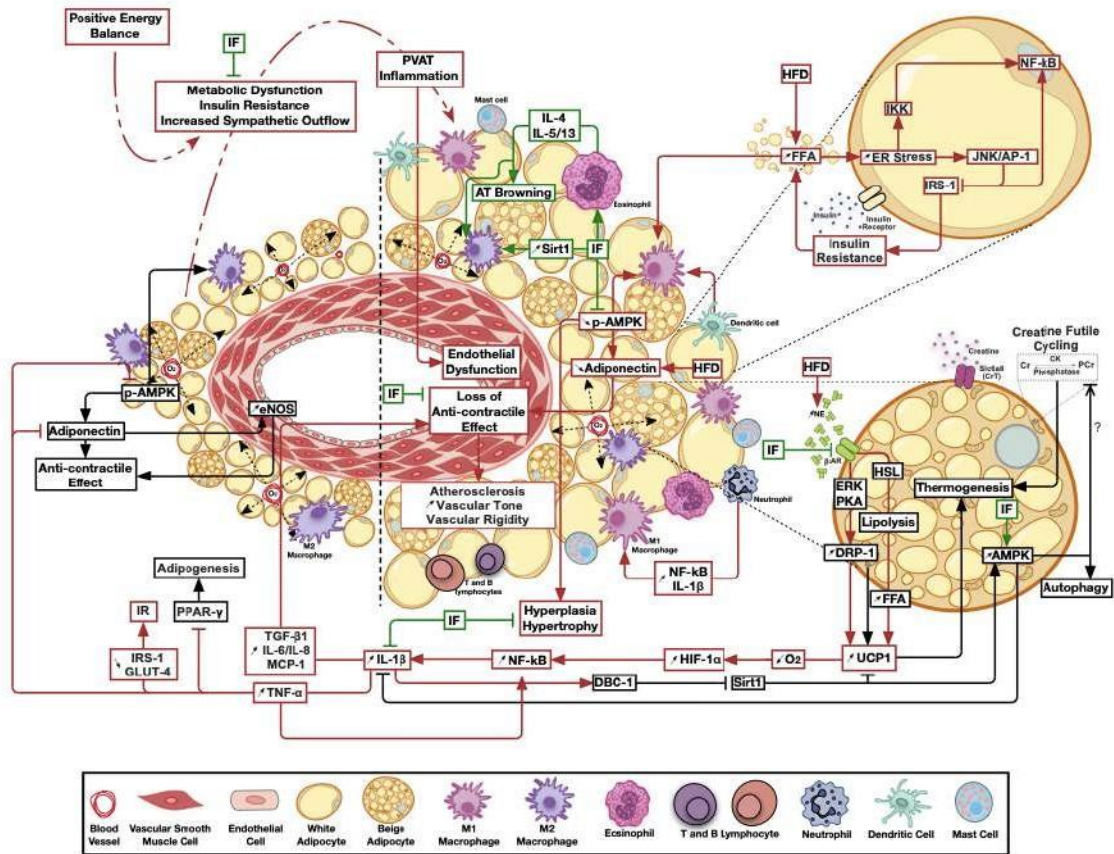


**Figure 1 The emerging ameliorative role of intermittent fasting on perivascular adipose tissue inflammation and thermogenesis.**

Calorie excess resulting in metabolic dysfunction triggers perivascular adipose tissue chronic low-grade inflammation, leading to the loss of its anticontractile effects and the subsequent negative paracrine modulation of vascular structure and function. Intermittent fasting ameliorates inflammatory, thermogenic and bioenergetic pathways favoring adipose tissue homeostasis. Pathways involved in adipose tissue homeostasis are shown in black, those activated by metabolic dysfunction in red, while those modulated by intermittent fasting in green arrows. AT, Adipose tissue; AMPK, AMP-activated protein kinase;  $\beta$ 3AR, Beta 3 adrenergic receptor; CK, Creatine kinase; Cr, Creatine; DBC-1, Deleted in bladder cancer protein 1; DRP-1, Dynamin related protein 1; eNOS, Endothelial nitric oxide synthase; ER, Endoplasmic reticulum; ERK, Extracellular signal-regulated kinase; FFA, Free fatty acids; HFD, High fat diet; HIF-1 $\alpha$ , Hypoxia-inducible factor 1-alpha; HSL, Hormone sensitive lipase; IF, Intermittent fasting; IKK, IK $\beta$  kinase; IL, Interleukin; IRS-1, insulin receptor substrate 1; JNK/AP-1, c-jun N-terminal kinase/activator protein 1; MCP-1, Monocyte Chemoattractant protein 1; NE, Norepinephrine; NF- $\kappa$ B, Nuclear factor kappa B; O<sub>2</sub>, Oxygen; PVAT,

Perivascular adipose tissue; PCr, Phosphocreatine; PKA, Protein kinase A; Sirt1, Sirtuin 1; TGF- $\beta$ 1, Transforming growth factor beta 1; TNF- $\alpha$ , Tumor necrosis factor alpha; UCP1, Uncoupling protein 1.

b. Sex Differences in Therapeutic Fasting Effect on Adipose and Cardiovascular Dysfunction

The evidence is slowly growing, and the conclusions are still debatable regarding sex-mediated therapeutic fasting outcomes. On one hand, some human and animal studies on obese subjects, did not report any differences between sexes in metabolic parameters in response to fasting regimens, such as insulin sensitivity, glucose tolerance, plasma lipid profile, blood pressure, adiposity, and TBW [272-274]. Indeed, in the absence of endogenous estrogen, IF was able to exert beneficial effects in female mice, even while being freely fed on HFD these mice had better weight loss, insulin sensitivity, glucose tolerance and general activity than the non-fasting counterparts[275]. On the other hand, some researchers detected the sex dimorphic effect on the mechanistic level, as even in the presence of HFD, IF in female mice reduced adipocytes differentiation and storage markers in WAT with and without exercise. While in males, markers of FA oxidation were increased only in IF with exercise. Of note, in both genders IF attenuated leptin level with and without exercise[273]. Additionally, fasting was linked to higher circulating levels of FFA in women than men, despite the absence of differences in lipolysis, this was attributed the higher fat mass in women, in addition to some differences of AT distribution in response to insulin induced antilipolytic effect, which is found to be more pronounced in women with lower sWAT rather than in men with upper sWAT adiposity[180]. Noteworthy, calorie restriction seems to have some sex related differences, as female

rats responded with a better conservation of energy, and more reduction in fat mass than males, mediated by reducing UCP1 expression and activity in female BAT only[276].

Sex dimorphic differences in IF outcomes are grossly studied and there is no doubt that IF regimes yield positive results in both sexes. Still the exact mechanism of how IF paradigms affect cardiovascular and metabolic outcomes related to HFD induced AT negative remodeling are still understudied. Especially, that each adipose depot behaves differently in response to positive caloric intake, plus their sensitivity to either caloric or time restricted feeding regimens most likely won't be alike. Hence, advanced understanding of how fasting routines mechanistically generate these positive findings in both sexes is crucial, which will help to customize these fasting interventions based on the metabolic and hormonal status of individuals.

## ***2. Inorganic Phosphate Supplementation and Cardiovascular Diseases.***

Based on the previous sections regarding AT dysfunction in CVDs, UCP1 overexpression was mostly perceived as a desired outcome of dietary and nondietary interventions in alleviating AT mediated CV and metabolic insults. However, conclusions concerning browning in PVAT were bewildering, as some indicated the downregulation of UCP1 in PVAT in response to excess dietary intake and high fat feeding, while other indicated the opposite.

Since our data consistently showed an increased UCP1 level in PVAT alongside ACs hypertrophy, we hypothesized that these two major modulations accelerated hypoxia in this pool, which in turn exaggerated the proinflammatory response and macrophage infiltration, leading to the observed early cardiovascular dysfunction in the prediabetic rats [6, 7, 222, 238, 253, 277, 278]. Plus, UCP1 overexpression is associated

with a state of energy inefficiency, which fuels obesity and increased adiposity [279]. Additionally, UCP1 was found to be activated by free fatty acids, as they disrupt membrane potential and exaggerate the proton leak across the inner mitochondrial membrane [18, 76, 280, 281], which are more abundant in the serum of obese hosts and the ones on HFD [282]. Thus, we believe that interfering UCP1 activity and expression in PVAT might have a positive modulatory effect in diet-induced early CV distress.

Interestingly, inorganic phosphate (Pi) was recently identified as a selective UCP1 inhibitor. UCP1 in BAT was found to be inhibited by Pi and purine nucleotides (adenine and guanine) increasing membrane potential, reducing respiration, and enhancing energy efficiency [280]. High dietary phosphate (Pd) intake has been viewed to be associated with metabolic and cardiovascular diseases. These concerns come from the increased intake of processed foods, where P is an important component of the preservatives and food additives [283], indicating the possible toxicity by Pd overload [284]. Since phosphate is mainly excreted thru urine, renal insults and vascular calcifications are very common in high P intake [284-288]. For instance, high serum P level was positively associated with wide range of cardiovascular and renal insults [289-292]. It was even associated with increased in-hospital mortality among patients with CKD and CVDs [293]. However, others reported that ED in chronic kidney disease (CKD) human and animal subjects was independent of serum P level, however it was dependent on the P loading in the myography chambers and its effect was mediated by disrupting NO pathway and reducing eNOS expression [294]. Low Pd intake was found to reduce CV risk in CKD patients, by reducing fibroblast growth factor-23 [295], which is associated with increased CV risk with and without CKD [288]. Thus, it was

suggested that Phosphate restrictions might be useful for vascular function and arterial contractility [296].

On the contrary, recent review indicated the importance of having balanced phosphate intake to ensure longevity and healthful aging [297]. Additionally, high phosphate intake was linked to some positive metabolic outcomes in human subjects without CKD, including reduced adiposity [298, 299], increased lipogenesis[299] , improved post prandial lipemia, glycemia, insulin level and sensitivity[300-302]. Moreover, low phosphate diet in mice was associated with increased hepatic lipids induced by high cholesterol diet[303]. Also it was suggested that low phosphate diets to be a contributor to the onset of obesity[304]. Low serum phosphate was also associated with metabolic syndrome in men[290, 305]. Moreover, it was suggested that the interplay between P level and ATP level and the use of P in cellular phosphorylation of enzymes and receptors, is the key to its beneficial effects[304].

Hence, the mechanism of which phosphate level affect cardiovascular state remains unclear. As the amount of ingested Pi is hard to be accurately measured, and mostly is being grossly estimated[287, 297], and the fact that P serum level is not directly associated with the high Pd intake, as the regulation of P homeostasis is complex and many hormones and modulators are involved, such as parathyroid hormone, calcium level and others [306, 307].

The detrimental cardiovascular outcomes of high Pi intake were mostly reported from patients with CKD which have altered homeostatic regulation of P. However, evidence on Pi supplementation form obese or metabolically challenged subjects, showed different outcomes, suggesting the possible beneficial role of Pi in exerting positive outcomes in early metabolic and cardiovascular dysfunction.





## CHAPTER II

### SPECIFIC AIMS

Cardiovascular diseases (CVDs) are the leading cause of premature mortality among Type 2 Diabetes Miletus (T2DM) patients [3, 308]. It is well accepted that cardiovascular dysfunction in T2DM patients starts with early metabolic distress[6], which is usually accompanied with low grade inflammation[309, 310]. This stage of early metabolic insult is usually linked to higher body mass index and higher intake of fat and sugar. However, some recent evidence suggest that even in the absence of the obese phenotype, low grade- inflammation is linked to early cardiovascular (CV) dysfunction [9] such as; cardiac autonomic imbalance, endothelial dysfunction and elevated blood pressure[116, 222].

A series of investigations on a metabolically challenged Sprague-Dawley rat model at our laboratory showed that early CV damage was detected in even the absence of systemic inflammation, but rather with a confined inflammation in certain depots of adipose tissue (AT)[4, 7, 166, 311], more specifically, the tissue surrounding the thoracic aorta, which is referred to as thoracic perivascular AT (PVAT) [7, 45, 222]. Our findings showed that PVAT is one of the first pools to be affected by diet induced metabolic stress[7, 222]. Figure 2.1 summarizes our previous findings on PVAT inflammation. However, data on PVAT are mostly based on studies using male animals, henceforth, disregarding the possible role of sex in PVAT morphology, function, and reactivity to overnutrition.

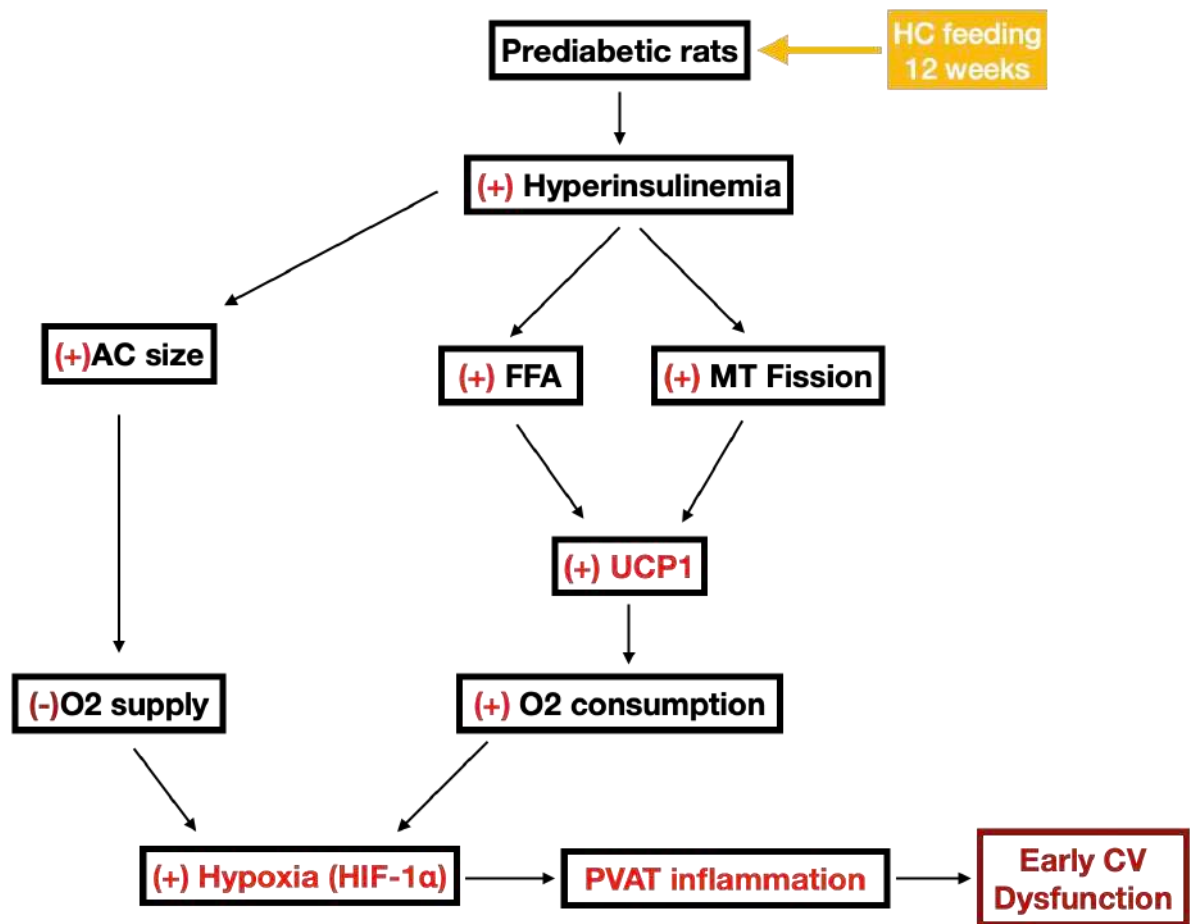


**Figure 2. Summary of previous data on PVAT dysfunction after twelve weeks of HC feeding in male rats.**

Twelve weeks of HC feeding in male rats will lead to prediabetes, evident by hyperinsulinemia and normoglycemia, which were accompanied by negative modulations of PVAT; hypertrophied adipocytes, mitochondrial dysfunction, and upregulation of UCP1, both adipocytes increased size and UCP1 will lead to state of hypoxia by reducing the oxygen supply and increasing the demand respectively, hypoxia will eventually provoke inflammation, PVAT inflammation will lead to a compromised cardiovascular function.

To our knowledge no pharmacological or non-pharmacological solutions were proposed to target PVAT inflammation in early metabolic distress and cardiovascular insult. Such interventions would be especially important to individuals in the compensation stage of diabetes prognosis, as the CV damage commences without any

overt hyperglycemia. Hence, such interventions would be of great value reducing the ensuing morbidity, mortality, and economic burden.

**2.1 Main Objective:** To investigate the sex-dependent differences in metabolic stress induced PVAT inflammation and cardiovascular dysfunction and examine impact of dietary interventions on cardiovascular dysfunction mediated through PVAT inflammation in a prediabetic rat model.

**2.2 Hypothesis:** With females being less prone to CVDs compared to males, they will show less PVAT involvement in response to the same metabolic stress patterns inducing PVAT inflammation in their male counterparts, Figure 3 . Moreover, simple dietary interventions encompassing therapeutic fasting and dietary phosphate supplementation will improve PVAT inflammation and preclude the early stages of cardiovascular dysfunction in metabolic disease.

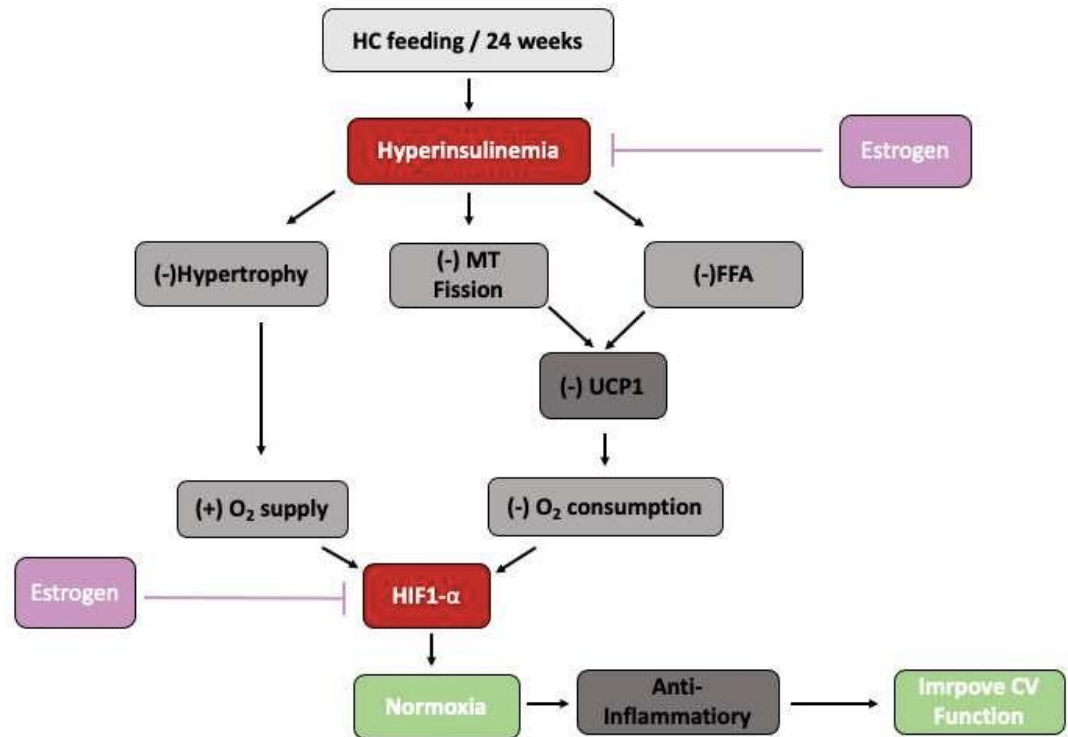


**Figure 3. Graphical presentation of the hypothesis.**

Twenty-four weeks of HC feeding in male rats will lead to prediabetes, while females will be protected from HC-induced prediabetes and cardiovascular dysfunction, as estrogen will protect from PVAT dysfunction by preserving insulin sensitivity which will prevent hypertrophy and promote better mitochondrial function, it also will target HIF-1 $\alpha$  which will prevent hypoxia and its downstream inflammatory response.

### 2.3 Specific Aims:

**2.3.1 To examine the effect of Phosphate (P) supplementation as a selective inhibitor of UCP1 on PVAT inflammation and CV function in metabolically challenged rats.**

**2.3.2 To assess sex differences in PVAT involvement in CV sensitivity to early metabolic challenge**

**2.3.2.a** Investigate the alterations in body composition and metabolic parameters in response to mild hypercaloric (HC) feeding in males vs females.

**2.3.2.b** Examine the development of PVAT inflammation in response to HC feeding.

**2.3.2.c** Delineate the differences in development of CV and autonomic dysfunction in response to HC feeding.

**2.3.3 To evaluate the impact of therapeutic fasting (TF) on cardiovascular dysfunction in early metabolic distress in male and female rats.**

**2.3.3.a** Investigate the alteration in body composition and metabolic parameters in response to TF.

**2.3.3.b** Examine PVAT morphological and metabolic changes in response to TF.

**2.3.3.c** Assess the Impact of TF on cardiovascular dysfunction.

**2.3.3.d** Study the browning of other adipose depots in response to TF.

# CHAPTER III

## METHODS AND MATERIALS

### A. Animal Model

#### 1. *Ethical approval and experimental design.*

All animal experiments were conducted in accordance with an experimental protocol approved by our institutional Animal Care and Use Committee in complying with the National Institutes of Health Guide for the Care and Use of Laboratory Animals, 8<sup>th</sup> edition [312].

- a. Five-week-old male Sprague-Dawley rats weighing 180-200 g were divided into four groups according to the diet they were kept on. Group 1 received a control diet (NC: 0.75) offering 3.8 Kcal/g with 0.75 mg free phosphorous per Kcal. The control diet composition (AIN-93 G, Table 1) and Pi content were based on the American Institute of Nutrition (AIN) recommendation for adult rat maintenance diets [313]. Group 2 was fed a mild hypercaloric (HC) diet offering 4.5 Kcal/g with 0.375 mg free phosphorous per Kcal (HC: 0.375). The HC diet composition was based on our previous studies showing that a 12-week feeding of HC diet, offering ~39% calories from fat with a 5% saturated fat content by weight, led to a non-obese prediabetic phenotype [7, 111, 253, 314, 315]. Animals were fed for a total of twelve weeks. Two additional groups were included. The first received HC diet with 0.375 mg phosphorous/Kcal for 10 weeks and then given HC diet with 1.5 mg phosphorous/Kcal (HC: +1.5). The second group received a control diet with low phosphorous content (0.375 mg/Kcal) for twelve weeks (NC: 0.375). Littermates were ordered in batches of six, one rat per treatment group. Upon receipt, rats were

caged individually by the animal facility technicians in cages given pre-assigned numbers randomly corresponding to the six treatment groups (each consisting of 6 rats). Animals were kept at controlled temperature and humidity and a 12-hour light/dark cycle. Daily food intake was recorded, and calorie intake was calculated.

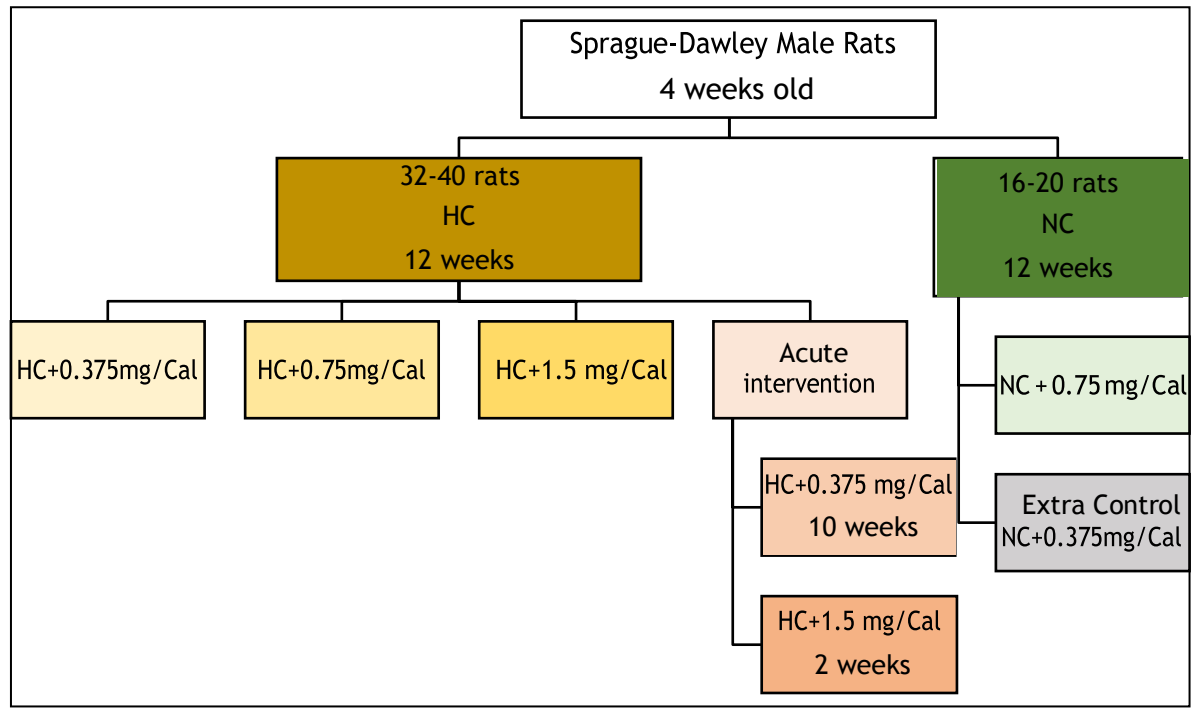


**Figure 4. Sprague-dawley male rats fed for twelve weeks on either control or hypercaloric diet with different levels of inorganic phosphate (mg of Pi/Cal).**

- b. Female and male Sprague-Dawley rats weighing 180-200 g were divided into three groups according to the diet they were kept on for twenty-four weeks: NC, HC and HC with 12 weeks of 12 hours daily fasting. Therapeutic Fasting is referred to time restricted feeding for 12 hours daily during the dark period (7pm:7am), during which the rats will have no access to food but free access to water. The rats will be fed freely on HC during the light period. The timeline and different groups are explained in Figure 5 . The term TF will be used instead of intermittent fasting for several reasons, first, the rats will have free access to water during the fasting hours,



and free access to HC during the feeding hours with no calorie restriction. Plus, the aim of this regimen is not weight loss, but rather improved adiposity. Second, the regimen we will adopt is 12 hours daily fasting, which will be introduced for 12 weeks after establishing the metabolic insult. Hence the purpose of this regimen is to be translational as an early intervention for metabolic stress in prediabetes. This TF regimen is applicable and requires minimal changes in dietary intake, which is the main challenge in lifestyle modifications in prediabetic individuals.

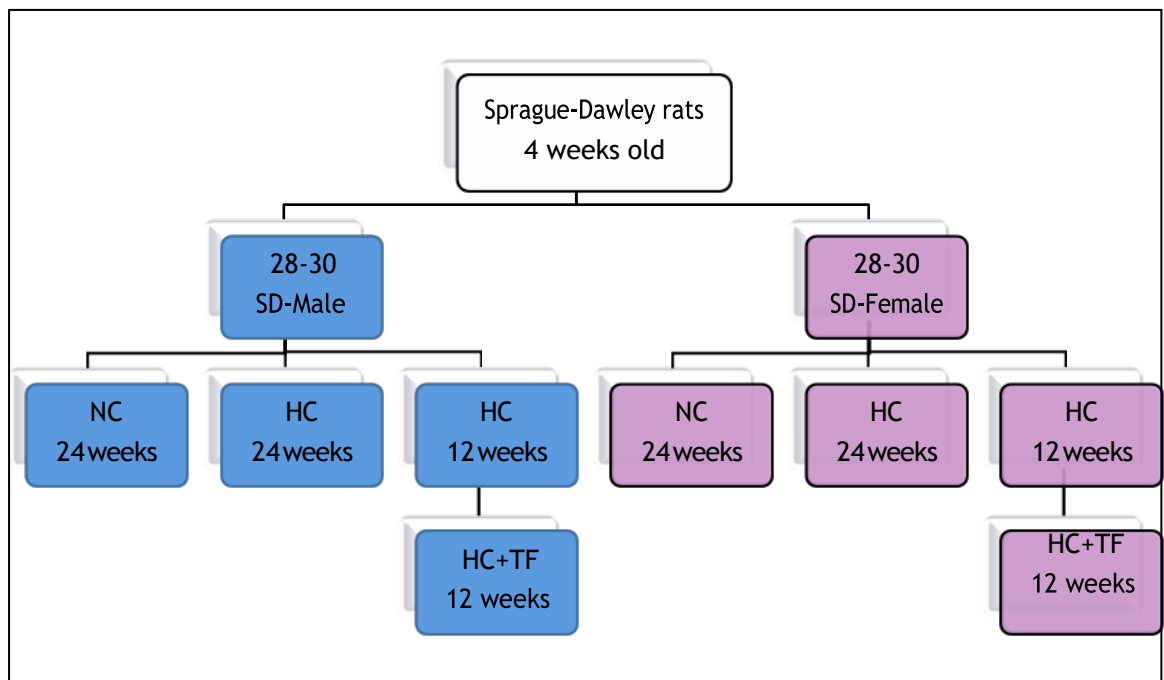


**Figure 5. Male and Female Sprague-dawley rats assigned for twenty-four weeks on control diet, hypercaloric diet and hypercaloric diet and therapeutic fasting.**

- c. Another batch of female rats were included, either fed on NC or HC for 24 weeks, and on at week 12 bilateral ovariectomy was performed thru a 2 cm dorsal incision, after anesthetizing the animals. Then they either continue HC and NC for another 12 weeks without treatment or with  $17\beta$ -estradiol (E2) 2.8  $\mu\text{g}/100$  gm of body weight,

an additional group was added to the HC OVX arm, 12 weeks of the same fasting regimen explained above (Fig 6).

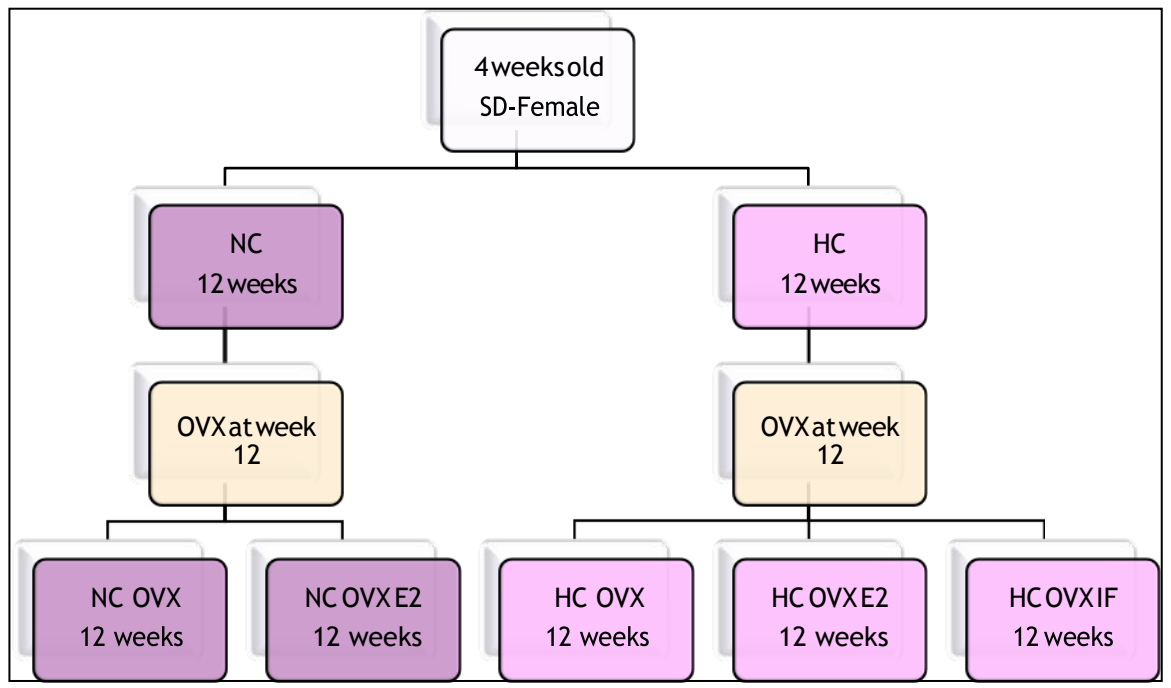


**Figure 6. Female Sprague-dawley rats with bilateral ovariectomy fed for twenty-four weeks fed on normal chow or hypercaloric diet with or without 17 beta-estradiol (E2) treatment.**

## **2. Diet.**

A loss of 50% of the Pi content was assumed in the previous studies due to nutrient displacement during preparation. The two additional groups were fed HC diet with phosphorous content of 0.75 (HC: 0.75) and 1.5 mg/Kcal (HC: 1.5), which are equal to and twice as much as the AIN recommended content. Diets were prepared in house using Pi free purified diet mix, then different amounts of potassium Phosphate were added to each diet to reach the desired phosphorous levels. Diet ingredients including

casein, L-methionine, cellulose, mineral mix (AIN-93G MX), Pi-free mineral mix (AIN-93G phosphorus free), vitamin mix (AIN-93VX), and potassium Phosphate monobasic were obtained from (Dyets Inc., Bethlehem, Pennsylvania, USA). Detailed diet composition is shown in Table 1.

**Table 1. Diet composition analysis of control and hypercaloric diet, presented in calorie percentage.**

<b>Diet</b>	<b>Cal/g</b>	<b>Carbohydrate (%)</b>	<b>Fat (%)</b>	<b>Protein (%)</b>	<b>Phosphate (mg/Cal)</b>
<b>NC</b>	4.6	53%	23.5%	23.5%	0.75
<b>HC</b>	5.15	*47%	**40%	13%	0.37

\*15.5% of calories from fructose

\*\*26.2% of calories from saturated fatty acids

## **B. *In-vivo* and *ex-vivo* techniques**

### **1. *Noninvasive blood pressure measurement.***

Non-invasive blood pressure (BP) was measured using a CODA tail-cuff High Throughput Monitor (Kent Scientific, Torrington, CT) at *weeks 0, 8, 9, 10, 11, and 12* [6, 277].

## ***2. Echocardiography.***

To assess heart structure and function echocardiography along the parasternal long axis M- and B-modes was done on *weeks 0,4, 8, 10, and 12* using SonixTouch Q+ ultrasound (BK ultrasound, Peabody, MA)[277].

## ***3. Pressure myography.***

Pressure myography experiments on middle cerebral arterioles were performed as described previously [316]. The intravascular pressure was gradually raised in a series of steps to 10, 20, 40, 60, 80, 100, 120, 140 mm Hg. The outer diameter of the vessel was measured at each pressure point. The pressure was then dropped back to 10 mm Hg and the vessel was washed and kept in a calcium-free buffer containing (NaCl 130 mM, KCl 4 mM, MgSO<sub>4</sub>.7H<sub>2</sub>O 1.2 mM, NaHCO<sub>3</sub> 4 mM, HEPES 10 mM, KH<sub>2</sub>PO<sub>4</sub> 1.18 mM, Glucose 6 mM, EDTA 0.03 mM, EGTA 2 mM, pH 7.4) and the ramp was repeated. Active tone was calculated as the difference in the outer diameter of the middle cerebral artery when in calcium-containing and calcium-free buffer at the respective pressure points.

## ***4. Nuclear Magnetic Resonance.***

Animals were weighed regularly, and body composition was determined using an LF10 Minispec Nuclear Magnetic Resonance (NMR) machine (Bruker, MA, USA). Different tissue densities were detected to measure fat:lean ratio. The values obtained from each rat were compared to a standardized, calibrated rat.

### **5. Blood chemistry parameters.**

Random blood glucose levels (RBG) at *weeks 0, 4, 8 and 10 and* fasting blood glucose levels (FBG) were measured after 6-8 hours of fasting at weeks 4, 8, 10 and on the day of sacrificing the animals were measured by lateral tail vein puncture, using an Accu-Chek glucometer (Roche Diagnostics, Basel, Switzerland). On the day of euthanization, 6-mL blood samples were obtained. Rat serum levels of Adiponectin, Leptin and insulin were measured using ELISA kits according to the manufacturer's protocol (Thermo Fisher Scientific, Waltham, MA). Serum lipid profile including triglycerides, total cholesterol, HDL and LDL, were measured using Vitros 350 chemistry system (Ortho-clinical diagnostic, Johnson&Johnson, New York, USA).

### **6. Invasive hemodynamic recordings.**

At the end of twelve weeks of feeding, anesthetized rats were instrumented with catheters inserted in the carotid artery and the jugular vein for invasive hemodynamic assessment as described previously [111]. Briefly, mean arterial pressure (MAP) and heart rate (HR) were measured through the carotid artery catheter connected to a Millar pressure transducer to measure. Data acquisition was performed by PowerLab (AD Instruments Ltd, Dunedin, New Zealand) and recorded using LabChart Pro 8 (AD Instruments Ltd., Dunedin, New Zealand) software. After a 45-minute stabilization period, baroreceptor sensitivity (BRS) was assessed by the vasoactive method as previously described [317]. Increasing doses of phenylephrine (PE, 0.25, 0.5, 0.75, 1, 2  $\mu\text{g}$ ) and sodium nitroprusside (SNP, 0.5, 1, 2, 4, 8  $\mu\text{g}$ ) were injected into the jugular vein at five-minute intervals, which were enough for MAP and HR to return to baseline values. Peak changes in mean arterial pressure ( $\Delta\text{MAP}$ ) and heart rate ( $\Delta\text{HR}$ ) were

recorded.  $\Delta$ HR was plotted as a function of  $\Delta$ MAP in each treatment group, and the mean slope of the linear regression of  $\Delta$ HR vs.  $\Delta$ MAP together with its confidence interval and SEM were calculated using GraphPad Prism software to represent baroreflex sensitivity and compared among groups. The maximal rate of rise of ventricular pressure ( $dP/dt_{\max}$ ), indicative of left ventricular function, was extracted from the LabChart recording.

### **C. Molecular and *in-vitro* techniques.**

#### ***1. Histopathology and immunohistochemistry.***

Serial sectioning and staining of formalin-fixed heart mid-section, brainstem, aortic segments, renal cortices, PVAT, epididymal and infra-scapular adipose were performed simultaneously for accurate comparison as previously described [314]. Hematoxylin & Eosin (H&E) staining was used for gross examination of cardiac and aortic tissue structure and to compare adipocyte size in different adipose depots across treatments. Medial thickness was measured in aortic sections, while inter-fibrillar edema as indicated by myocardial fiber separation in the papillary muscle, was considered indicative of possible focal ischemic injury [318]. Masson's trichrome staining was used to assess connective tissue fiber deposition in heart and aorta. Renal cortical sections were stained with periodic acid Schiff (PAS) stain for the examination of glomerular and mesangial matrix area alterations as previously described [319]. Mesangial matrix index was calculated as the ratio of the mesangial area to the glomerular area. In order to evaluate calcium deposition in rat kidneys, the Von Kossa stain was used as previously described [320]. Dihydroethidium (DHE) staining was performed on cryosections to demonstrate reactive oxygen species (ROS) load.

Fluorescent images were obtained through Alexa Fluor 568 filter for the DHE red fluorescence. In vascular tissue, the red fluorescence was measured against the green collagen autofluorescence obtained through the Alexa Fluor 488 filter.

Immunohistochemical detection of CD68 in the heart and IBA1 in brainstem was performed using 1:100 and 1:1000 concentrations of rabbit anti-CD68 and rabbit anti-IBA1, respectively (Abcam, Cambridge, UK), and visualized using Novolink Polymer Detection Kit (Leica Biosystems, Buffalo Grove, IL) according to the manufacturer's protocol. Control experiments were performed by omitting primary antibodies and using rabbit IgG controls. Images were taken using OLYMPUS CX41 light microscope (Olympus, Shinjuku, Tokyo, Japan). In each representative slide, DHE fluorescence or trichrome staining was semi-automatically quantified in 20 fields and expressed as a percentage of staining of total surface area, and the results from all fields were averaged. H&E was used to assess adipocyte size and papillary edema measured by ImageJ. At least 10 adipocytes were measured from five random areas in the slide in question and total interfibrillar space was calculated from heart sections. Quantification was performed by a blinded assessor via isolation and quantification of the staining intensity using ImageJ software and normalization to the tissue area in each slide.

## ***2. Western blotting***

Experiments were carried out as described previously [316, 321]. PVAT, epididymal and infra-scapular adipose tissue samples were homogenized on ice, and the protein extracts were separated by SDS-polyacrylamide gel electrophoresis. Proteins were then blotted to nitrocellulose membranes and were incubated in primary antibodies (1:500 for rabbit polyclonal anti-IL-1 $\beta$ , 1:1000 for rabbit monoclonal anti-GAPDH,

rabbit polyclonal anti-hypoxia inducible factor 1  $\alpha$  (HIF1- $\alpha$ ), Abcam, Cambridge, UK, and rabbit polyclonal anti-uncoupling protein 1 (UCP1), Cellsignaling, Danvers, MA) overnight at 4°C. Membranes were then washed with 0.02% TBST (Tris-buffered saline with 0.1% Tween 20) and incubated for 1 hour at room temperature in 1:40,000 biotinylated conjugated goat anti-rabbit Ig. Membranes were then washed and incubated for 30 minutes at room temperature with 1:200,000 HRP-conjugated streptavidin (Abcam, Cambridge, UK). After two washes with 0.02% TBST (5min) and two washes with TBS (5 min), the blots were exposed to Clarity Western ECL substrate (BioRad, Hercules, California) for 5 min and then detected by Chemidoc imaging system (BioRad, Hercules, CA). Densitometric analysis of the protein bands was performed using ImageJ software. Measurements were normalized to the density of GAPDH.

### ***3. Fluorescence activated cell sorting (FACS).***

Stromal vascular cells were isolated from freshly dissected PVAT as described previously [322]. CD45/CD68/CD86 staining was used to identify M1 polarized macrophages, while M2 macrophages were identified by CD45/CD68/CD163 staining [323]. An aliquot of the stromal fraction containing  $10^6$  cells was incubated in FACS buffer with DAPI (1:100), 1:50 APC-Cy780-conjugated anti-CD45, 1:10 PE-conjugated anti-CD68, 1:125 FITC-conjugated anti-CD86 (Thermo Fisher Scientific, Waltham, MA), and 1:200 APC647-conjugated anti-CD163 (Bioss Antibodies, Woburn, MA) on ice for 30 minutes in the dark. Cells were gently washed for three times and resuspended in FACS buffer. Stained cells were counted using a BD FACSAria Cell Sorter (BD Biosciences, San Jose, CA) and M1/M2 ratio was determined. Antibody-



beads mixtures, fluorophore-conjugated isotypes, and unstained cells were used to set compensation and gating.

### ***3. In-vitro experiments.***

The induction of adipogenic differentiation of human bone marrow-derived mesenchymal stem cells (BMMSCs) was done as previously described with slight modification [324]. Briefly, BMMSCs were seeded in 6 well plates at a density of 50,000 cells/well in Dulbecco's Modified Eagle's Medium – low glucose (DMEM-LG) containing 10% fetal bovine serum and 1% penicillin/streptomycin and were allowed to reach 80-90% confluency before the induction of adipogenic differentiation. Cells were washed twice with phosphate-buffered saline and media was then replaced with adipogenic induction medium (AIM) containing 0.1 mM 3-isobutyl-1-methylxanthine (IBMX), 1  $\mu$ M dexamethasone, 2  $\mu$ M pioglitazone and 40mIU/L insulin for ten days. Adipogenic differentiation was followed visually under the microscope through the formation of intracellular lipid droplets. AIM was then replaced with maintenance media containing 40mIU/L insulin and 2  $\mu$ M pioglitazone for five days. Following adipogenic differentiation, adipocytes were incubated with either DMEM-LG (1mmol/L Pi) or phosphate-supplemented DMEM-LG (4mmol/L Pi) for 24 hours. The 4-fold increase was meant to simulate the increase of Pi intake in HC diet from 0.375 mg/Kcal to 1.5 mg/Kcal used in the *in vivo* experiment. Thereafter, cells were either incubated with DMEM-LG or DMEM-LG containing 1.6 mM palmitic acid and 40mIU/L insulin for 24 hours in the continued presence of 4 mmol/L Pi. At this stage, adipocytes were cocultured with THP-1 human leukemic monocytes (primarily cultured in RPMI containing 10% fetal bovine serum and 1% penicillin/streptomycin) at a density of

50,000 cells/well for an extra 24 hours, following which cells were lysed and protein was extracted as described below. In other experiments, cells were trypsinized, stained with anti-CD45 and anti-CD86, and subjected to FACS as described above. For the THP-1 adhesion assay, adipocytes were seeded into a 96-well plate at a concentration of 5000 cells/well and were left to attach for 24 hours and then exposed to either normal medium or the medium containing 1.6 mM palmitic acid and 40mIU/L insulin. THP-1 cells labelled with Hoescht Molecular Probes stain (Nuc Blue, Sigma) were added at a density of 20,000 cells per well into each well. After 30 minutes incubation time at 37°C, the THP-1 containing medium was aspirated and the wells washed twice with PBS 1X (Sigma). Images of the adherent cells were later taken using a Zeiss Axio microscope at the same excitation/emission spectra for monocytes, and superimposed on brightfield images in order to visualize the non-labelled cells.



## CHAPTER IV

### RESULTS

#### **A. Sexual Dimorphism of Metabolic and Cardiovascular Dysfunction in Prediabetic Rat Model.**

##### ***1. Metabolic and gross hemodynamic outcomes after 24 weeks of HC feeding in male and female rats.***

The metabolic parameters presented in this section reveal a new aspect of our prediabetic model establishing the sex differences in the prediabetes metabolic phenotype driven by HC feeding. After 24 weeks of HC feeding and consistent with our previous findings, cumulative energy intake was higher among the HC arm in male rats. A similar pattern was observed in females on HC diet, however, they had a lower total caloric intake compared to males (Fig 7. A). Although total body weight did not differ between control and HC fed female and male rats, fat to lean ratio (F/L) was consistently higher in the HC group in both sexes indicating an increased adiposity compared to control males, and no intragroup difference was detected in females (Fig 7. B and C). The energy imbalance between total caloric intake and total body weight in HC arms can be explained by the altered metabolic efficiency (ME). Furthermore, both arms of females had lower ME compared to males (Fig 7. D).

As for the blood glucose homeostasis, normoglycemia and hyperinsulinemia were observed in HC fed male rats only, however, intact females seemed to maintain normal glucose and insulin levels despite HC feeding (Fig 7. E and F). HOMA-IR was only elevated in HC males. As such, twenty-four weeks of HC feeding did not seem to induce prediabetes in female rats.

As for the non-invasive hemodynamic measurements, on one hand, SPB seemed to be affected by HC feeding only in males. Surprisingly, in control females SPB was higher than their male counterparts (Fig 7. G). On the other hand, left ventricle ejection fraction did not change in response to HC feeding in both sexes (Fig 7. H).

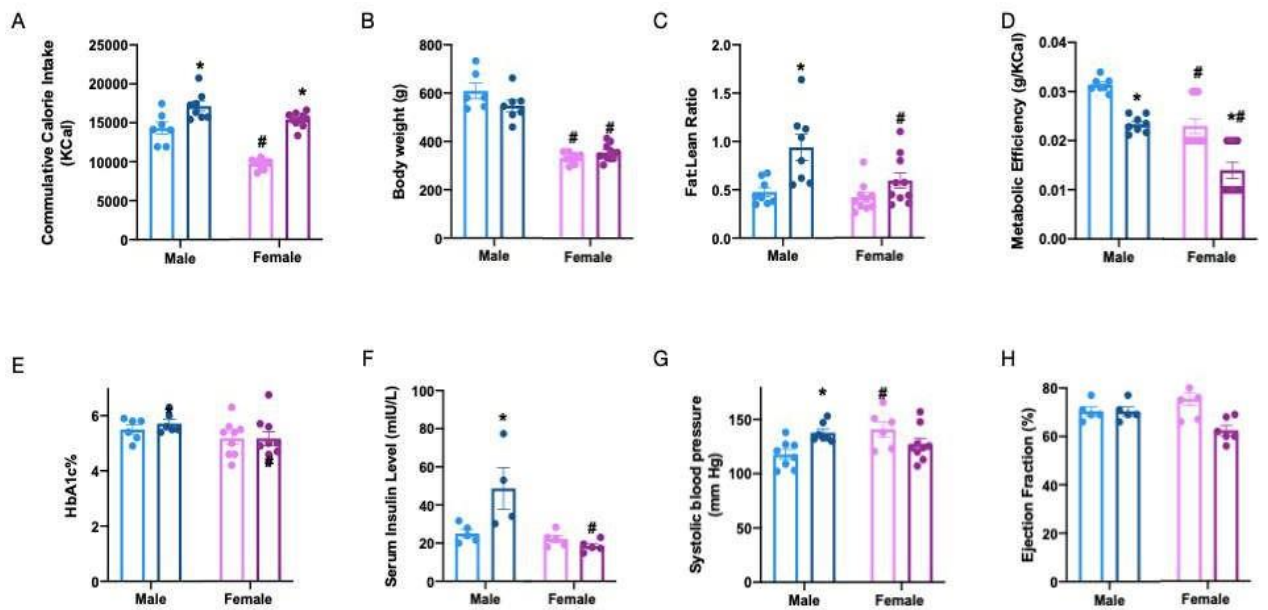


**Figure 7. Metabolic and gross hemodynamic impact of 24 weeks HC feeding in male and female rats.**

After twenty-four weeks on either HC or NC several important metabolic and cardiovascular parameters were assessed; cumulative calorie consumption (A) body weight (B), fat:lean ratio (C) metabolic efficiency (D), glycosylated hemoglobin A1c level (E), and fasting insulin level (F) were tested on serum sample on the day of the sacrifice, systolic blood pressure(G), and Ejection fraction (H)). The effects of HC feeding during the full twenty-four duration are depicted and compared to rats receiving normal chow (NC). Results shown are mean  $\pm$  SEM of observations from six different rats per group. Statistical significance was tested by two-way ANOVA followed by Tukey *post hoc* test. \* denotes a *P*-value < 0.05 vs. NC in each sex, while # denotes a *P*-value < 0.05 vs. the corresponding male group.

## ***2. Sexual dimorphism in HC-induced adipose tissue negative remodeling.***

Our previous work showed consistent PVAT negative remodeling in response to 12 weeks of HC feeding in male rats. Here, our data presented similar results in male rats. Twenty-four weeks of HC feeding seemed to promote ACs hypertrophy in PVAT of male rats, whereas in intact females it did not (Fig 8. A). Moreover, HC feeding in males provoked negative remodeling of PVAT, as ACs hypertrophy was accompanied with molecular changes with increased MT fission indicated by an increase in P-ser616 DRP1, UCP1 overexpression, concurrently with an increase in marker of inflammation and hypoxia, IL-1 $\beta$  and HIF1- $\alpha$ , respectively (Fig 9. B). On the contrary, females were protected from HC induced PVAT negative remodeling, except for the increase in UCP1 expression (Fig 9. F).

Our previous work confirmed the unique response of each depot to the same energy stimulus. Indeed, unlike PVAT, hypertrophy was observed in BAT in both sexes, while the size of GAT ACs was not affected (Fig 8. B). Although BAT had mitochondrial fission and increased expression of UCP1, neither hypoxia nor inflammation were detected in males (Fig 9. C). While in females no molecular changes were observed (Fig 9. G). Surprisingly, both epididymal and periovarian depots were less sensitive to 24 weeks of HC feeding (Fig 8. C and Fig 9. D&H).

Of note and in accordance with our previous findings, no markers of inflammatory spill into the circulation were detected in both male and female rats, indicated by serum IL-1  $\beta$  levels (Fig 9. D). Confirming the confined inflammation in PVAT of male fed on HC diet.

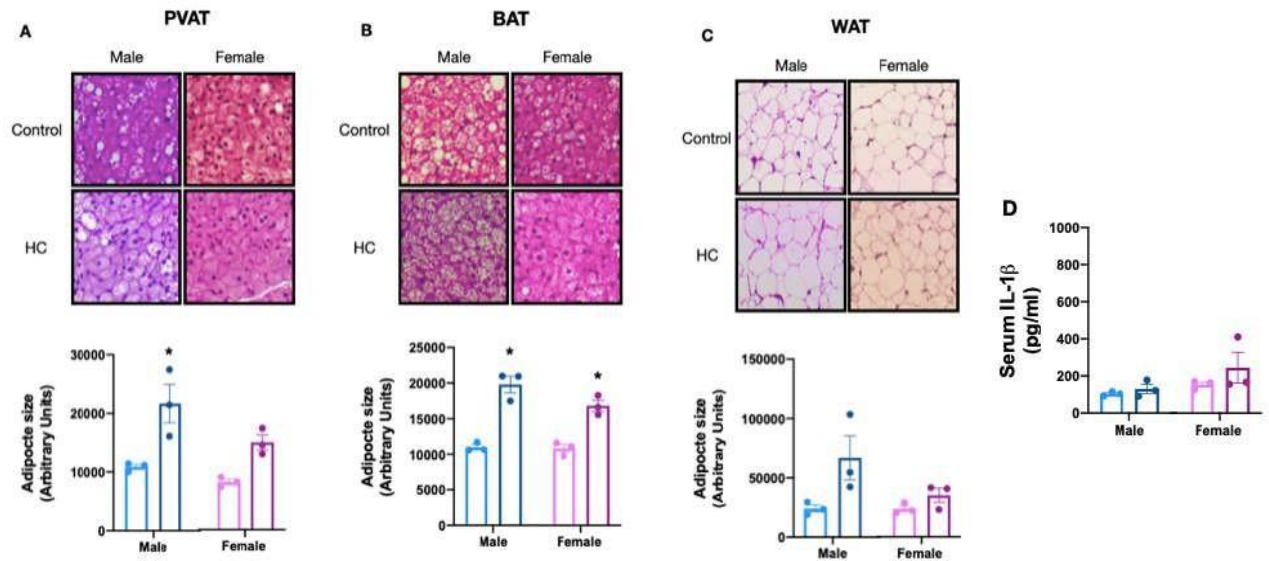


**Figure 8. Sex differences of the impact of twenty-four weeks of HC feeding on adipocytes size of different depots.**

Representative micrographs (top) and summary of the quantified data (bottom) showing the adipocyte size in H&E stained PVAT (A), infra-scapular BAT (B) and Gonadal WAT (epididymal in males and periovarian in females, C) sections, Serum IL-1 $\beta$  measured (D). Scale bars are 25  $\mu$ m, summary data for micrographs are obtained from nine sections from three different rats per group. Results shown are mean  $\pm$  SEM. Statistical significance was tested by one-way ANOVA followed by Tukey multiple comparisons test for A-F, and two-way ANOVA followed by Tukey *post hoc* test for G. \* denotes a *P*-value < 0.05 vs. NC-fed rat values.

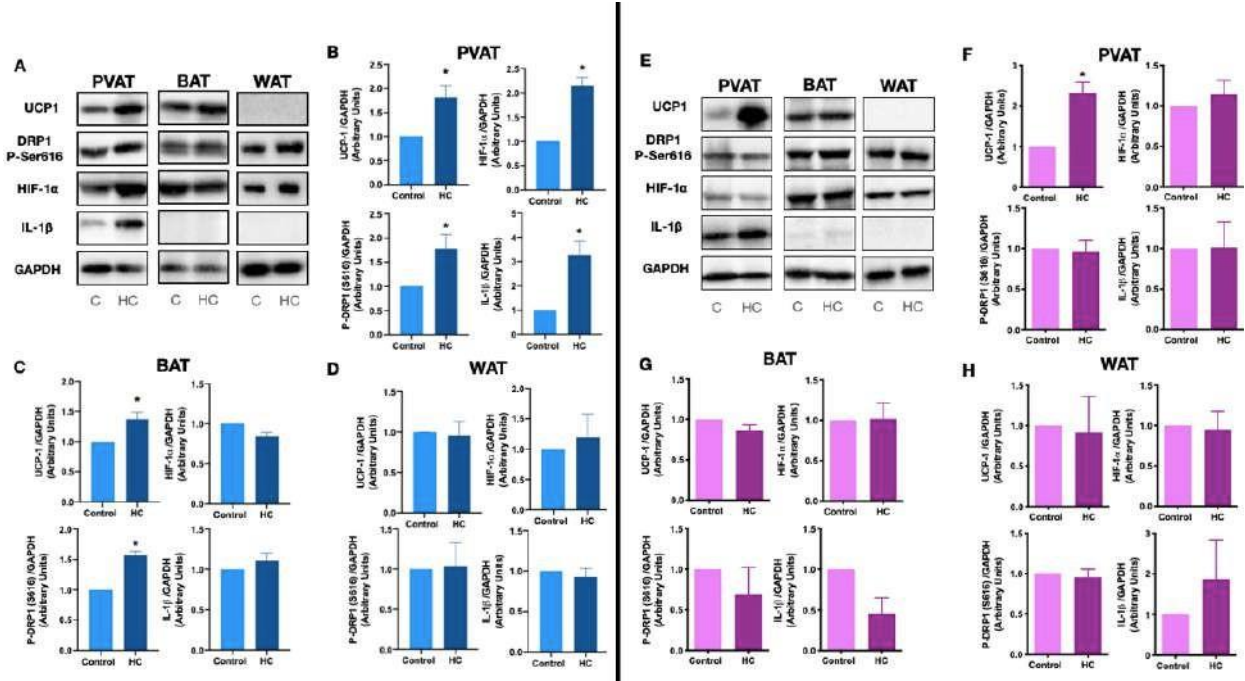


**Figure 9. Sex differential molecular manifestations of twenty-four weeks of HC feeding on adipose tissue remodeling.**

A & E Representative western blotting in males and females respectively, and summary of the quantified data for PVAT (B & F) showing the expression levels of UCP1 (upper left), HIF1- $\alpha$  (upper right), P-DRP1(ser616) (lower left) and IL-1 $\beta$  (lower right), in response to HC and NC feeding, same parameters were assessed for infra-scapular BAT (C & G) and Gonadal WAT (epididymal in males and periovarian in females , D & H respectively). The blots shown are representatives of experiments on tissues from three different sets of rats. Results shown are mean  $\pm$  SEM. Statistical significance was tested by two-way ANOVA followed by Tukey multiple comparisons test for A-F, and two-way ANOVA followed by Sidak *post hoc* test for G. \* denotes a  $P$ -value  $< 0.05$  vs. NC-fed rat values.

### 3. Sex differences in HC diet induced Cardiovascular dysfunction in vivo and in ex-vivo settings.

In line with the literature and as expected, early signs of cardiovascular dysfunction were only detected in HC fed males, as the recordings of invasive hemodynamics showed a dose-dependent blunted bradycardic response and increased pressor effect to PE (Fig 10. B&C), indicating an impaired parasympathetic regulation of BP, and altered



baroreceptor sensitivity (Fig 10. E). However, the tachycardiac response to different doses of SNP did not seem to be different between HC and NC fed males, which presents the cardio-regulatory autonomic imbalance, which is a manifestation of the subclinical phase of CAN[107]. On the contrary, females regardless of the diet did not seem to develop any sign of autonomic dysfunction or imbalance (Fig 11).

Additionally, ex-vivo functional testing of isolated aortic rings showed that the vasopressor effect of different concentrations of PE was not the same between males and females. As HC provoked increased sensitivity to PE in males, indicated by the shifting of concentration-response curve to the right (Fig 12. C). Interestingly, in females both arms had lower EC50 for PE compared to control males (Fig 12. E).

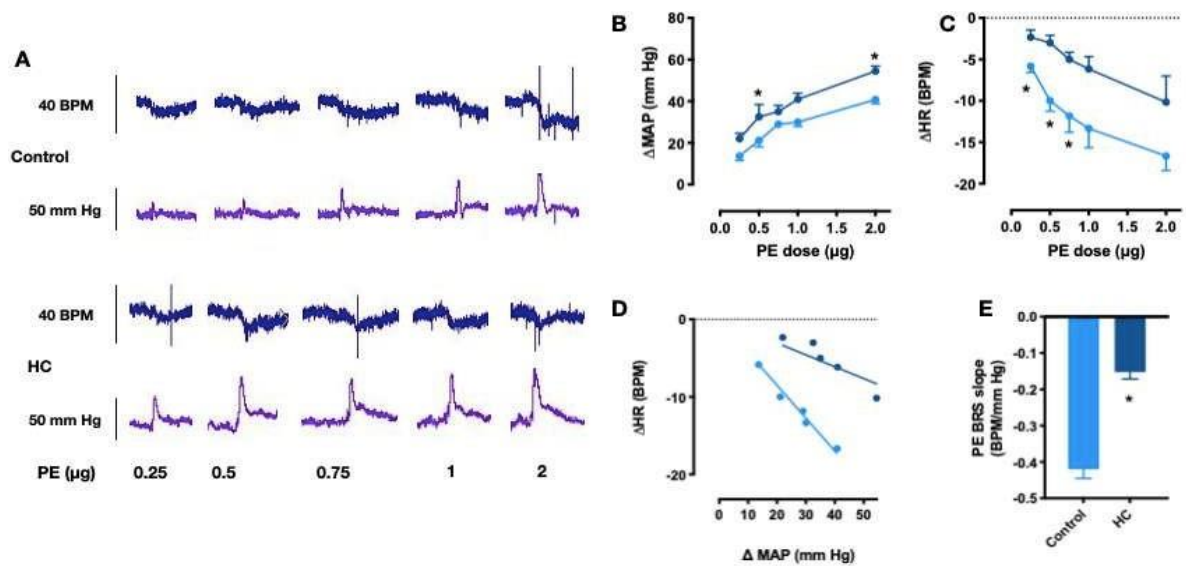


**Figure 10. Cardiac autonomic modulation by HC feeding in male rats.**

A, Representative tracings of pressor (MAP) and cardiac (HR) responses to increasing PE doses in NC- and HC-fed male rats. Vertical scale bars represent MAP (60 mmHg) and HR (40 BPM) while horizontal scale bars represent time (60 sec); B, The pressor responses to increasing doses of PE; C, Reflex bradycardiac responses to increasing BP; D, Best fit regression line for the correlation between  $\Delta$ MAP and reflex changes in HR in response to increasing doses of PE in NC- and HC-fed rats; E, Slope of the linear regression of the relationship between  $\Delta$ HR and  $\Delta$ MAP reflecting parasympathetic baroreceptor sensitivity (BRS). Depicted data represent mean $\pm$ SEM of values obtained from 6 rats/group. Statistical analysis was done by two-way ANOVA followed by

Sidak's multiple comparisons test for B & C, and one-way ANOVA followed by Tukey multiple comparisons test for E. \* denote  $P < 0.05$  vs. NC.

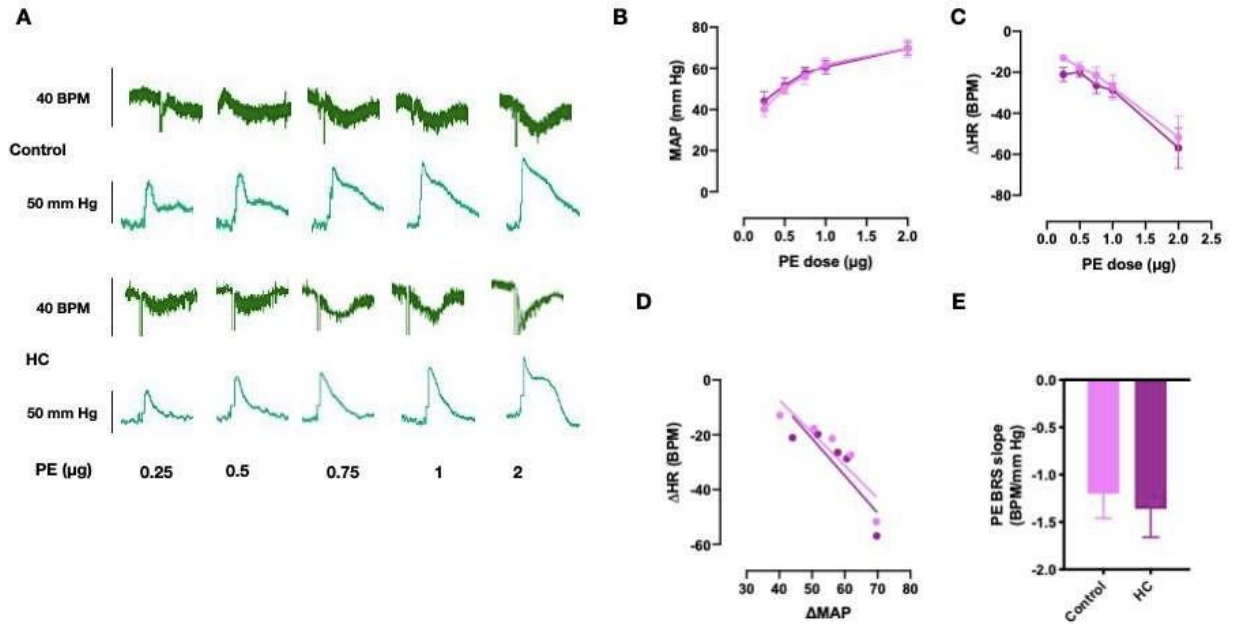


**Figure 11. Cardiac autonomic modulation by HC feeding in female rats.**

A, Representative tracings of pressor (MAP) and cardiac (HR) responses to increasing PE doses in NC- and HC-fed female rats. Vertical scale bars represent MAP (60 mmHg) and HR (40 BPM) while horizontal scale bars represent time (60 sec); B, The pressor responses to increasing doses of PE; C, Reflex bradycardic responses to increasing BP; D, Best fit regression line for the correlation between  $\Delta$ MAP and reflex changes in HR in response to increasing doses of PE in NC- and HC-fed rats; E, Slope of the linear regression of the relationship between  $\Delta$ HR and  $\Delta$ MAP reflecting parasympathetic baroreceptor sensitivity (BRS). Depicted data represent mean $\pm$ SEM of values obtained from 6 rats/group. Statistical analysis was done by two-way ANOVA followed by Sidak's multiple comparisons test for B & C, and one-way ANOVA followed by Tukey multiple comparisons test for E. \* denote  $P < 0.05$  vs. NC.

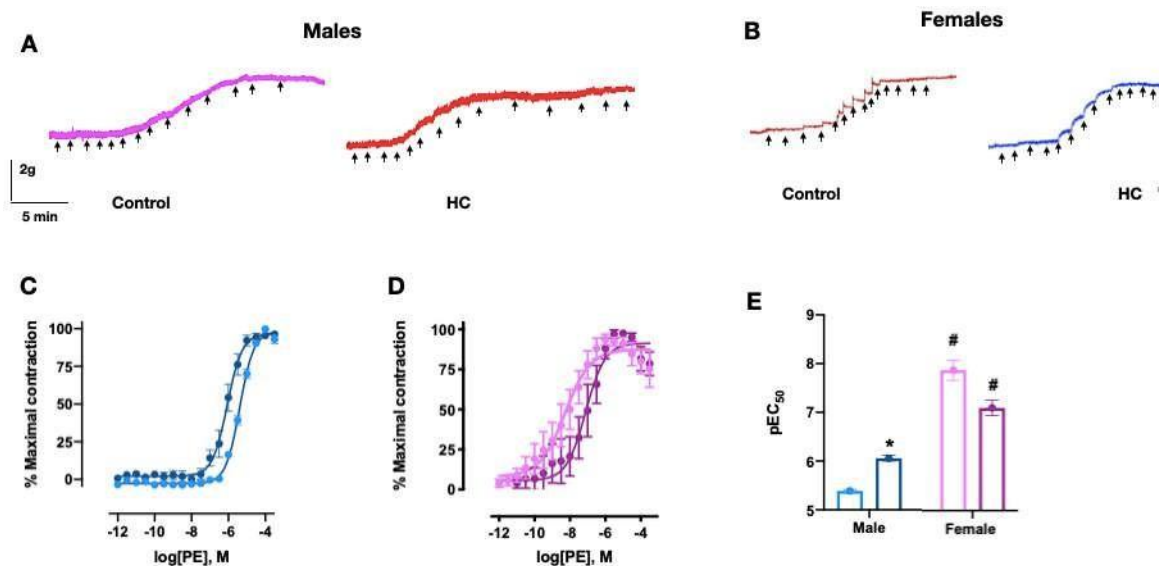


**Figure 12. Ex vivo evaluation of the impact of twenty-four weeks NC or HC feeding in male and female rats on endothelial function.**

A & B, representative tracings of vasopressor effect of different concentrations of PE in aortic rings from male and female rats respectively. C&D, PE concentration-response curve of aortic rings of 24 weeks HC fed male and female rats respectively. E, PE pEC<sub>50</sub> values for the different groups obtained from the best fit values determined by the non-linear regression of the curves in C and D. Statistical significance was tested by two-way ANOVA followed by Sidak multiple comparisons tests for E \* denote a P-value < 0.05 vs. NC fed rats, and # denotes a P-value < 0.05 vs. NC fed male rats.

#### ***4. The role of estrogen in HC-feeding induced PVAT inflammation and consequent cardiovascular dysfunction.***

After 12 weeks of HC or NC feeding, bilateral ovariectomy was performed. Rats were then either treated with a daily dose of exogenous 17 $\beta$ -estradiol (E2) 2.8  $\mu$ g/ 100 gm of body weight or untreated for 12 weeks. E2 treatment in ovariectomized (OVX) rats for 12 weeks induced a response to HC feeding similar to that observed in intact females. However, the loss of endogenous estrogen in the OVX batch seemed to exacerbate HC induced metabolic derangement, as they had higher caloric intake compared to intact females. However, NC fed OVX rats also showed a higher caloric intake compared to intact females (Fig 13. A). Still, total body weight and F/L ratio

were higher in OVX untreated batch regardless of the diet, which was corrected with E2 treatment (Fig 13. B&C). Relatedly, ME was higher in OVX batch explaining the increased adiposity and weight gain, again E2 treatment seemed to reduce ME in both arms (Fig13. D). Only OVX HC arm developed prediabetes, as it had normal glucose level with high fasting serum insulin (Fig 13. E&F) and a higher HOMA-IR score compared to other groups. These lines of evidence further confirm the protective role of estrogen against diet induced prediabetes in female rats. However, neither SPB nor EF were changed among groups (Fig 13. G&H).

As expected, the prediabetic metabolic phenotype in OVX HC fed arm triggered some changes in PVAT which were corrected by E2 treatment such as ACs hypertrophy (Fig 14. B), hypoxia and inflammation. Interestingly though, E2 did not seem to affect UCP1 levels (Fig 14. A). OVX also induced hypertrophy in BAT and WAT, which was prevented by E2 treatment. Parallel to prediabetic male rats, PVAT dysfunction evoked by HC feeding in OVX females induced cardiovascular dysfunction, indicated by impaired BRS in response to PE, and disrupted autonomic regulation in the parasympathetic arm, which was corrected with E2 treatment (Fig 15. E).

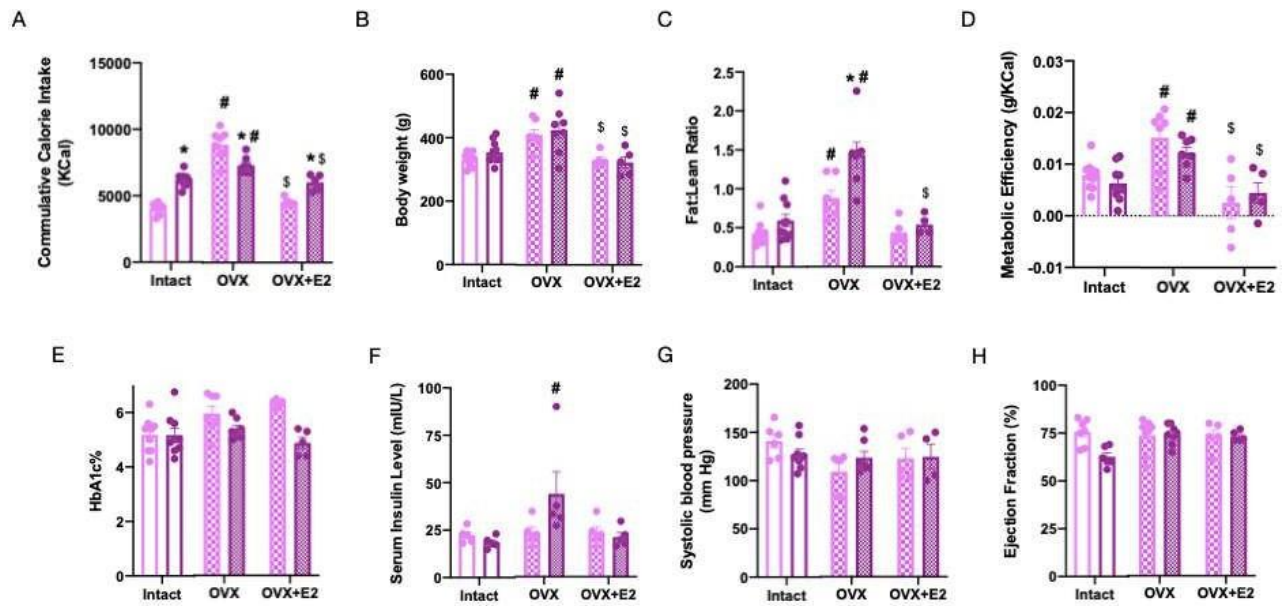


**Figure 13. Metabolic and gross hemodynamic impact of 12 weeks Estradiol treatment in HC and NC fed ovariectomized female rats.**

Cumulative caloric intake in intact, OVX and E2 treated female rats after 24 weeks of either HC or NC feeding (A), body weight (B) and fat:lean ratio at week 24 (C), metabolic efficiency (D), glycosylated hemoglobin A1c level (E), fasting insulin level, (F) systolic blood pressure, (G), Ejection fraction (H) were measured at week 24. The effects of E2 treatment for 12 weeks in rats fed on either HC or NC are described and compared to intact and ovariectomized rats receiving the same diets. Results shown are mean  $\pm$  SEM of observations from six different rats per group. Statistical significance was tested by two-way ANOVA followed by Tukey *post hoc* test. \* denotes a  $P$ -value  $< 0.05$  vs. NC, while # denotes a  $P$ -value  $< 0.05$  vs. intact, and \$ denotes a  $P$ -value  $< 0.05$  vs. OVX.

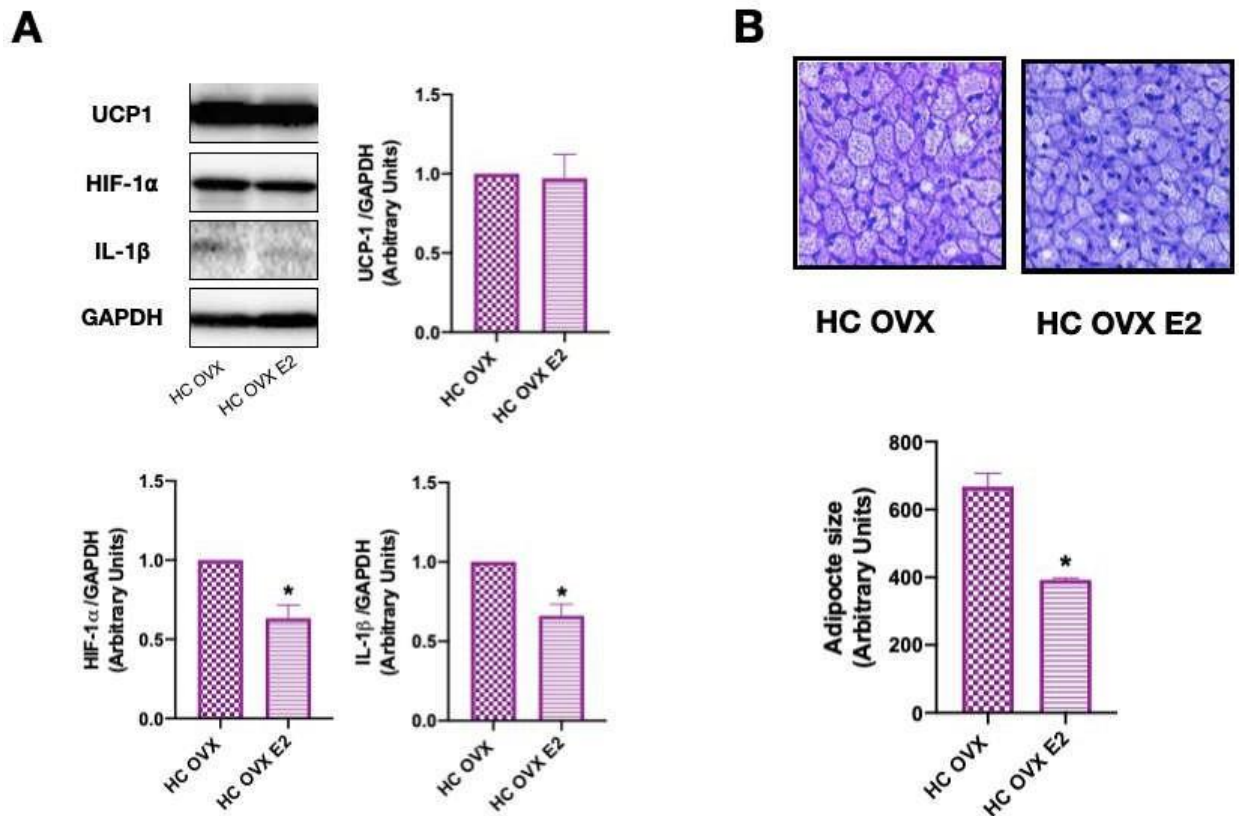


**Figure 14.** Impact of E2 treatment on PVAT of HC fed ovariectomized rats.

A representative western blotting (top left) and summary of the quantified data (top right and bottom) showing the expression levels of UCP1, HIF1- $\alpha$ , and IL-1 $\beta$  in PVAT between HC fed OVX with and without E2 treatment, B representative micrographs (top) and summary of the quantified data (bottom) showing the adipocyte size in H&E stained PVAT. Scale bars are 25  $\mu$ m. The blots shown are representatives of experiments on tissues from three different sets of rats, while summary data for micrographs are obtained from nine sections from three different rats per group. Results shown are mean  $\pm$  SEM. Statistical significance was tested by Student's t-test. \* denotes a *P*-value < 0.05 vs. HC-fed OVX rat values.



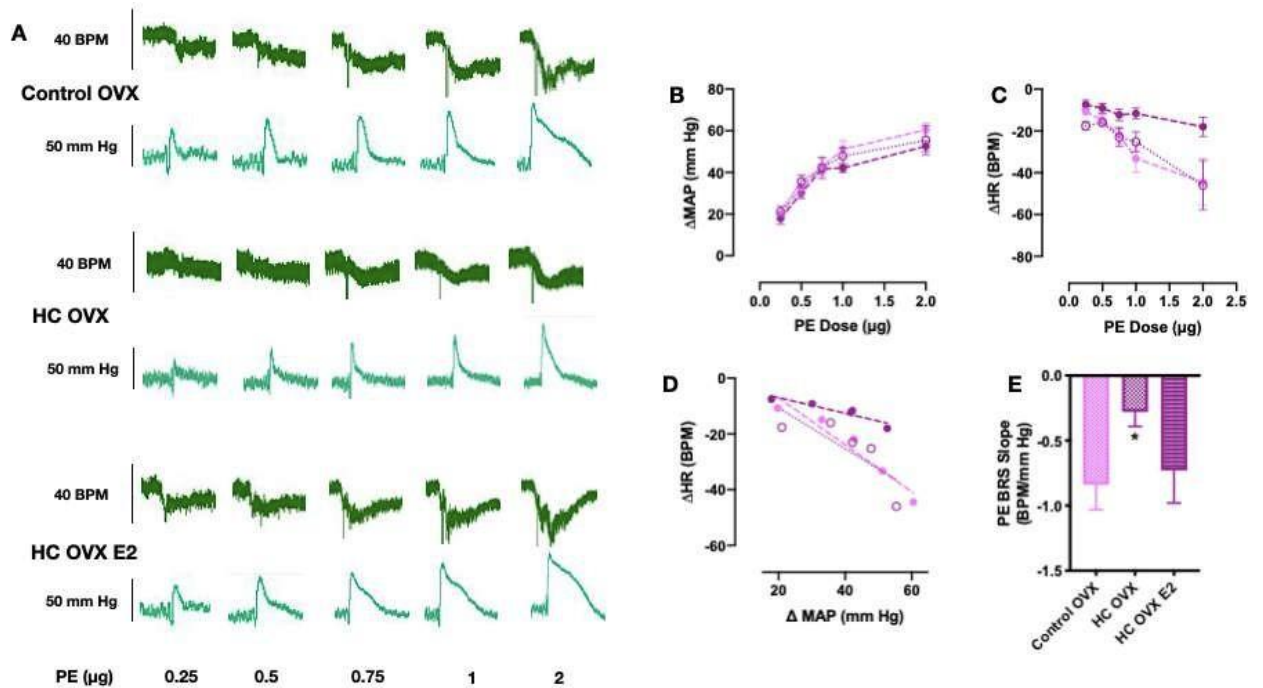


**Figure 15. Cardiac autonomic modulation by ovariectomy and E2 treatment in female rats.**

A, Representative tracings of pressor (MAP) and cardiac (HR) responses to increasing PE doses in ovariectomized NC- and HC-fed females and E2 treatment in HC OVX rats. Vertical scale bars represent MAP (60 mmHg) and HR (40 BPM) while horizontal scale bars represent time (60 sec); B, The pressor responses to increasing doses of PE; C, Reflex bradycardic responses to increasing BP; D, Best fit regression line for the correlation between  $\Delta$ MAP and reflex changes in HR in response to increasing doses of PE; E, Slope of the linear regression of the relationship between  $\Delta$ HR and  $\Delta$ MAP reflecting parasympathetic baroreceptor sensitivity (BRS). Depicted data represent mean  $\pm$  SEM of values obtained from 6 rats/group. Statistical analysis was done by two-way ANOVA followed by Sidak's multiple comparisons test for B & C, and one-way ANOVA followed by Tukey multiple comparisons test for E. \* denote  $P < 0.05$  vs. NC OVX arm.

## B. Therapeutic fasting impact on early cardiovascular dysfunction in HC fed rats.

### 1. The impact of 12 weeks of therapeutic fasting on metabolic and gross hemodynamic outcomes in prediabetic male rats.

Twelve weeks of HC feeding were followed by another twelve of intermittent fasting (IF) or therapeutic fasting (TF). TF was implemented as 12 hours fasting in the

dark period, while giving free access to HC diet during the remaining 12 hours, daily for 12 weeks. As expected in our model HC induced increased cumulative energy intake and fat to lean ratio with no change in weight, which was explained by the reduced energy efficiency in males (Fig 16. A-D). Despite the free access to HC diet, TF was able to reduce cumulative energy intake (Fig 4.10. A), however, total body weight did not change (Fig 16. B). Still, fat:lean ratio was rescued by TF (Fig 16. C), however, ME was not (Fig 16. D). It also prevented hyperinsulinemia and improved IR (Fig 16. E-G). Not only did TF correct and improve metabolic parameters, it also reduced HC induced systolic blood pressure (Fig 16. H)

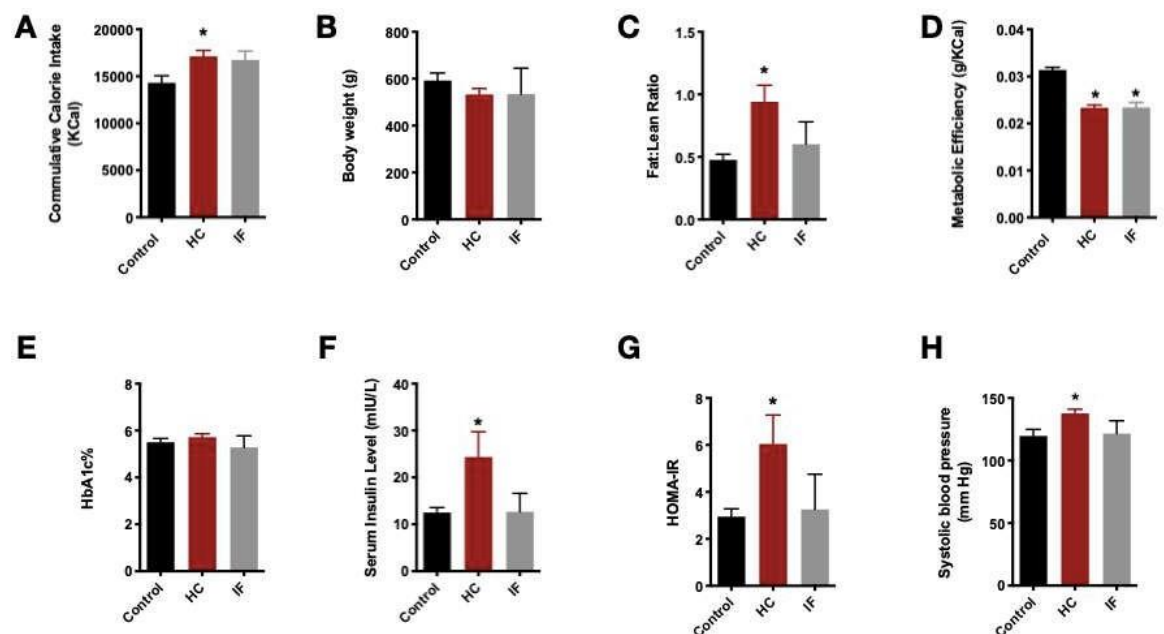


**Figure 16. Metabolic and gross hemodynamic impact of therapeutic fasting and HC feeding in male rats for twelve weeks.**

After twelve weeks on therapeutic fasting (daily 12 hours fasting) and HC free feeding, several important metabolic and cardiovascular parameters were assessed; cumulative calorie consumption (A) body weight (B), fat:lean ratio (C) metabolic efficiency (D), glycosylated hemoglobin A1c level (E), and fasting insulin level (F) were tested on serum sample on the day of the sacrifice, homeostatic model assessment of insulin



resistance (HOMA IR) (G), and systolic blood pressure (H)). The effects of therapeutic fasting regimen during the twelve weeks duration and HC feeding are depicted and compared to rats receiving normal chow (NC). Results shown are mean  $\pm$  SEM of observations from six different rats per group. Statistical significance was tested by one-way ANOVA followed by. \* denotes a  $P$ -value  $< 0.05$  vs. NC fed rats.

## ***2. Effect of therapeutic fasting on markers of adipose tissue inflammation in HC-fed rats.***

Consistent with our previous findings, HC-fed male rats developed PVAT dysfunction, in the absence of systemic inflammation (Fig 17. D). TF seemed to induce positive outcomes in PVAT as it corrected hypertrophy (Fig 17. A) and other molecular hallmarks of negative adipose remodeling; UCP1, P-DRP1 (ser616), HIF1- $\alpha$  and IL-1 $\beta$  in PVAT (Fig 18. A) and promoted positive transformation in PVAT of prediabetic rats without calorie restriction.

BAT ACs as well were rescued from HC induced expansion (Fig 17. B) and MT dysfunction (Fig 18. B). Since eWAT was not affected by HC feeding, TF did not seem to induce any changes (Fig 17. C and Fig 18. C).

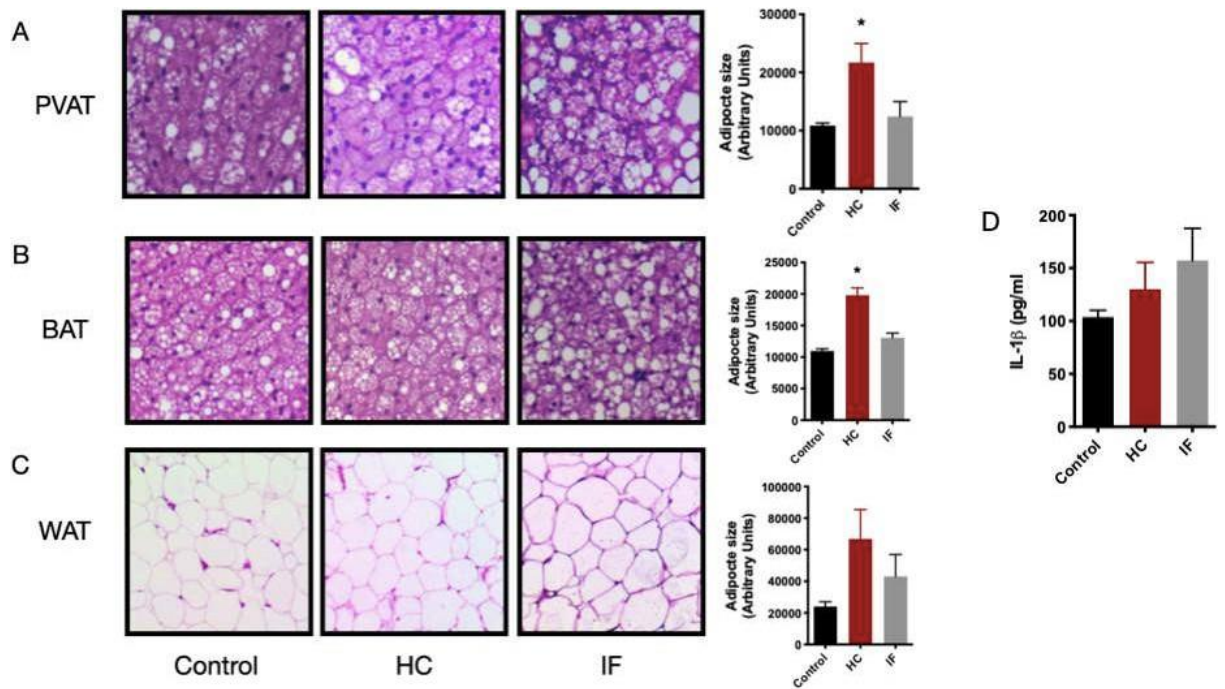


**Figure 17. The impact of twelve weeks of fasting on adipocytes size of different depots.**

Representative micrographs (Right) and summary of the quantified data (left) showing the adipocyte size in H&E stained PVAT (A), infra-scapular BAT (B) and epididymal WAT (C) sections, Serum IL-1 $\beta$  measured (D), from male rats fed on NC, HC and HC with fasting. Scale bars are 25  $\mu$ m, summary data for micrographs are obtained from nine sections from three different rats per group. Results shown are mean  $\pm$  SEM. Statistical significance was tested one-way ANOVA followed by Sidak *post hoc* test for (A-D) \* denotes a *P*-value < 0.05 vs. NC-fed rat values.

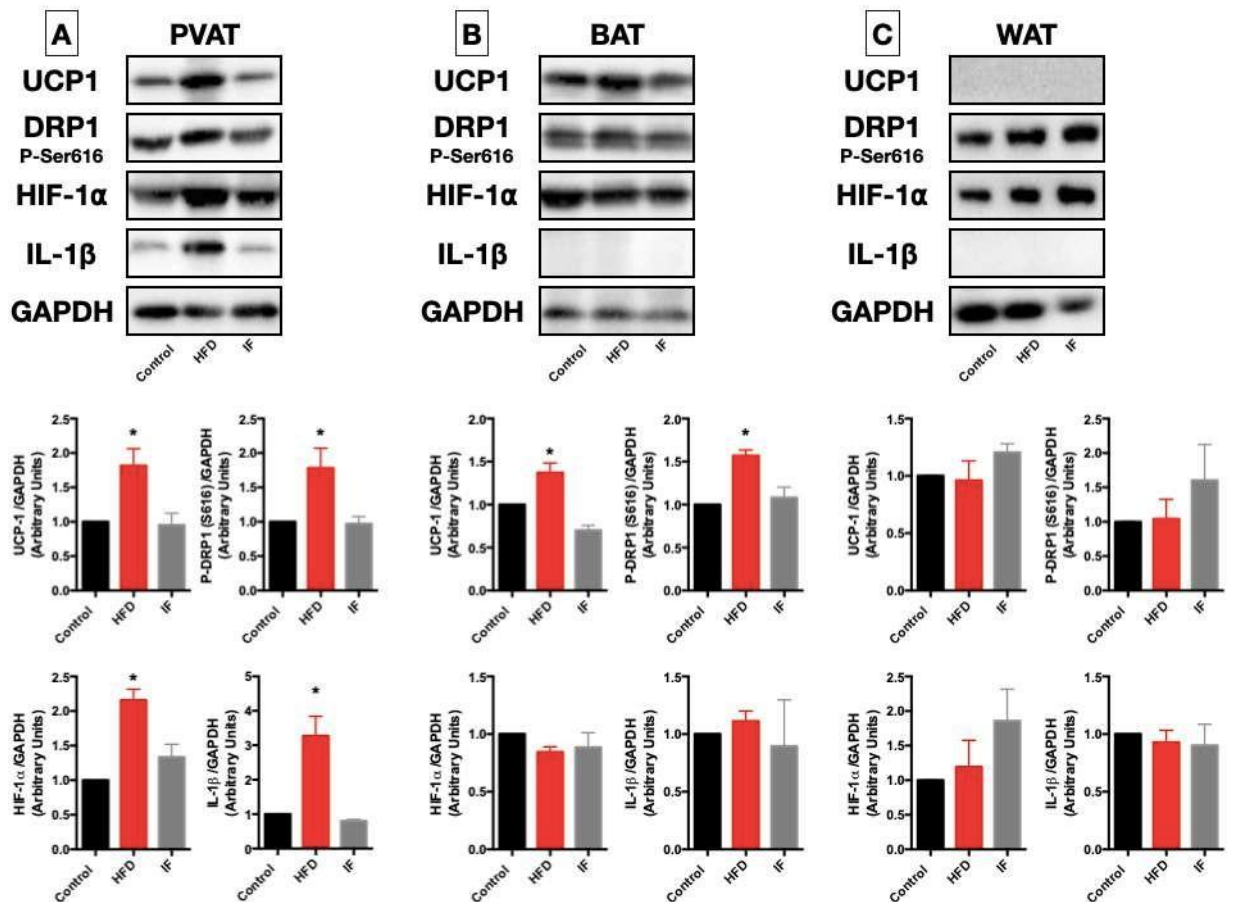


**Figure 18. Sex differential molecular manifestations of twenty-four weeks of HC feeding on adipose tissue remodeling.**

Representative western blotting (upper A-C)) in males Control, HC and HC with fasting respectively, and summary of the quantified data (bottom A-C) for PVAT (A) showing the expression levels of UCP1 (upper left), HIF1- $\alpha$  (upper right), P-DRP1(ser616) (lower left) and IL-1 $\beta$  (lower right), in response to NC, HC and TF, same parameters were assessed for infra-scapular BAT (B) and epididymal WAT (C). The blots shown are representatives of experiments on tissues from three different sets of rats. Results shown are mean  $\pm$  SEM. Statistical significance was tested by one-way ANOVA followed by Tukey multiple comparisons test for A-F, and two-way ANOVA followed by Sidak *post hoc* test for G. \* denotes a *P*-value  $< 0.05$  vs. NC-fed rat values.

### 3. Therapeutic fasting impact on HC induced Cardiovascular dysfunction in vivo and in ex-vivo settings.

PVAT inflammation in our non-obese prediabetic state induced by HC-diet feeding in male rats was associated with parasympathetic cardiac autonomic

neuropathy, manifested as a blunting of the bradycardic baroreflex in response to PE. An increased pressor effect was observed in these rats in response to increasing PE doses compared to rats on control diet [325] in line with the reported increased vascular contractility at this stage [7]. Significantly, both effects were ameliorated 12 weeks of fasting with HC feeding (Fig 19. B&C). Restoration of parasympathetic autonomic function was confirmed by examination of the baroreceptor sensitivity in response to PE (Fig 19. E). As observed previously, no change in the sympathetic arm of the baroreflex was observed following HC feeding or fasting (data not shown). Moreover, HC-induced increased sensitivity to PE was improved by 12 weeks of fasting (Fig 19. B). Figure 20. A depict the representative tracings for NC-, HC- fed and HC-fasting rats. In our group, we observed endothelial dysfunction in HC-fed male rats, which was mainly driven by impaired EDH due to dysfunctional Kir channels [116]. Indeed, we tested the aortic function in male rats after 24 weeks of HC feeding with and without fasting. ACh dependent relaxation was blunted in HC fed males (Fig 20. C, left), while IF seemed to reduce residual constriction with increased concentrations of ACh compared to HC fed arm (Fig 20. C, right).

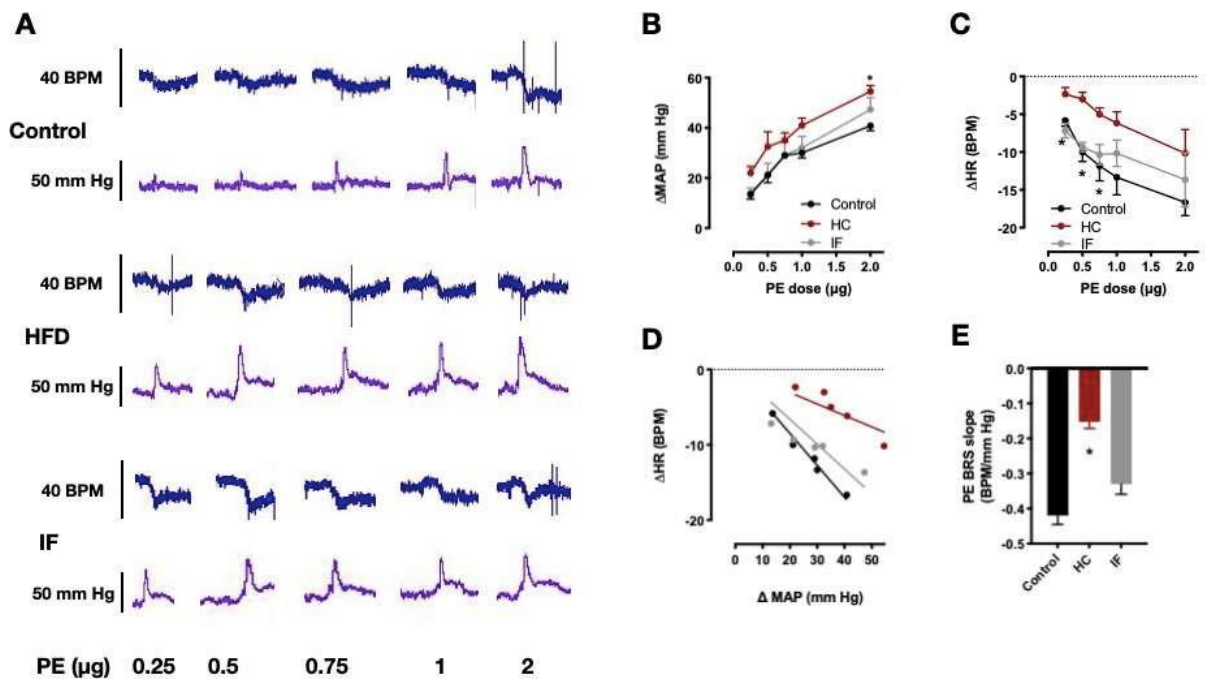


**Figure 19. Therapeutic Fasting restores parasympathetic cardiac autonomic function.**

A, Representative tracings of pressor (MAP) and cardiac (HR) responses to increasing PE doses in NC- and HC-fed rats with different concentrations of P supplementation. Vertical scale bars represent MAP (60 mmHg) and HR (40 BPM) while horizontal scale bars represent time (60 sec); B, The pressor responses to increasing doses of PE; C, Reflex bradycardic responses to increasing BP; D, Best fit regression line for the correlation between  $\Delta$ MAP and reflex changes in HR in response to increasing doses of PE in NC-, HC-fed and HC fasting rats with different concentrations of P supplementation; E, Slope of the linear regression of the relationship between  $\Delta$ HR and  $\Delta$ MAP reflecting parasympathetic baroreceptor sensitivity (BRS). Depicted data represent mean $\pm$ SEM of values obtained from 6 rats/group. Statistical analysis was done by two-way ANOVA followed by Sidak's multiple comparisons test for B & C, and one-way ANOVA followed by Tukey multiple comparisons test for E. \* denote  $P < 0.05$  vs. NC.

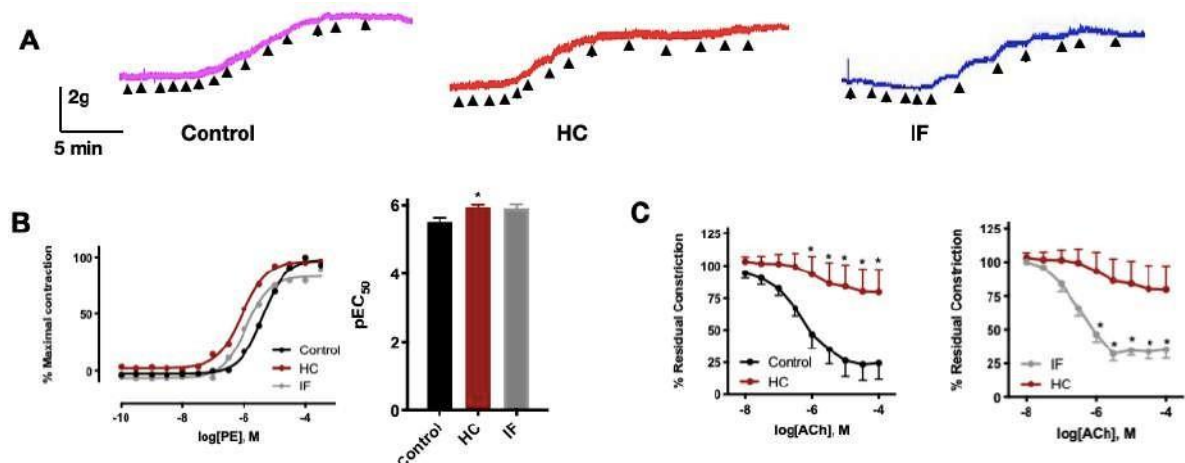


**Figure 20. Ex vivo evaluation of the impact of therapeutic fasting on HC mediated impaired endothelial function.**

A, representative tracings of the vasopressor response to PE concentrations. The dotted line represents the incremental increase in PE concentrations; B, PE concentration-response curve on aortic rings of NC and HC fed rats with and without fasting (top), PE pEC<sub>50</sub> values for the different groups (bottom); C, mean normalized ACh-evoked relaxations in aortic rings pre-constricted with PE for the different groups. Statistical significance was tested by two-way ANOVA followed by Sidak's multiple comparisons test. \* denote a P-value < 0.05 vs. control in B& C, left. And it denotes P-value < 0.05 vs. HC rats in C, right.

#### ***4. Therapeutic fasting alleviates signs of cardiovascular deterioration.***

In addition to the altered hemodynamics and vascular dysfunction induced by HC feeding, histochemical examination of heart mid-section from 24 weeks HC-fed male rats showed signs of focal injury demonstrated by an elevated papillary muscle edema, as well as increased fibrosis (Fig 21. B). Our fasting regimen appeared to have reversed these changes. On the other hand, similar changes were observed for aortic tissue. While HC feeding led to increased aortic medial thickness and fibrosis, again even in the presence of HC feeding intermittent fasting was able to reverse these changes (Fig 21. A).



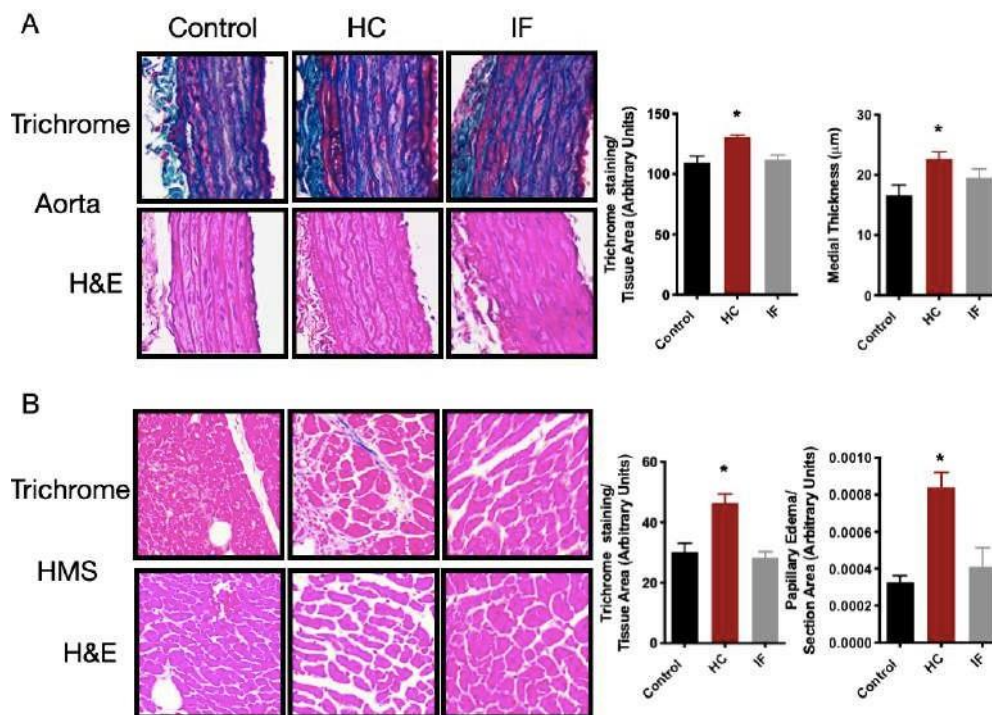


**Figure 21. Impact of 12 weeks therapeutic fasting on histopathological and molecular signs of cardiac and aortic impairment induced by hypercaloric feeding.**

A, Representative micrographs of histopathological staining (left) in thoracic aorta (A) and heart mid-section (B) of rats on NC, HC and HC- fasting regimen. Data presented are serial sections taken from the same tissues and are representative of 9 sections from 3 different rats in each group. Scale bars are (top to bottom): 25, 25, 50, and 50 μm. Fibrotic staining appears as a blue color on a red background. Quantification values of area of interfibrillar edema (B, bottom right) as well as the intensity of Masson trichrome (A&B, upper right). Quantification values of aortic medial thickness (A, upper right). Statistical significance was determined by one-way ANOVA followed by Tukey *post hoc* test. \* denote  $P < 0.05$  compared to NC rats.

### **5. The role of TF in PVAT inflammation induced cardiovascular dysfunction in HC fed ovariectomized rats.**

Since OVX female rats fed HC diet demonstrated a detrimental phenotype similar to that observed in males, the effect of TF introduction for twelve weeks was examined.

IF did not seem to reduce cumulative caloric intake nor change body weight compared to OVX controls (Fig 22. A&B), however, IF reduced adiposity despite estrogen loss

and HC feeding (Fig 22. C). Still, ME did not change in response to IF (Fig 22.D). Interestingly, twelve weeks of IF corrected prediabetes in ovariectomized HC fed females, prevented HC provoked hyperinsulinemia (Fig 22. E) and improved HbA1c level (Fig 22. F).

Moreover, twelve weeks of fasting were able to reverse HC induced PVAT dysfunction in OVX rats, as it prevented hypertrophy not only in PVAT but also in BAT (Fig 23.). It also corrected UCP1 upregulation, hypoxia, and inflammation (Fig 24.). Similar to our previous findings, PVAT inflammation provoked cardiovascular dysfunction, here, IF was able to improve BRS in response to PE despite estrogen deficiency and HC feeding (Fig 25. E).

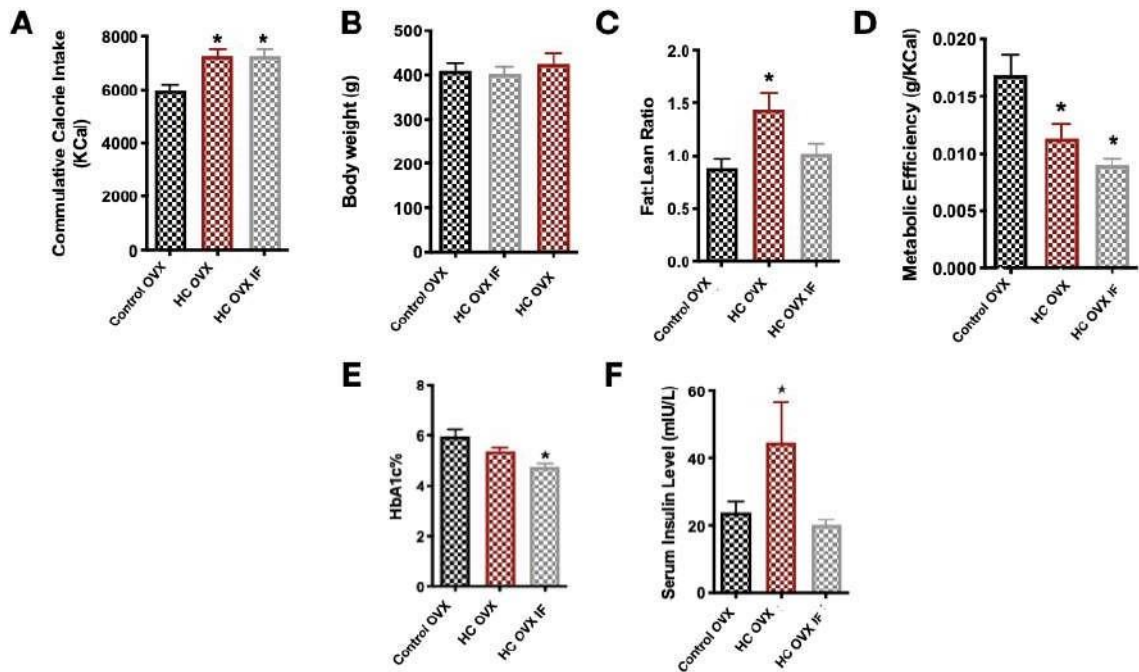


**Figure 22. Metabolic and gross hemodynamic impact of 12 weeks fasting in HC fed ovariectomized female rats.**

Cumulative caloric intake in ovariectomized NC-, HC- fed and HC- fed with 12 weeks IF (A), body weight (B) and fat:lean ratio at week 24 (C), metabolic efficiency (D), glycosylated hemoglobin A1c level (E), serum fasting insulin level (F). The effects of IF for 12 weeks in rats fed on HC are described and compared to intact controls and



ovariectomized rats receiving HC diet. Results shown are mean  $\pm$  SEM of observations from six different rats per group. Statistical significance was tested by one-way ANOVA followed by Tukey *post hoc* test. \* denotes a *P*-value  $< 0.05$  vs. Ovariectomized NC fed rats.

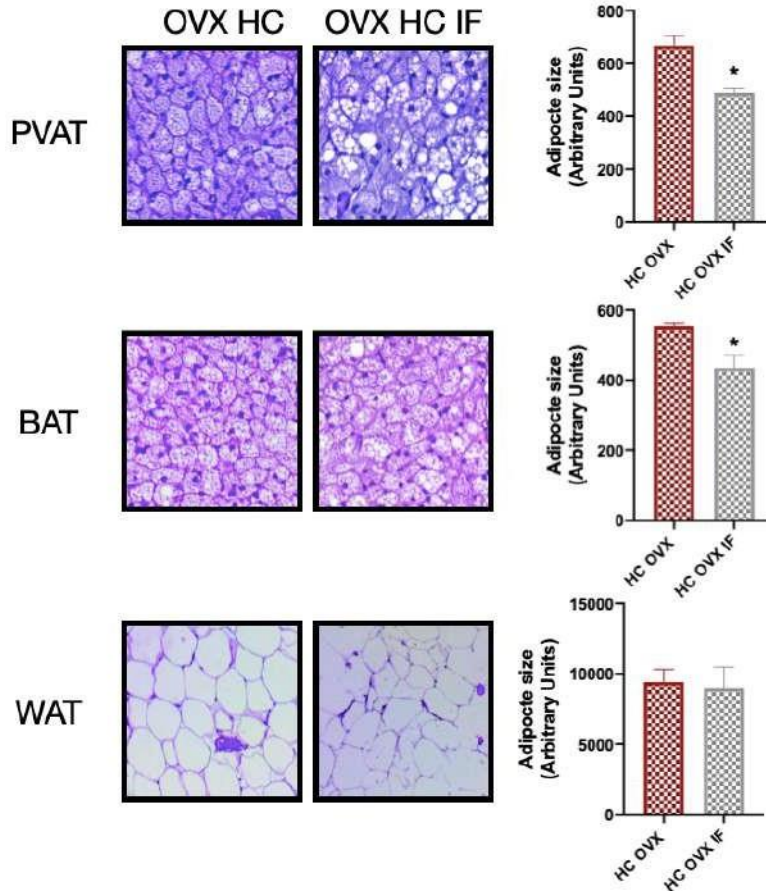


**Figure 23. The impact of twelve weeks of fasting on adipocytes size of ovariectomized female rats.**

Representative micrographs (Right) and summary of the quantified data (left) showing the adipocyte size in H&E stained PVAT (A), infra-scapular BAT (B) and epididymal WAT (C) sections, Serum IL-1 $\beta$  measured (D), from ovariectomized female rats fed on HC diet with or without twelve weeks of fasting. Scale bars are 25  $\mu$ m, summary data for micrographs are obtained from nine sections from three different rats per group. Results shown are mean  $\pm$  SEM. Statistical significance was tested one-way ANOVA followed by Tukey *post hoc* test for (A-D) \* denotes a *P*-value  $< 0.05$  vs. HC-fed ovariectomized rats.

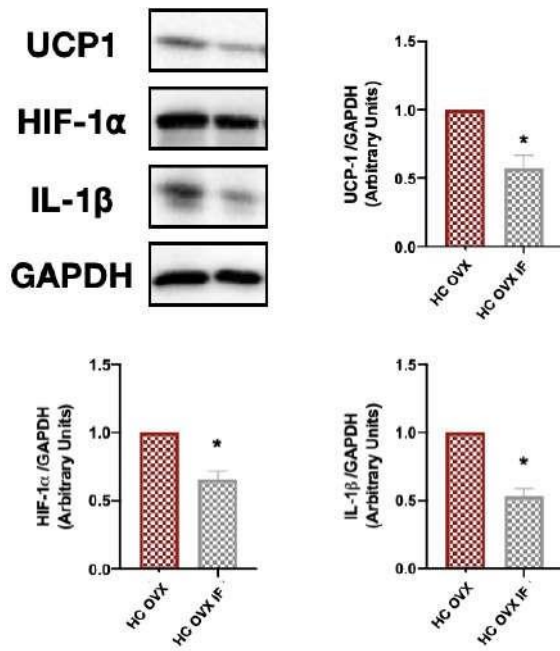


**Figure 24. Impact of therapeutic fasting on PVAT of HC fed ovariectomized rats.**

A representative western blotting (top left) and summary of the quantified data (top right and bottom) showing the expression levels of UCP1, HIF1- $\alpha$ , and IL-1 $\beta$  in PVAT between HC fed OVX with and without IF. The blots shown are representatives of experiments on tissues from three different sets of rats, while summary data for micrographs are obtained from nine sections from three different rats per group. Results shown are mean  $\pm$  SEM. Statistical significance was tested by one-way ANOVA followed by Tukey multiple comparisons test for , and two-way ANOVA followed by Sidak *post hoc* test for G. \* denotes a  $P$ -value  $< 0.05$  vs. HC-fed OVX rat values.

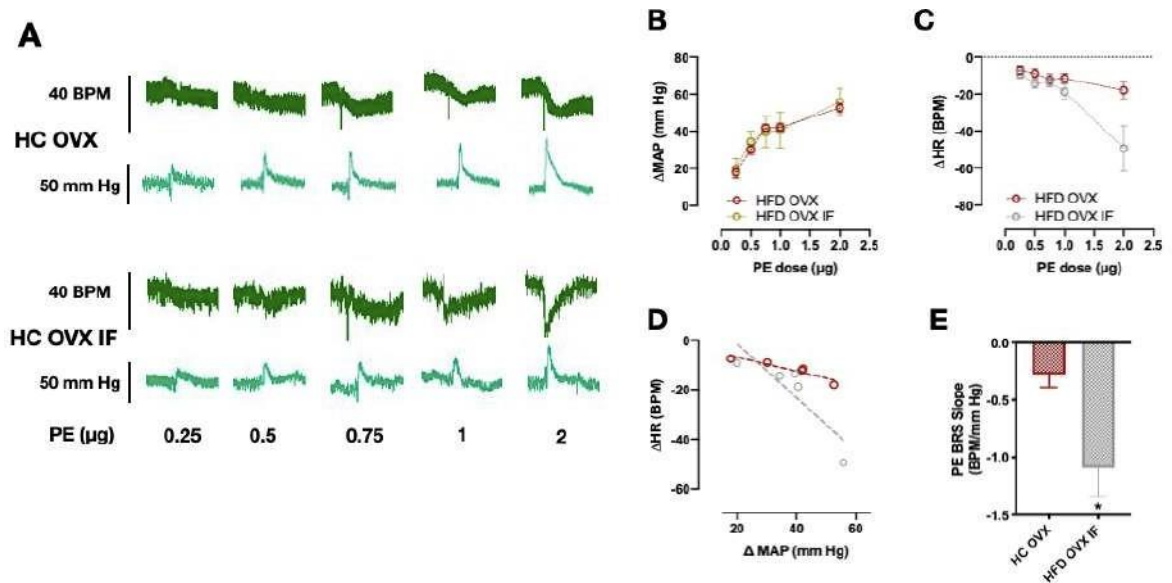


**Figure 25. Cardiac autonomic modulation by therapeutic fasting in ovariectomized female rats.**

A, Representative tracings of pressor (MAP) and cardiac (HR) responses to increasing PE doses in ovariectomized HC-fed females with and without IF. Vertical scale bars represent MAP (60 mmHg) and HR (40 BPM) while horizontal scale bars represent time (60 sec); B, The pressor responses to increasing doses of PE; C, Reflex bradycardic responses to increasing BP; D, Best fit regression line for the correlation between  $\Delta$ MAP and reflex changes in HR in response to increasing doses of PE; E, Slope of the linear regression of the relationship between  $\Delta$ HR and  $\Delta$ MAP reflecting parasympathetic baroreceptor sensitivity (BRS). Depicted data represent mean $\pm$ SEM of values obtained from 6 rats/group. Statistical analysis was done by two-way ANOVA followed by Sidak's multiple comparisons test for B & C, and one-way ANOVA followed by Tukey multiple comparisons test for E. \* denote  $P < 0.05$  vs. HC OVX arm.

### C. The impact of Inorganic Phosphate as a UCP1 inhibitor on PVAT Induced Cardiovascular Dysfunction.

#### 1. Metabolic and gross hemodynamic impact of HC feeding with different levels of phosphorus.

The metabolic and gross hemodynamic profile of rats fed HC-diet with low Pi has been characterized in our previous work [7, 253, 315]. Indeed, the present study showed similar results with an increased cumulative calorie intake that is equivalent to the

previously observed daily increase of ~14 Kcal (Fig 26. A). This occurred in absence of increased body weight or fasting blood glucose level (Fig 26. B & C). As for non-invasive hemodynamic measurements, no changes in systolic blood pressure and ejection fraction were detected (Fig 26. G & H). As previously observed, HC-fed rats demonstrated an increased adiposity as indicated by an elevated fat:lean ratio, which was not affected by different levels of Pi supplementation (Fig 26. D). On the other hand, the characteristic increase in serum triglyceride that appeared in this model of early metabolic challenge was reversed by Pi supplementation at both 0.75 and 1.5 mg/Kcal (Fig 26. E). Moreover, while the 0.75 mg/Kcal supplementation level did not affect the elevated serum insulin levels in HC-fed rats, supplementation at 1.5 mg/Kcal appeared to be associated with fasting serum insulin levels that were not different from those in control rats (Fig 26. F). Interestingly, despite the observed increase in adiposity, serum concentrations of leptin and adiponectin did not appear to vary in different rat groups (Fig 26. H & I). Significantly, despite a trend to increase, serum Pi levels in rats receiving the HC-diet deficient in Pi was not different from that in rats receiving control diet or the HC-diet with the intermediate Pi dose of 0.75 mg/Kcal (Fig 27. A). Importantly though, rats receiving HC diet supplemented by 1.5 mg/Kcal Pi had serum levels that were significantly less compared to those with Pi-deficient diet. Moreover, the different rat groups showed similar serum concentrations of calcium (Fig 27. B) and magnesium (Fig 27. C). Interestingly, the general trends observed after the 12-week feeding period were preserved, albeit with lesser differences at the earlier time point of eight weeks (Fig 28) indicating a consistent trajectory over the feeding period.

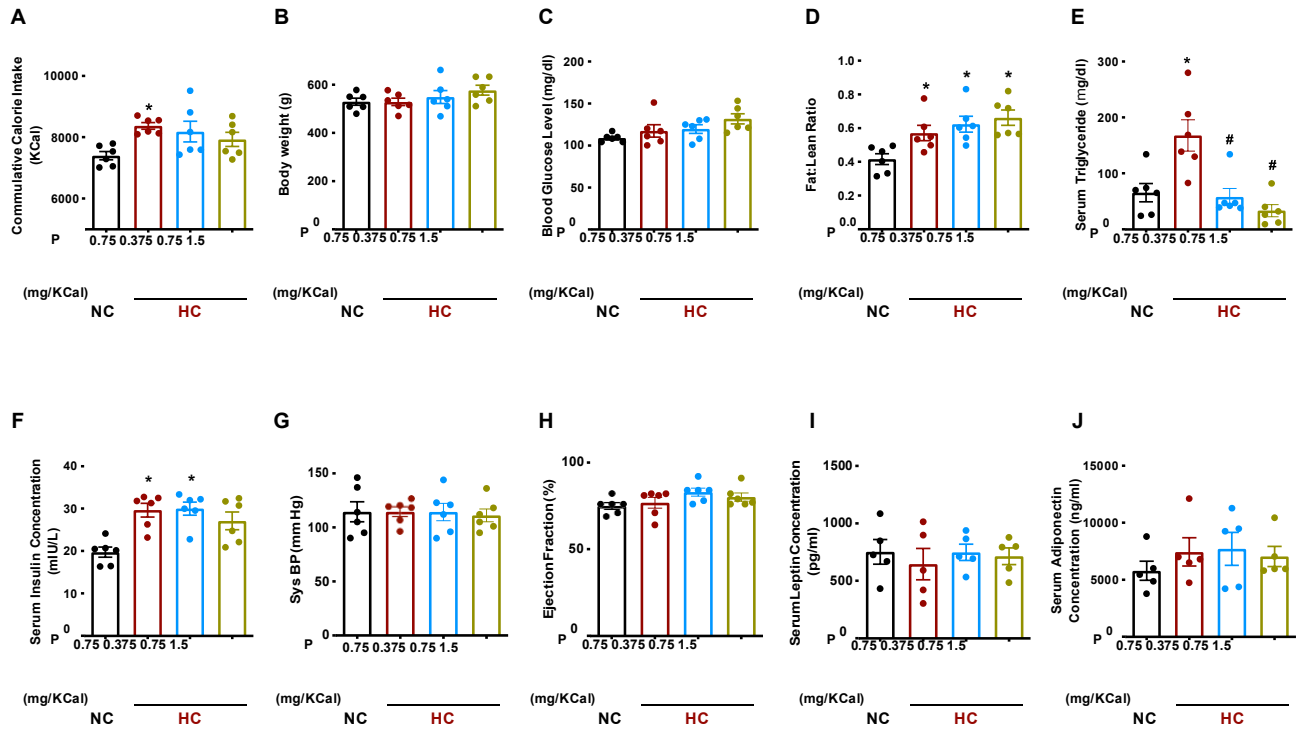


**Figure 26. Metabolic and gross hemodynamic impact of inorganic phosphorus supplementation of hypercaloric diet.**

Twelve weeks of increased calorie consumption (A) due to hypercaloric (HC) diet feeding induce a non-obese prediabetic phenotype in rats without an increase in body weight (B), fasting blood glucose (C), systolic blood pressure (Sys BP, G), Ejection fraction (H), Serum Leptin (I), and serum adiponectin (J); but with increased fat:lean ratio (D), serum triglycerides (E), and fasting serum insulin (F). The effects of inorganic phosphorus (P) supplementation at 0.75 and 1.5 mg/Kcal during the full twelve-week duration are depicted and compared to rats receiving normal chow (NC). Results shown are mean  $\pm$  SEM of observations from six different rats per group. Statistical significance was tested by one-way ANOVA followed by Tukey *post hoc* test. \* denotes a *P*-value < 0.05 vs. NC while # denotes a *P*-value < 0.05 vs. HC: 0.375 mg/Kcal P.

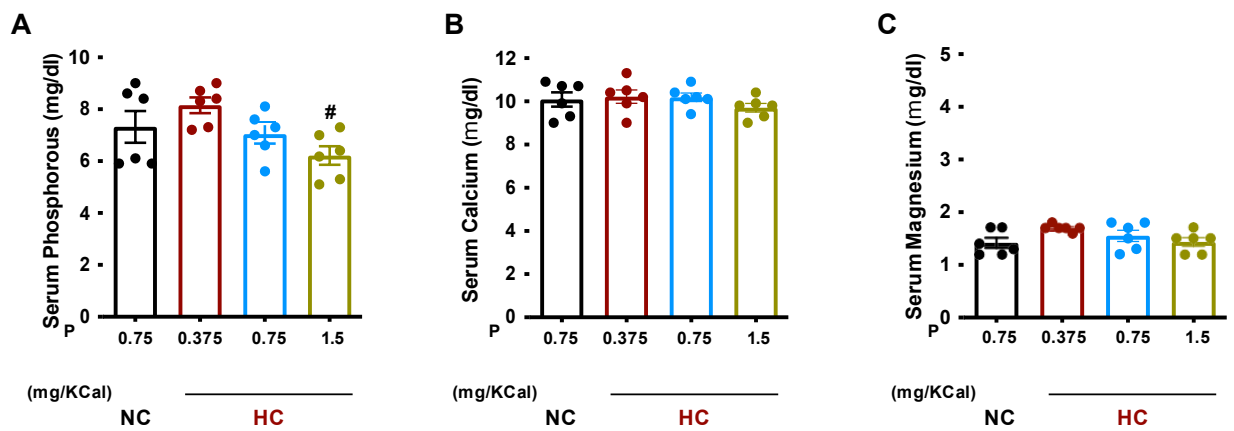


**Figure 27. Phosphorus supplementation does not affect serum Pi, calcium, or magnesium concentrations.**

Phosphorus (Pi) deficient hypercaloric feeding (HC: 0.375 mg/Kcal) does not affect serum Pi (A), calcium (B) or magnesium (C) concentrations. Results shown are mean  $\pm$  SEM of observations from six different rats per group. Statistical significance was tested by one-way ANOVA followed by Tukey multiple comparisons test.

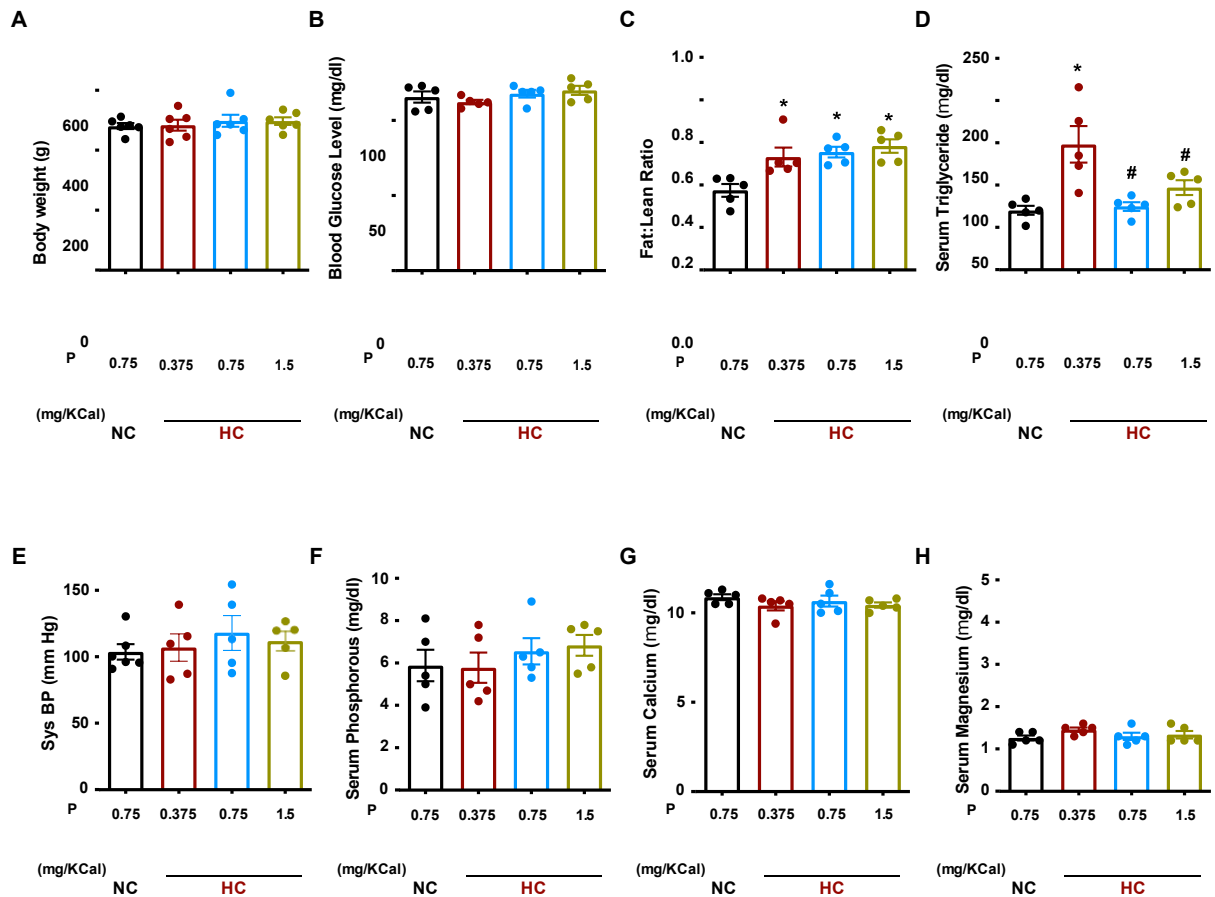


**Figure 28. Impact of 8 weeks of inorganic phosphorus supplementation of hypercaloric diet on metabolic and gross hemodynamic parameters as well as Pi, calcium, and magnesium concentration.**

Eight weeks of feeding had no effect on body weight (A), fasting blood glucose (B), systolic blood pressure (Sys BP, E), serum Pi (F), serum calcium (G), and serum magnesium (H); but increased fat:lean ratio (E) and serum triglycerides (D). Results shown are mean  $\pm$  SEM of observations from five different rats per group. Statistical significance was tested by one-way ANOVA followed by Tukey *post hoc* test. \* denotes a *P*-value < 0.05 vs. NC while # denotes a *P*-value < 0.05 vs. HC: 0.375 mg/Kcal P.

## ***2. Impact of phosphorus supplementation on markers of adipose tissue inflammation in HC-fed rats and in vitro in cultured adipocytes.***

Our previous studies showed that HC feeding was associated with increased UCP1 expression in PVAT but not in other adipose depots, which was accompanied by increased markers of hypoxia and inflammation [7]. Similar findings were obtained in the present study whereby HC: 0.375 Pi diet was found to induce an increased UCP1

expression with parallel increases in HIF1- $\alpha$  and IL-1 $\beta$  (Fig 29. A). Pi supplementation



led to a dose-dependent decrease in UCP1 PVAT expression. Parallel reduction in HIF1- $\alpha$  and IL-1 $\beta$  expression was seen particularly with the 1.5 mg/Kcal Pi dose (Fig 29. A). Interestingly, while PVAT adipocyte size increased upon HC feeding, Pi supplementation led to a reversal of this effect (Fig 29. B). Upon examination of the impact of dietary changes on *bona fide* WAT and BAT, UCP1 expression was not detected and did not change in epididymal and infra-scapular adipose tissue, respectively (Fig 29. C & E). In parallel, HIF1- $\alpha$  expression did not change in either tissue with any of the diets, whereas no IL-1 $\beta$  expression was seen (Fig 29. C & E). Nevertheless, an increase adipocyte size was observed in both WAT and BAT representative tissues from rats fed HC: 0.375 Pi diet. This change was reversed was Pi supplementation, particularly at the 1.5 mg/Kcal dose (Fig 29. D & F).

In attempt to establish a direct effect of Pi on PVAT changes, we have developed an *in vitro* cell culture model to simulate the inflammatory changes occurring upon exposure to increased calorie intake and hyperinsulinemia. Adipocytes differentiated from human bone marrow-derived mesenchymal stem cells showed lipid droplet accumulation and UCP1 expression (Fig 30 A&B). Differentiated adipocytes stressed by exposure to 40 mIU/L and 1.6 mM palmitic acid appeared to develop a phenotype that favors inflammation demonstrated by increased THP-1 monocyte adhesion compared to adipocytes incubated in control media (Fig 30. C). The adherent monocytes developed macrophage markers indicative of initiation of inflammatory response (Fig 30. D). Interestingly, HIF-1 $\alpha$  and IL-1 $\beta$  expression levels increased in the stressed adipocytes exposed to THP-1 monocytes as observed in the PVAT of prediabetic rats receiving HC: 0.375 (Fig 30. G). Significantly, when this experiment

was repeated in 4 mM Pi, the increase in the expression of both HIF-1 $\alpha$  and IL-1 $\beta$  was attenuated.

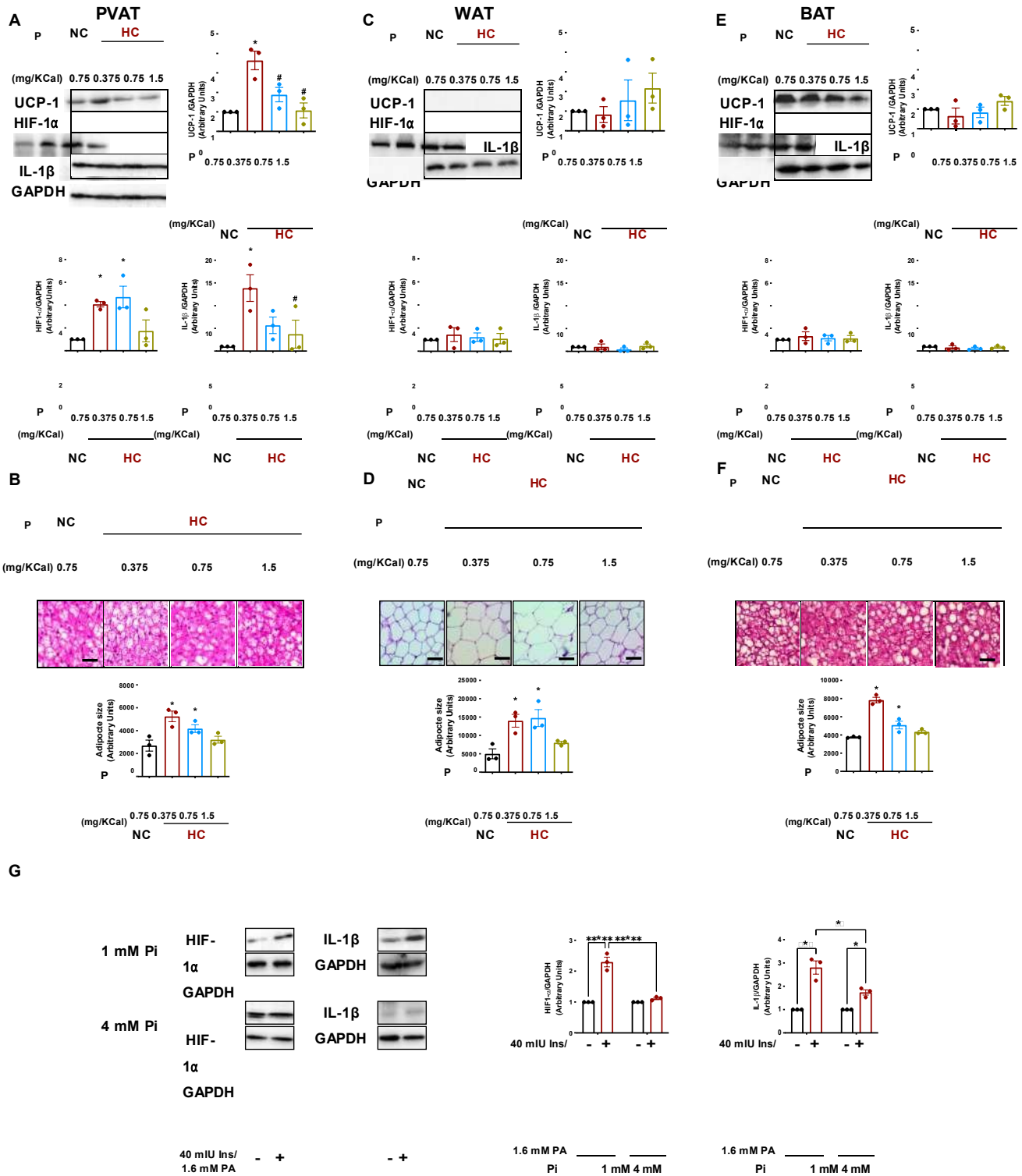


**Figure 29.** Manifestations of PVAT inflammation in HC-fed rat compared to changes in a visceral WAT and BAT pools and the ameliorative effect of inorganic phosphorus supplementation.

A, C & E, Representative western blotting (top left) and summary of the quantified data (top right and bottom) showing the expression levels of UCP1, HIF1- $\alpha$ , and IL-1 $\beta$  in PVAT, epididymal WAT and infra-scapular BAT, respectively, of NC- and HC-fed rats with different concentrations of P supplementation; B, D & F, Representative micrographs (top) and summary of the quantified data (bottom) showing the adipocyte size in H&E stained PVAT epididymal WAT and infra-scapular BAT sections, respectively. Scale bars are 25  $\mu$ m. G, Representative western blotting (left) and summary of the quantified data (right) showing the expression levels HIF1- $\alpha$  and IL-1 $\beta$  in cultured adipocytes differentiated from mesenchymal stem cells at 1 and 4 mM P in culture media with or without insulin and palmitic acid challenge. The blots shown are representatives of experiments on tissues from three different sets of rats, while

summary data for micrographs are obtained from nine sections from three different rats per group. Results shown are mean  $\pm$  SEM. Statistical significance was tested by one-way ANOVA followed by Tukey multiple comparisons test for A-F, and two-way ANOVA followed by Sidak *post hoc* test for G. \* denotes a *P*-value  $< 0.05$  vs. NC-fed rat values.

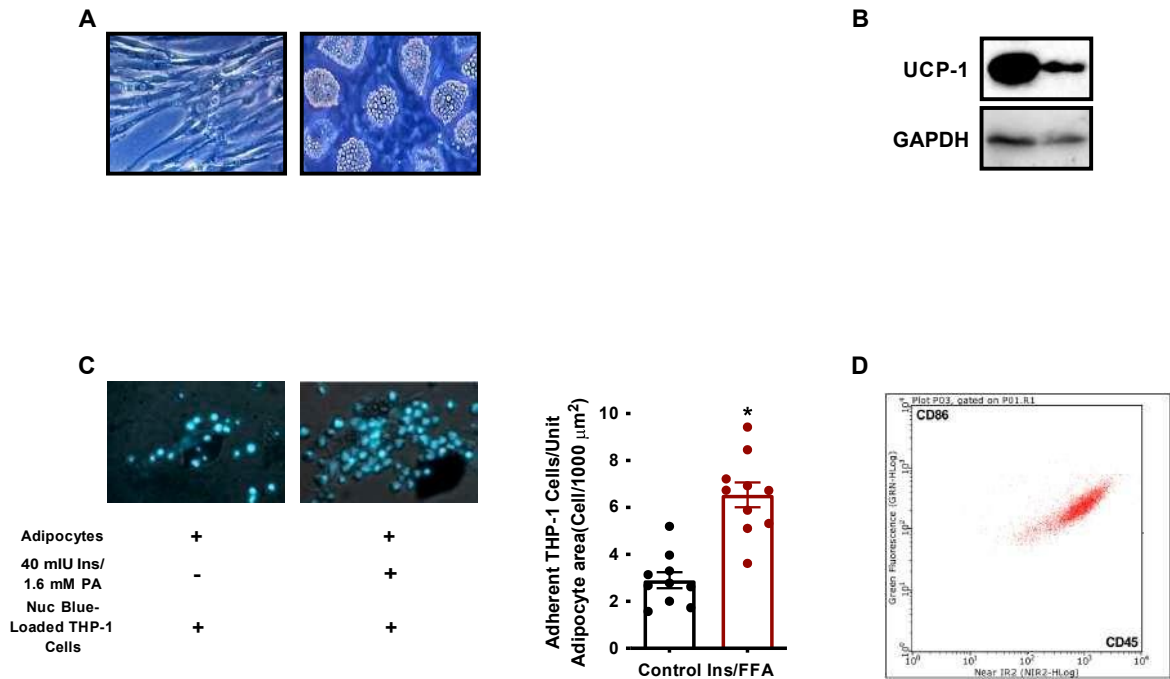


**Figure 30. Adipocytes differentiated from human bone marrow-derived mesenchymal stem cells respond to stress by 40 mIU/L insulin and 1.6 mM palmitic acid by an inflamed phenotype.**

Bone marrow mesenchymal stem cells before (left) and after (right) differentiation to adipocytes; (B) Representative western blotting showing UCP1 expression in different batches of differentiated adipocytes; (C) adipocyte exposure to a high insulin and palmitic acid stress leads to increased recruitment and adhesion of THP-1 monocytes; (D) Recruited monocytes show markers of differentiation into macrophages. For (C), statistical significance was tested by *t* test. \* denotes a *P*-value  $< 0.05$  vs. control culture medium without the increased insulin and palmitic acid.

### 3. Phosphorus supplementation ameliorates HC-induced alteration of PVAT macrophage polarization.

Resident macrophages contribute to adipose tissue homeostasis by adopting a wide range of activation phenotypes within the M1/M2 model of polarization. While M2 polarization is prevalent in a healthy adipose tissue, obesity and adipose expansion tend to alter the macrophages towards the M1 polarization concomitant with adipose tissue inflammation [326]. In line with the inflammatory changes, flow cytometric examination of the SVF of PVAT for macrophage markers showed that the ratio of CD45+/CD68+/CD86+ cells corresponding to M1 polarized macrophages to the CD45+/CD68+/CD163+ corresponding to M2 cells increased in animals receiving low Pi HC diet (Fig 31. A & B). Importantly, parallel decreases in M1/M2 cell ratio were seen in PVAT from rats fed HC diet with 0.75 and 1.5 mg/Kcal Pi (Fig 31. C & D). Results of the FACS experiments are summarized in Fig 31. E.

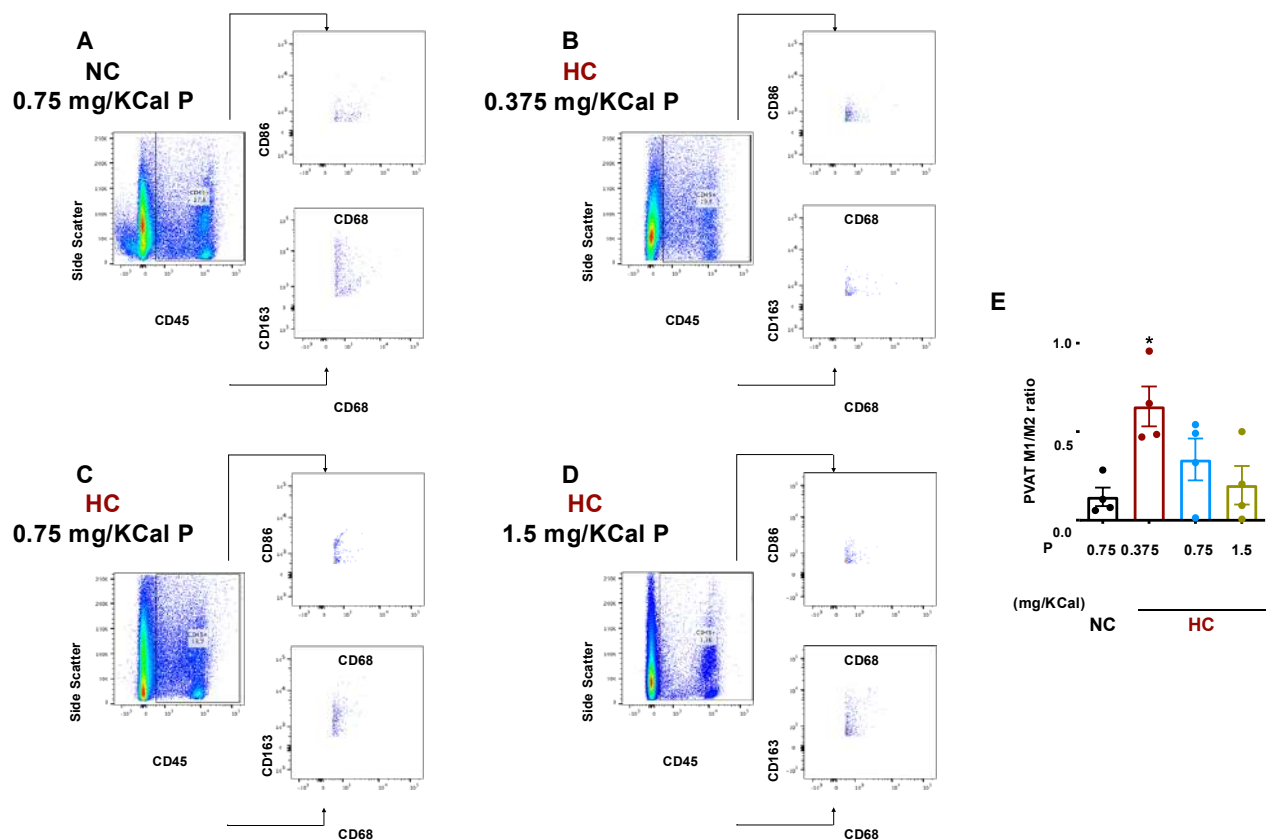


**Figure 31. Phosphorus supplementation restores PVAT macrophage polarization in rats fed a hypercaloric diet.**

A, B, C & D, Representative FACS scattergrams showing PVAT leukocytes expressing M1 vs. M2 macrophage polarization markers in rats fed normal chow (NC) or hypercaloric (HC) diet with different inorganic phosphorus (P) concentrations; E, summary of the ratio of M1/M2 PVAT macrophages from four different animals per group. Results shown are mean  $\pm$  SEM. Statistical significance was tested by one-way ANOVA followed by Tukey multiple comparisons test. \* denotes a  $P$ -value  $< 0.05$  vs. NC-fed rat values.

#### 4. Impact of dietary phosphorus on metabolic efficiency and protein metabolism.

Metabolic efficiency (weight gained in g/Kcal of energy intake) was assessed for every rat in the different diet groups as a measure of energy stored somatically vs. that dissipated by mitochondrial uncoupling [327]. As could be inferred from the increased energy intake without an equivalent rise in body weight, energy efficiency decreased in rats receiving HC: 0.375 Pi diet (Fig 32. A). Consistent with the putative UCP1 inhibitory effect, energy efficiency increased in rats receiving Pi supplemented HC diet (Fig 32. A). Interestingly, this reduced energy efficiency did not appear to be associated with increased protein metabolism as BUN did not change among control and HC-fed rat groups at different Pi levels (Fig 32. B).

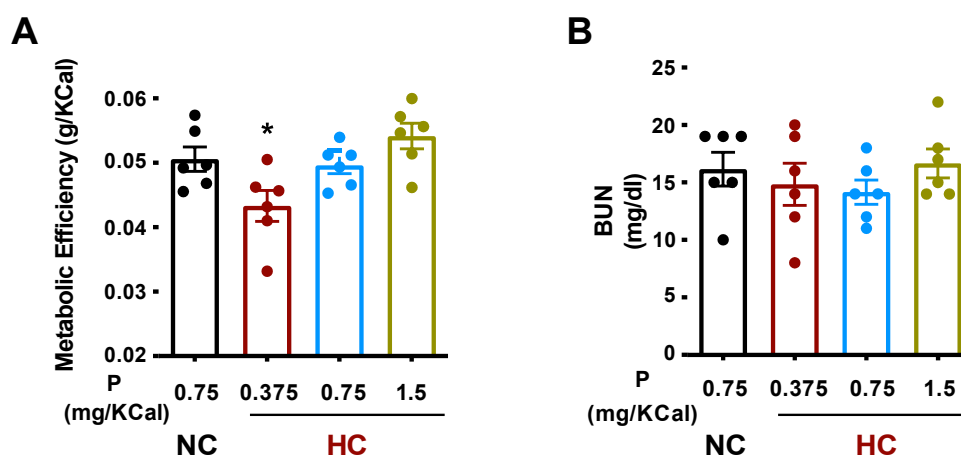


**Figure 32. Phosphorus supplementation restores metabolic efficiency without affecting protein metabolism.**

Phosphorus (Pi) deficient hypercaloric feeding (HC: 0.375 mg/Kcal) is associated with reduced metabolic efficiency (A) that is restored by Pi supplementation without affecting protein breakdown measured by blood urea nitrogen (BUN, B). Results shown are mean  $\pm$  SEM of observations from six different rats per group. Statistical significance was tested by one-way ANOVA followed by Tukey multiple comparisons test. \* denotes a *P*-value < 0.05 vs. NC-fed rat values.

**5. Phosphorus supplementation reverses cardiac autonomic neuropathy in HC-fed rats.**

PVAT inflammation in the non-obese prediabetic state induced by 12-week HC-diet feeding was consistently shown to be associated with parasympathetic cardiac autonomic neuropathy manifesting as a blunting of the bradycardic baroreflex in response to vasopressors [111, 314]. This was indeed the case in rats fed low Pi HC diet. An increased pressor effect was observed in these rats in response to increasing PE doses compared to rats on control diet (Fig 33.A & B) in line with the reported increased vascular contractility at this stage [7]. This was accompanied with an attenuation of the bradycardic response (Fig 33.. C). Significantly, both effects were ameliorated in rats fed HC diet supplemented with 1.5 mg/Kcal Pi. Restoration of parasympathetic autonomic function was confirmed by examination of the baroreceptor sensitivity in response to PE (Fig 33. D). Whereas the slope of the  $\Delta$ HR vs.  $\Delta$ MAP line was blunted in the low Pi HC-fed group, an increased sensitivity was observed in the 1.5 mg/Kcal supplemented HC group (Fig 33. E). As observed previously, no change in the sympathetic arm of the baroreflex was observed following HC feeding or after Pi supplementation (Data not shown).

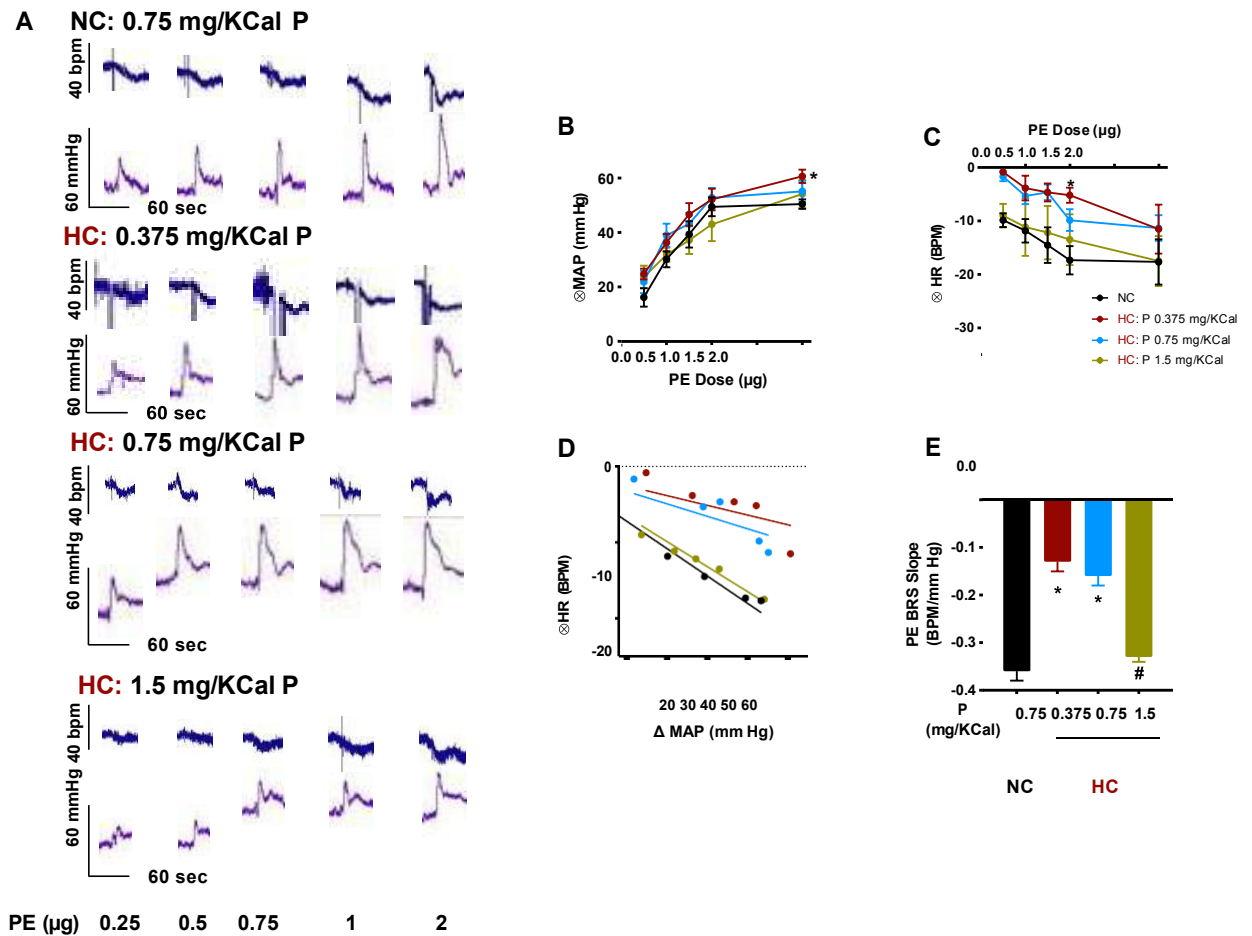


**Figure 33. Phosphorus supplementation of hypercaloric diet restores parasympathetic cardiac autonomic function.**

A, Representative tracings of pressor (MAP) and cardiac (HR) responses to increasing PE doses in NC- and HC-fed rats with different concentrations of P supplementation. Vertical scale bars represent MAP (60 mmHg) and HR (40 BPM) while horizontal scale bars represent time (60 sec); B, The pressor responses to increasing doses of PE; C, Reflex bradycardic responses to increasing BP; D, Best fit regression line for the correlation between  $\Delta$ MAP and reflex changes in HR in response to increasing doses of PE in NC- and HC-fed rats with different concentrations of P supplementation; E, Slope of the linear regression of the relationship between  $\Delta$ HR and  $\Delta$ MAP reflecting parasympathetic baroreceptor sensitivity (BRS). Depicted data represent mean $\pm$ SEM of values obtained from 6 rats/group. Statistical analysis was done by two-way ANOVA followed by Sidak's multiple comparisons test for B & C, and one-way ANOVA followed by Tukey multiple comparisons test for E. \* and # denote  $P < 0.05$  vs. NC and HC: 0.375 mg/Kcal P, respectively.



## 6. Phosphorus supplementation alleviates signs of cardiovascular deterioration.

Histochemical examination of heart mid-section from low Pi HC-fed rats showed signs of focal injury demonstrated by an elevated papillary muscle edema, as well as increased fibrosis, macrophage infiltration, and oxidative stress (Fig 34. A & B-E).

Pi supplementation appeared to have reversed these changes in a dose-dependent manner with the 1.5 mg/Kcal dose being consistently effective. In parallel, the low Pi HC-induced impairment of ventricular function shown as a decreased  $dP/dt_{max}$  was mitigated in rats fed Pi supplemented HC diet (Fig 34. F).

On the other hand, similar changes were observed for aortic tissue. While low Pi HC feeding led to increased aortic medial thickness, fibrosis, and oxidative stress, Pi supplementation, particularly the 1.5 mg/Kcal dose, was able to reverse these changes. Representative micrographs are shown in Fig 35.A and summary data in Fig 35. B-D.

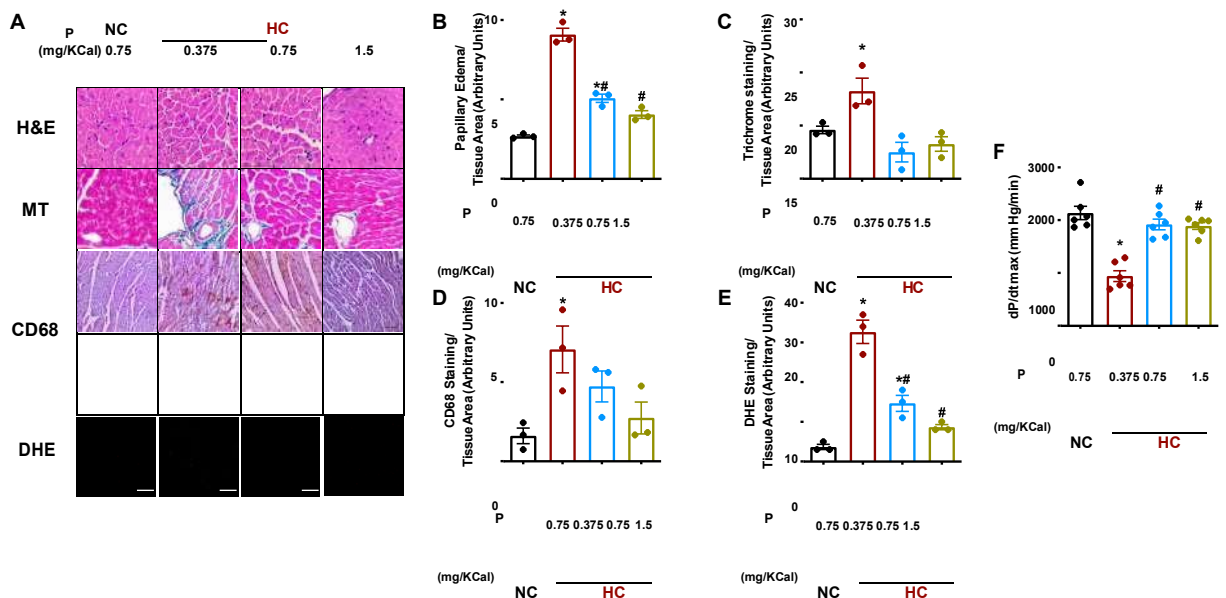


**Figure 34. Impact of inorganic phosphorus supplementation on histopathological and molecular signs of cardiac impairment induced by hypercaloric feeding.**

A, Representative micrographs of histopathological, immunohistochemical, and DHE staining in heart mid-section of NC- and HC-fed rats with different concentrations of P supplementation. Data presented are serial sections taken from the same tissues and are representative of 9 sections from 3 different rats in each group. Scale bars are (top to bottom): 25, 25, 50, and 50  $\mu$ m. Fibrotic staining appears as a blue color on a red

background, CD68 staining appears as a brown color on a background of H&E counter

stain, while DHE staining appears as red fluorescence on a black background. Quantification values of area of interfibrillar edema (B), as well as the intensity of Masson trichrome (C), CD68 (D), and DHE (E) staining normalized to ventricular tissue area. F, Cardiac contractility assessed by maximal rate of rise of ventricular pressure ( $dP/dt_{max}$ ). Statistical significance was determined by ANOVA followed by Tukey *post hoc* test. \* and # denote  $P < 0.05$  compared to NC and HC: 0.375 mg/Kcal rats, respectively.

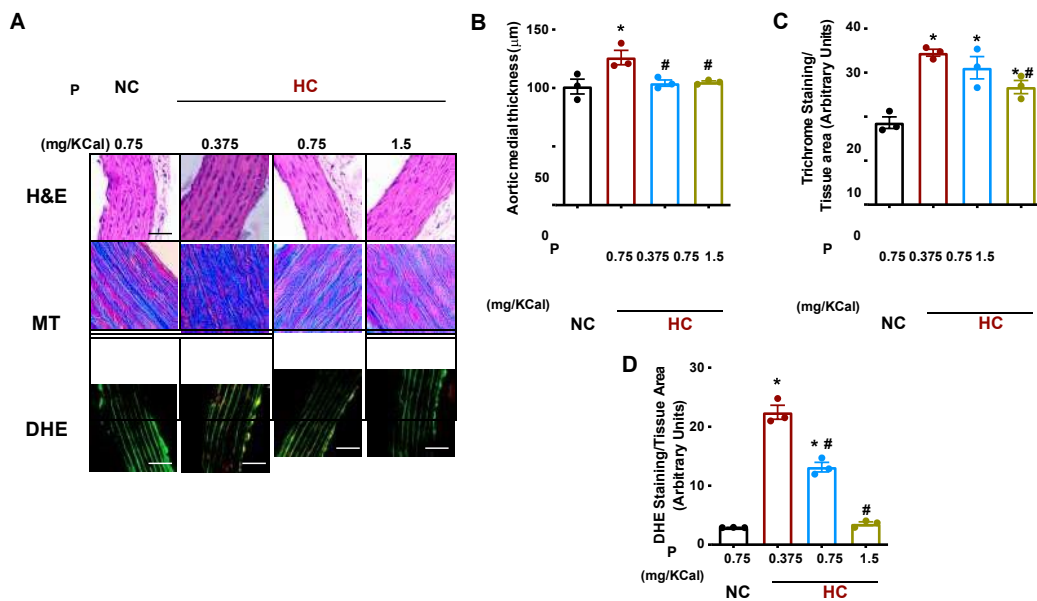


**Figure 35. Impact of inorganic phosphorus supplementation on histopathological and molecular signs of vascular impairment induced by hypercaloric feeding.**

A, Representative micrographs of histopathological and DHE staining in aortas of NC- and HC-fed rats with different concentrations of P supplementation. Data presented are serial sections taken from the same tissues and are representative of 9 sections from 3 different rats in each group. Scale bars are (top to bottom): 50, 25, and 50 µm. Fibrotic staining appears as a blue color on a red background while DHE staining appears as red fluorescence on a background of green collagen autofluorescence. Quantification values of medial thickness (B), as well as the intensity of Masson trichrome (C) and DHE (D) staining normalized to aortic tissue area. Statistical significance was determined by ANOVA followed by Tukey *post hoc* test. \* and # denote  $P < 0.05$  compared to NC and HC: 0.375 mg/Kcal rats, respectively.

**7. Phosphorus supplementation ameliorates HC-diet induced cerebrovascular dysfunction and the associated brainstem changes.**

Consistent with our previous results [253], HC feeding was associated with increased cerebrovascular myogenic tone (Fig 36. A & B). Such an increased cerebrovascular reactivity within the operational pressure range of the middle cerebral arteriole was associated with cerebral hypoxia and increased neuroinflammation [253]. This was indeed the case in HC-fed rats showing increased oxidative stress and IBA1 staining indicative of microglial activation in the brain stem (Fig 36. C). Interestingly, consistent with its effect on PVAT inflammation, cardiac autonomic and cardiovascular functions, Pi supplementation reduced the cerebrovascular tone and the associated brainstem oxidative stress and microglial activation (Fig 36. D & E).

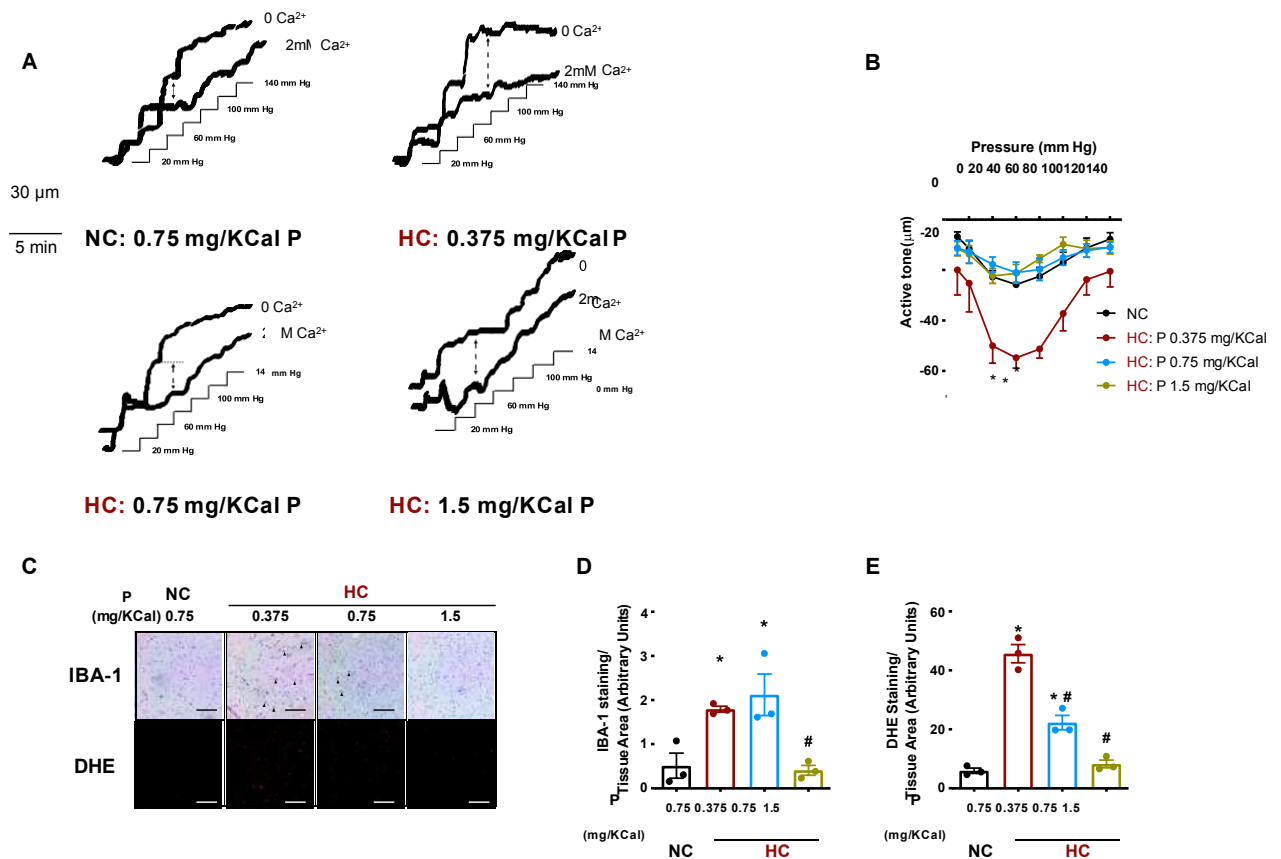


**Figure 36. Inorganic phosphorus supplementation reverses cerebrovascular**

**hypercontractility and brainstem inflammation induced by hypercaloric feeding.**

A, Representative tracings of pressure myography experiments depicting changes in rat middle cerebral artery diameter as a function of change in intravascular pressure in vessel segments from NC- (top left), HC: 0.375 mg/Kcal P-fed (top right), HC: 0.75 mg/Kcal P-fed (bottom left), and HC: 1.5 mg/Kcal P-fed (bottom right) rats in presence (2 mM Ca) and absence (-Ca) of calcium in the bath solution; B, Active tone generated by rat middle cerebral artery in vessel segments as a function of pressure change ( $n = 4$ ). Active tone is the difference in diameter of the vessel at a given intravascular pressure value in absence and presence of calcium as indicated by the double-headed arrow on the tracings at 60 mm Hg; C, Representative micrographs of IBA1 immunohistochemical and DHE staining in brainstems of NC- and HC-fed rats with different concentrations of P supplementation. Data presented are serial sections taken from the same tissues and are representative of 9 sections from 3 different rats in each group. Scale bars are 100  $\mu\text{m}$ . IBA1 staining appears as a brown color on a background of H&E counter stain, while DHE staining appears as red fluorescence on a black background. Quantification values of IBA1 staining (D), as well as the intensity DHE staining (E) normalized to brainstem tissue area. Statistical significance was determined by two-way ANOVA followed by Sidak's *post hoc* test for (B) and one-way ANOVA followed by Tukey *post hoc* test for (D) and (E). \* and # denote  $P < 0.05$  compared to NC and HC: 0.375 mg/Kcal rats, respectively.

**8. *Hypercaloric intake, rather than phosphorus deficiency, precipitates PVAT, metabolic, and cardiovascular alterations, which can be reversed upon reinstating dietary phosphorus.***

To examine whether PVAT inflammation and the associated cardiovascular changes in rats fed HC diet occur due to increased calorie intake or Pi deficiency, an additional group of rats fed a control diet with a Pi concentration equivalent to that in HC diet (0.375 mg/Kcal) was used. Moreover, the impact of Pi reinstatement after a ten-week exposure to low Pi HC diet was examined by switching these rats to HC diet supplemented with 1.5 mg/Kcal Pi for the last two weeks of the feeding duration. Fig. 8.1 depicts the gross hemodynamic and metabolic outcome of these protocols compared to rats fed control and low Pi HC diet for twelve weeks. While rats in the HC diet with Pi reinstatement consumed more calories as expected, those on low Pi control diet did not (Fig 37. A). Whereas these dietary manipulations had no bearing on blood glucose

level, blood pressure and ejection fraction (Fig 37. B, C, G & H), only HC-fed rats with Pi reinstatement had an increased adiposity and serum insulin like those in rats on low Pi HC-fed rats (Fig 37. D & F). Moreover, a two-week reinstatement of Pi at the 1.5 mg/kcal dose did not appear to alter metabolic efficiency (Fig 37. I). However, despite the lack of effect on insulin, Pi reintroduction reduced serum triglyceride levels. Serum triglyceride level in rats fed a low Pi control chow was also comparable to that in rats receiving control diet with normal Pi content (Fig 37. E). Serum Pi, calcium, and magnesium levels in the low Pi control diet group and those in the Pi reinstatement group were not different from either the control diet or Pi-deficient HC diet groups (Fig 4.32 ). Significantly, while Pi reinstatement on top of HC-diet improved ventricular function as measured by  $dP/dt_{max}$ , rats on a low Pi control diet appeared to have a reduced ventricular contractility (Fig 37. J).

From a different perspective, molecular examination revealed no signs of PVAT inflammation in either rat group. Indeed, UCP1 and HIF1- $\alpha$  PVAT expression levels were similar both in rats fed HC: 0.375 and receiving a two-week 1.5 mg/Kcal Pi supplementation as well as those receiving the low Pi control diet compared to control rats (Fig 38. A). PVAT IL-1 $\beta$  levels were very low in both groups and no different from those in rats receiving control chow (Fig 38. A). As opposed to rats receiving 1.5 mg/Kcal Pi supplemented HC-diet for the full duration, those in which Pi was reintroduced for the last two weeks of feeding showed increased PVAT adipocyte size. No such increase was seen in rats fed a low Pi control diet (Fig 38. B).

The lack on inflammatory changes in PVAT of these rats reflected on the histological and molecular markers of cardiac and vascular damage elevated in rats fed HC: 0.375 Pi diet. No signs of papillary muscle focal injury, cardiac fibrosis,

macrophage infiltration, and oxidative stress were seen in heart mid-sections of either rats group (Fig 38. C). Similarly, aortic intimal thickness, trichrome and DHE staining were within the same levels as in rats receiving control diet with standard phosphate content (Fig 38. D).

On the other hand, though increased vascular contractility in response to PE lingered in both groups, the lack of Pi in control diet did not seem to induce parasympathetic autonomic neuropathy, and Pi reinstatement reversed the bradycardic reflex blunting induced by HC: 0.375 Pi diet feeding as evident from the baroreflex slopes (Fig 39. B). Indeed, the correction of parasympathetic neuropathy could be related to the lack of signs of brainstem neuroinflammation. Both IBA1 and DHE staining were at levels very similar to control rats in both groups (Fig 39. C & D).

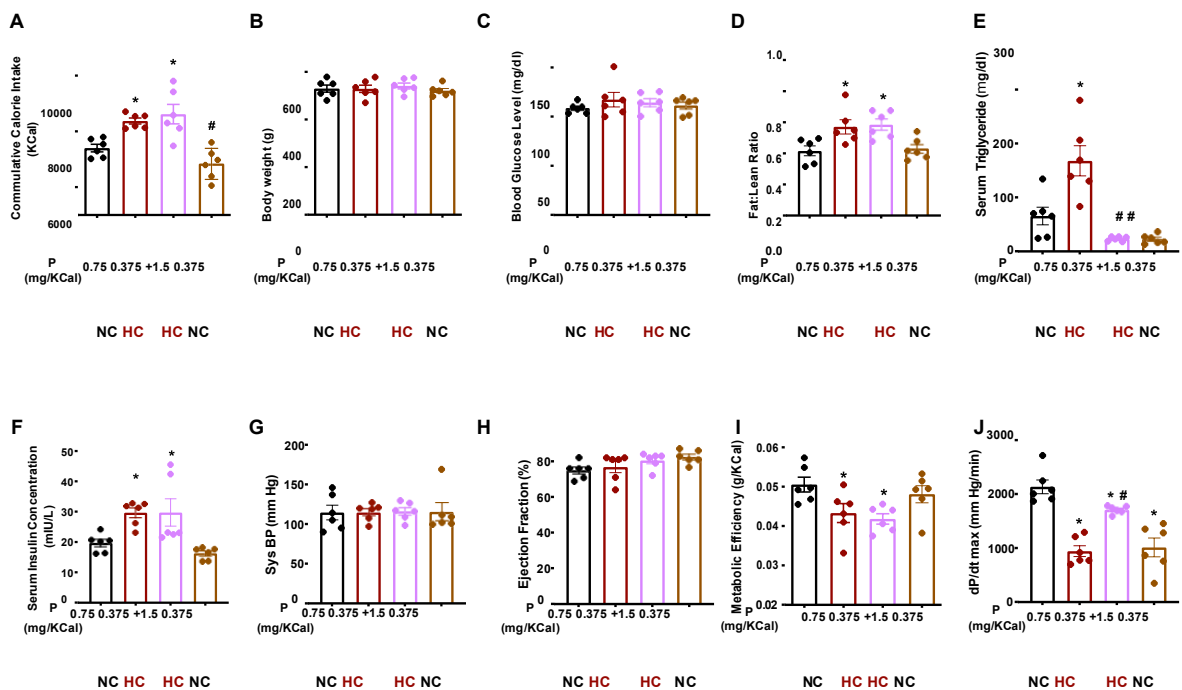


**Figure 37. Gross metabolic and functional parameters following low phosphorus control diet feeding or phosphorus reinstatement after a ten-week high calorie phosphorus deficient diet feeding.**



The differences in calorie consumption (A) in different groups for the twelve-week duration did not reflect into changes in body weight (B), fasting blood glucose (C),

systolic blood pressure (Sys BP, G), and Ejection fraction (H); yet increased fat:lean ratio (D), serum triglycerides (E), and fasting serum insulin (F) were not seen in the low Pi control diet group with only serum triglycerides reversed by Pi reinstatement. Low Pi control diet and Pi reinstatement did not affect metabolic efficiency (I) compared to control rats or those receiving low Pi HC diet, respectively. J, Systolic ventricular function in different groups measured as  $dP/dt_{max}$ . Results shown are mean  $\pm$  SEM of observations from six different rats per group. Statistical significance was tested by one-way ANOVA followed by Tukey *post hoc* test. \* denotes a *P*-value  $< 0.05$  vs. NC while # denotes a *P*-value  $< 0.05$  vs. HC: 0.375 mg/Kcal P.

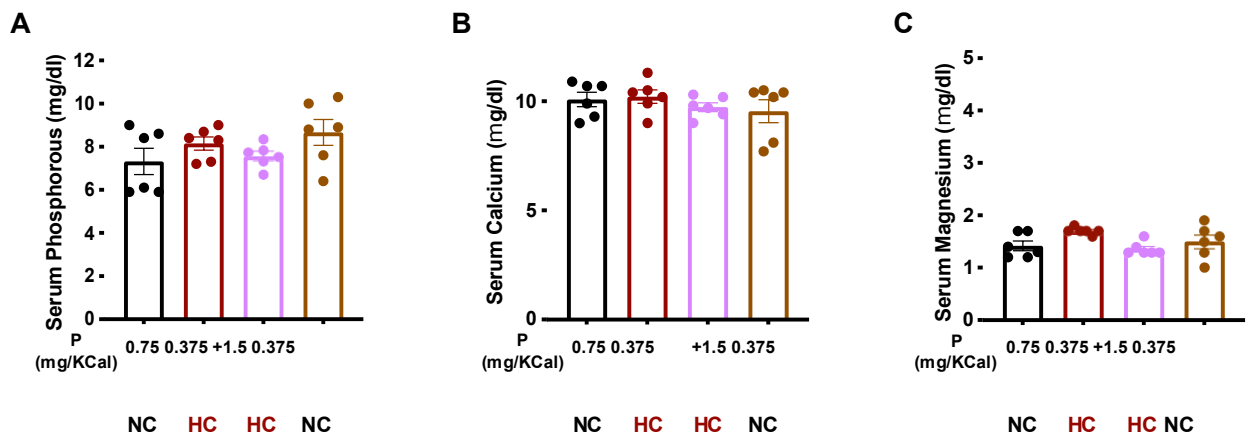


**Figure 38. Serum Pi, calcium and magnesium following low phosphorus control diet feeding or phosphorus reinstatement after a ten-week high calorie phosphorus deficient diet feeding.**

Different dietary interventions do not affect serum Pi (A), calcium (B) or magnesium (C) concentrations. Results shown are mean  $\pm$  SEM of observations from six different rats per group. Statistical significance was tested by one-way ANOVA followed by Tukey multiple comparisons test.

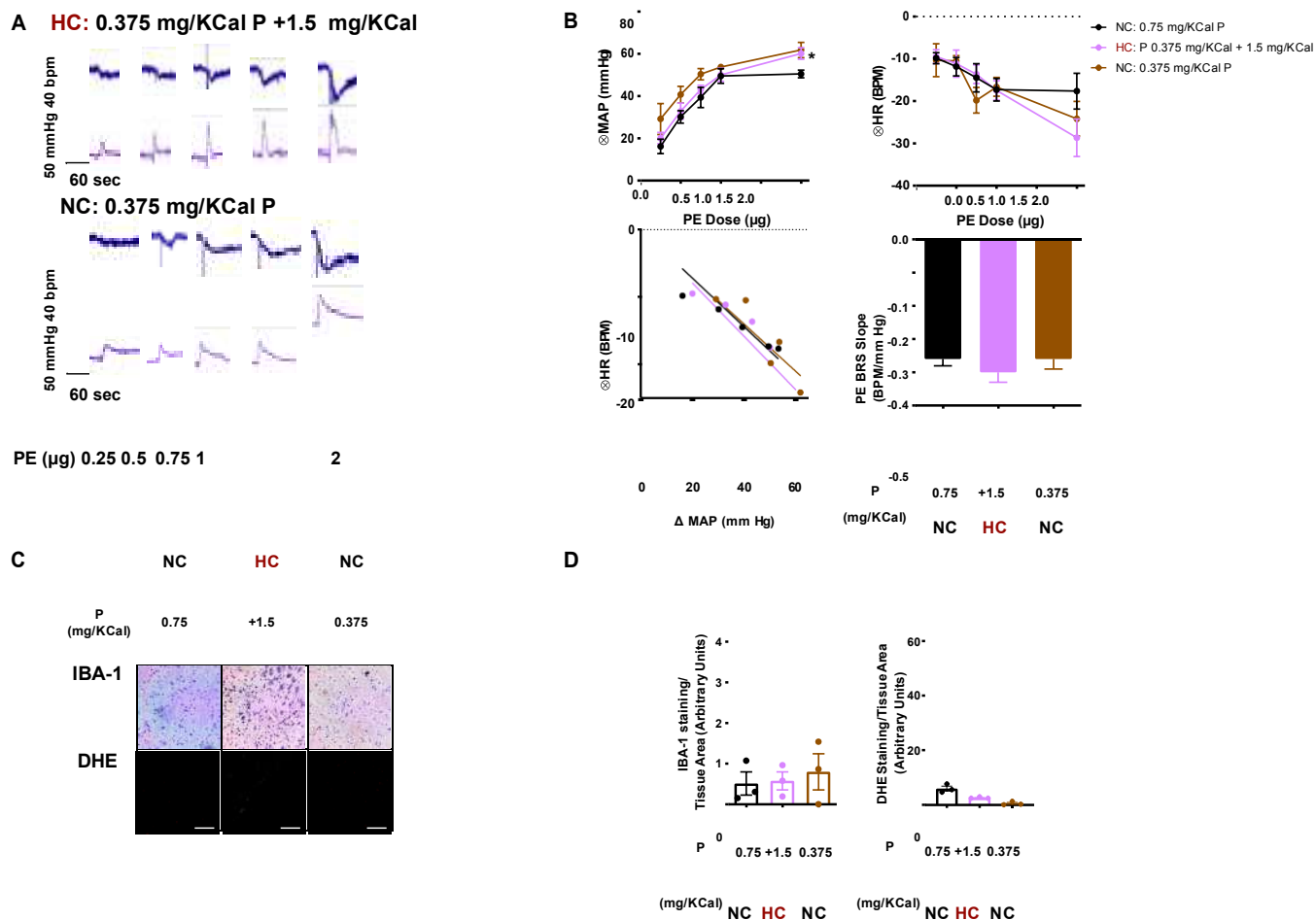


**Figure 39. Impact of low phosphorus control diet feeding or phosphorus reinstatement after a ten-week high calorie phosphorus deficient diet feeding on parasympathetic cardiac autonomic function and brainstem inflammation.**

A, Representative tracings of pressor (MAP) and cardiac (HR) responses to increasing PE doses in low Pi NC-fed and Pi reinstatement rats. Vertical scale bars represent MAP (50 mmHg) and HR (40 BPM) while horizontal scale bars represent time (60 sec); B, The pressor responses to increasing doses of PE (top left), reflex bradycardic responses to increasing BP (top right), best fit regression line for the correlation between  $\Delta$ MAP and reflex changes in HR in response to increasing doses of PE (bottom left), and slope of the linear regression of the relationship between  $\Delta$ HR and  $\Delta$ MAP reflecting parasympathetic baroreceptor sensitivity (BRS, bottom right) Depicted data represent mean $\pm$ SEM of values obtained from 6 rats/group. C, Representative micrographs of IBA1 immunohistochemical and DHE staining in brainstems of low Pi NC-fed and Pi reinstatement rats. Data presented are serial sections taken from the same tissues and are representative of 9 sections from 3 different rats in each group. Scale bars are 100  $\mu$ m. IBA1 staining appears as a brown color on a background of H&E counter stain, while DHE staining appears as red fluorescence on a black background; D, Quantification values of IBA1 staining (left), as well as the intensity DHE staining (right) normalized to brainstem tissue area. Statistical analysis was done by two-way ANOVA followed by Sidak's multiple comparisons test for  $\Delta$ MAP and  $\Delta$ HR, and one-way ANOVA followed by Tukey multiple comparisons test for the BRS slope and quantification values in E. \*

denotes  $P < 0.05$  vs. NC.

**9. *Dietary interventions with different phosphorus levels do not appear to induce renal structural alterations.***

Increased dietary Pi carries the risk of renal damage characterized by tubular necrosis and calcium phosphate deposition [328]. To investigate whether the Pi amounts used in the present study induced renal changes, we have undergone histological examination of kidneys from all groups. PAS staining demonstrated no changes in tubular or glomerular structure (Fig 40 ). Similarly, von Kossa staining showed no calcium deposits in the renal cortices of kidneys from rats in different groups (Fig 40 ).

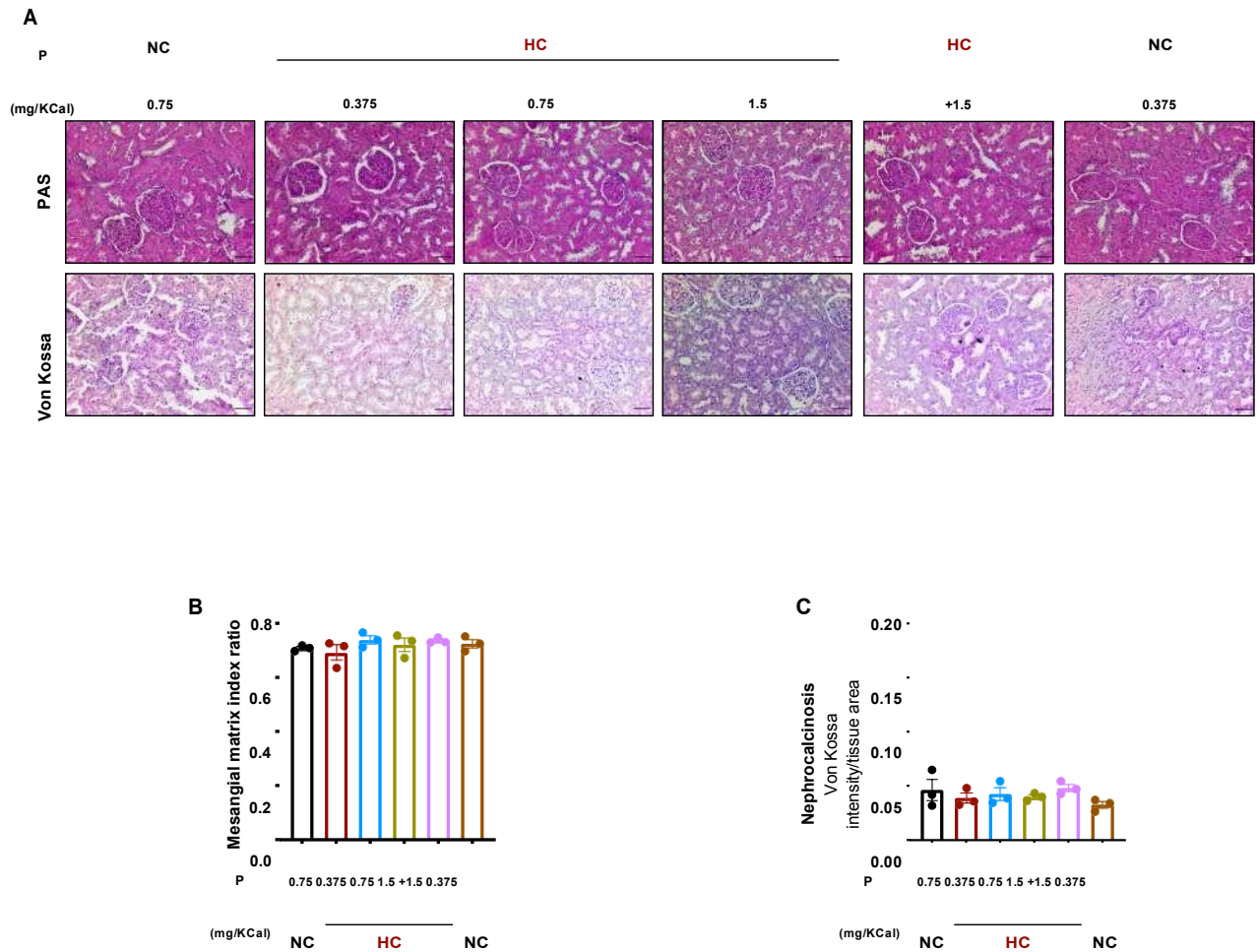


**Figure 40. Impact of different phosphate and fat levels in diet on renal microscopical structure and calcium deposition.**

A, Representative micrographs of PAS (top) and von Kossa (bottom) stained renal cortical sections showing normal glomerular and tubular structure and absence of calcium deposits in kidneys from different treatment groups. Data presented are serial sections taken from the same tissues and are representative of 9 sections from 3 different rats in each group. Scale bars are 50  $\mu$ m. von Kossa staining typically appear as brown staining on a background of H&E counter stain. Quantification values of mesangial matrix ratio reflecting glomerular structure (B), as well as the intensity of von Kossa stain (C). Statistical significance was tested by one-way ANOVA followed by Tukey multiple comparisons test.

## CHAPTER V

### DISCUSSION

#### **A. Sexual Dimorphism of Adipose Tissue Remodeling and Cardiovascular Dysfunction in Prediabetes.**

It is well established that the incidence of T2DM and its complications are affected by a wide set of factors; of which some are modifiable such as caloric intake, macro- and micronutrient modifications, and physical activity. Non-modifiable factors include genetic predisposition, age, and sex hormones [1, 148]. These factors have a significant impact not only in symptomatic patients, but also in the subclinical stages, such as prediabetes, where early cardiovascular and metabolic derangements occur [8]. Indeed, the state of sex hormones remains one of the most important non-modifiable risk factors in metabolic and cardiovascular dysfunction [148-150, 329, 330]. It is widely accepted that premenopausal women are more resilient to metabolic and cardiovascular diseases than men in the same age, however, this advantage is lost after menopause [149, 330].

Indeed, non-obese prediabetes characterized by hyperinsulinemia and insulin resistance in presence of normal blood glucose levels was induced by HC feeding in male rats, whereas intact females were protected from this prediabetic metabolic phenotype. Moreover, ovariectomized (OVX) female rats were more vulnerable to diet induced prediabetes like their male counterparts. As expected, HC feeding in OVX rats induced obesity and increased adiposity (F:L ratio). Adiposity and weight gain are usually recorded in postmenopausal women [156]. Additionally, estrogens appear to protect against adipocyte hypertrophy in different depots regardless of the diet [151, 172], and the metabolic and cardiovascular privilege in premenopausal women and in

those who are receiving HRT is mainly driven by estrogens [149, 155]. Indeed, exogenous estrogen treatment was found to correct metabolic and cardiovascular abnormalities [167, 331]. Besides, the shielding properties of estrogen from diet induced adipose expansion and inflammation, are suggested to be mediating its cardio protective effect [172, 212].

In our rat model, intact females did not suffer from negative remodeling of PVAT except for UCP1 upregulation, which seemed to be estrogen independent, as in E2 treated OVX rats it was not affected. Sex differential expression of UCP1 and the role of estrogen in modulating UCP1 in adipocytes is controversial. For instance some studies found that estrogen is only involved in the early stages of adipogenesis [332], mainly via ER $\alpha$  [333], where its selective agonist increased UCP1 expression in *in vitro* experiments in a manner mediated by AMPK activation [334]. At the same time, others found it to be positively associated with ERs levels and age, and was depot dependent [335]. On the other hand, data from human adipose tissue and murine models showed that premenopausal females have higher UCP1 and MT activity in BAT compared to men, an observation that was lost after ovariectomy [336]. Nevertheless, one study reported the increase of PVAT UCP1 mRNA in intact female mice in response to WD [197]. Conversely, another study on Wistar female rats reported the decrease of UCP1 expression, hypertrophy and reduced MT density in PVAT in response to WD [223]. Interestingly, our HC diet did not appear to affect MT functional balance in females, the fission:fusion rate in the mitochondrial mesh, as P-DRP1 (ser616), which is an indicator of MT fission, only increased in HC fed male rats but not their female counterparts. Increased mitochondrial sensitivity and adaptive response to HFD and obesity in females was observed mainly in BAT and WAT, which was lost in



males [194, 337, 338]. In this context, female mice on HFD had adaptive modulation in MT community in BAT, as they had higher complex I and II and optimized respiratory rate compared to Lean females and males on HFD [337]. Mitochondrial fission in PVAT was observed consistently in HC fed males [222], but in this cohort of female rat MT fission was not observed, which suggest a more resilient or adaptive MT in the adipose. Moreover, our previous findings on PVAT detected an increase in HIF1- $\alpha$  in response in HC feeding in males explained by the increased oxygen consumption in response to UCP1 upregulation together with the reduced supply due to hypertrophy, leading to an exacerbated hypoxic state [325]. Interestingly, in females despite the increase of PVAT UCP1 in response to HC feeding, they were protected from ACs hypertrophy, which compensated for the oxygen demand by increased UCP1. Moreover, estrogen plays an important role in HIF1- $\alpha$  degradation and hence inhibiting the hypoxia machinery and downstream effect [339, 340]. A parallel result was observed in HC-fed OVX female rats where E2 treatment reduced HIF1- $\alpha$  in PVAT. E2 treatment improved hypoxia, reduced AC size, and also reduced inflammatory markers. These findings further confirm the role of hypoxia in provoking inflammation in PVAT [325] making the hypoxic machinery a tempting target for preventing negative adipose remodeling and the subsequent metabolic and cardiovascular insults providing further context for the use of Pi at this stage as explained above.

Our rat model fed for 12 weeks on HC diet showed a very confined and PVAT specific adipose negative remodeling [222, 325, 341]. In addition to changes induced in PVAT after 24 weeks of HC feeding in male rats, BAT was the second depot to be affected by HC feeding. It had hypertrophic ACs, increased MT fission, and increased UCP1 expression. However, these changes were not enough to incite hypoxia and the

following inflammatory state in BAT. While in intact females HC only affected BAT adipocytes' size. Although one might expect UCP1 to be upregulated in intact female BAT, since it is a highly innervated tissue and females have high sympathetic activation [202, 336, 342]. Thus, one might speculate that the increased UCP1 expression induced in BAT of HC fed males is driven by the insulin mediated sympathetic overflow [343], where HFD was shown to activate sympathetic flow more prominently in males [225]. Moreover, it was reported that female Wistar rats had lower  $\beta_3$ -AR expression in BAT following HFD feeding [198]. Surprisingly, unlike HFD our HC diet did not provoke any dysfunction in WAT [344]. Neither males nor ovulating females had any changes in GAT in response to HC feeding, however OVX seemed to bring forth hypertrophy, which was corrected by E2 treatment, suggesting the sex-depot dependent variability in response to the same energy stimuli. Indeed, estrogen deficiency provoked hypertrophy in different depots such as PVAT [212] and GAT[170]. These results point to a possible elevated vulnerability of PVAT and then BAT in males upon mild energy stress, and despite being small pools they were able to significantly decrease metabolic efficiency in HC fed male and female rats as well as provoke metabolic and cardiovascular derangements.

Undoubtedly, insulin resistance and glucose intolerance remain the most vital players in fueling metabolic and cardiovascular derangements mediated by adiposopathy [12, 38, 150, 345]. Several mechanisms were suggested on how estrogen exert positive outcomes in adipose tissue via modulating its response to insulin. One suggested pathway is the role of estrogen in preserving insulin sensitivity [156, 175, 207, 344]. Estrogens are known to improve insulin sensitivity in ACs through the increased phosphorylation of IRS-1 [346]. Indeed, our results show that only male rats

develop hyperinsulinemia and insulin resistance in response to HC feeding. Moreover, estrogen deficiency in OVX rats triggered hyperinsulinemia and insulin resistance upon HC feeding, which was corrected by estrogen treatment. As such, hyperinsulinemia in our model can be considered the main driver of PVAT negative remodeling in males and OVX females, as both exogenous and endogenous estrogens appear to be sufficient to prevent insulin resistance.

Diet induced PVAT dysfunction is known to induce vascular complications more prominently in males [213]. Even in the absence of systemic inflammation, HC diet induced PVAT inflammation which aggravated cardiovascular dysfunction. In males it was associated with increased vascular reactivity and blunted parasympathetic baroreflex sensitivity, which were tied to increased paracrine IL-1 $\beta$  production from the inflamed PVAT [7, 314]. Intact females scored better cardiovascular and parasympathetic outcomes. However, HC fed OVX females had blunted parasympathetic baroreflex sensitivity, which was prevented with E2 treatment. Since hyperinsulinemia is known to induce sympathetic overflow [106], and our HC fed males and ovariectomized females had hyperinsulinemia and autonomic imbalance, we can safely suggest that our HC model develops the preclinical stage of CAN, similar to prediabetic humans [6, 107], indicative of the early cardiovascular dysfunction in the absence of apparent obesity or hyperglycemia in the case of males, and the obese prediabetic postmenopausal females.

## **B. Sex Dependent Effect of Therapeutic Fasting on Prediabetic Adipose and Cardiovascular Dysfunction.**

Since overnutrition and positive energy balance are key triggers of cardiometabolic dysfunction, calorie restriction becomes an attractive intervention to study as a possible

way to prevent, improve and even treat their manifestations. Time restricted feeding regimens, referred to as intermittent fasting (IF) [226, 227] showed a strong positive impact on the metabolic state of obese and non-obese human subjects and animal models [226, 228]. Nevertheless, the exact mechanism of how these fasting regimens improve the metabolic state are still not fully understood. Specifically, despite the many desired outcomes reported for calorie restriction, isocaloric IF seems to have a prominent effect on the metabolic health [228, 232, 233]. In our therapeutic fasting (TF) regimen caloric intake was not restricted, and cumulative caloric intake was similar to the controls. Body weight did not change as well, but adiposity was reduced. Indeed, the change in fat pad size was found to be triggered by TF alone, regardless of the daily caloric intake, and independent of the change in body weight as animal studies showed a decrease in size and weight of adipose depots, with mild or no change in total body weight [81, 235-237]. Moreover, TF reversed insulin resistance and hyperinsulinemia, which was observed in other animal models and human studies [228, 229].

Moreover, not only did TF improve insulin resistance, but it was also found to produce a positive impact on AT remodeling occurring in diet-induced metabolic dysfunction were [229, 238]. Different fasting regimens found to reduce AC size in different pools [238], and since HC induced hypertrophy in PVAT and BAT, both were corrected by TF in male and ovariectomized females. HC induced PVAT dysfunction was corrected by 12 weeks of fasting, it prevented diet induced MT fission, hypoxia, and inflammation, which were observed in our previous work [238]. Increased UCP1 expression has been considered one of the major outcomes of AT remodeling by IF, as fasting induced adipose browning was linked to many metabolic and cardiovascular positive outcomes [230, 231]. Moreover, both the same IF regimen and every other

day (EOD) fasting for 4 weeks were able to evoke an increased energy expenditure and UCP1 expression in WAT tissue in diet-induced obese mice in a manner that also involved reduction of inflammatory markers [81, 231]. Yet, while IF reduced WAT fat mass in both obese mice models and obese human subjects, no UCP1 upregulation was observed in humans [81]. In our non-obese prediabetic rat model, WAT was not affected by HC feeding in male rats, and did not exert any signs of adiposopathy, hence, fasting-induced browning in this case was not expected. However, TF was able to correct the pathological levels of UCP1 in PVAT and BAT of HC fed males, which is a positive outcome of IF that was not previously reported in the literature.

Taken together, one can conclude that the positive impact of IF on AT is expected to ameliorate the cardiovascular manifestations of cardiometabolic syndrome. Indeed, the American heart association (AHA) included IF as one of the dietary measures to prevent CVDs. Based on human studies, AHA concluded that that IF, regardless of its effect on weight, improves lipid profile, lowers LDL and cholesterol and increases HDL, in addition to improving insulin sensitivity, indicated by reduced HOMA-IR, with no change in blood glucose level [228]. As well, human and animal studies indicated that IF reduced blood pressure [261-263] and heart rate [262]. As expected, TF seemed to prevent systolic hypertension induced by HC feeding, improve vascular sensitivity to PE, preserve autonomic balance, and improve baroreceptor sensitivity. This might be also due to an effect on sympathetic flow as IF reduced the low frequency component in the diastolic blood pressure variability, a marker of reduced sympathetic activity, and increased high frequency component in heart rate variability, which is reflective of the parasympathetic tone, both being indicative of positive modulation of cardiovascular state [264]. Furthermore, IF improved endothelial dependent vasorelaxation in healthy

men [266]. Significantly, IF exerted a similar pattern in Wistar male rats, as it showed an improved aortic endothelial depend relaxation [267]. Indeed, TF in our prediabetic model appeared to improve ACh induced vasorelaxation and restoring HC induced endothelial dysfunction in male rats.

There has been no conclusive evidence regarding sex-mediated therapeutic fasting outcomes. Some human and animal studies indicated the absence of sex differences on some metabolic outcomes such as insulin sensitivity, glucose tolerance, plasma lipid profile, blood pressure, adiposity, and total body weight between obese men and women [272-274]. Since HC feeding in OVX rats induced similar metabolic and cardiovascular derangements to those in males, which were corrected by E2 treatment as explained in the previous section, we examined whether therapeutic fasting would correct HC induced metabolic anomalies in estrogen deficient female rats. In mice despite being ovariectomized, IF was able to exhibit its beneficial effects even while the animals being freely fed on HFD, as these mice had better weight loss, insulin sensitivity, and glucose tolerance compared to the non-fasting counterparts [275]. Indeed, twelve weeks of TF in ovariectomized female rats were able to correct the obese prediabetic metabolic phenotype induced by HC feeding in OVX females by improving adiposity and hyperinsulinemia. Moreover, TF appeared to prevent HC driven PVAT dysfunction, which was exaggerated in females after OVX, by correcting AC size and UCP1 level, consequently promoting a normoxic state and preventing the inevitable inflammation. Parallel to positive alterations in PVAT in response to TF, cardiovascular outcomes were promising, as it improved BRS in response to PE compared to the non-fasting OVX females.

Altogether, the current therapeutic fasting regimen induced positive metabolic and cardiovascular outcomes in prediabetic males and postmenopausal female rats, even without calorie restriction or dietary modifications. In the latter group, it was able to overcome the cardiovascular insults mediated by estrogen deficiency. Understanding the mechanism of how fasting generate its positive outcomes in this context will be our next step. In the absence of caloric restriction and dietary modifications, we hypothesize that gut microbiome (GM) and its metabolites play a crucial role in mediating these metabolic outcomes [347]. As GM composition seemed to be affected by not only the dietary value of food [347-350], but also by the diurnal patterns of food consumption [351-353]. Importantly, our proposed TF regime is non-intrusive, safe, and translational as it requires minimal changes in dietary intake, since adherence to strict dietary changes remains a huge challenge for patients [354] [355], making it a promising intervention in prediabetic men and postmenopausal women.

### **C. Inorganic Phosphate Supplementation and Adipose Mediated Cardiovascular Dysfunction.**

The complexity of the pathophysiology linking metabolic dysfunction in type 2 diabetes to cardiovascular complications has long been recognized to extend beyond simple perturbations of blood glucose and lipid levels [356]. Yet, it was not until fairly recently that investigation of pharmacological therapies for metabolic disease focused on their cardiovascular benefits as desirable outcomes independent of their impact on hyperglycemia and blood lipid levels [357-359]. While undoubtedly useful, these drugs were originally designed as hypoglycemic tools. Despite the long standing and exponentially growing evidence implicating the involvement of inflammation, particularly that in adipose tissue, in the cardiometabolic complications, direct

interventions with this pathology have not been forthcoming [137, 360-362]. Here, we propose dietary phosphate supplementation as a simple approach to mitigate PVAT inflammation and reduce the associated cardiovascular consequences. Not only did prolonged Pi supplementation of a hypercaloric western diet reduce signs of PVAT inflammation, cardiac autonomic and cerebrovascular dysfunction, in addition to molecular and histopathological indicators of damage in the heart, blood vessels and brainstem, a two-week treatment period had similar outcomes as well.

Typically, western diets known to induce cardiovascular impairment in humans and animal models are rich in refined sugars and saturated fat [363]. Such dietary shifts are associated with loss of micronutrients including Pi [364]. Indeed, the rat model used in the present study received a limited increase in daily caloric intake from saturated fats and refined sugars for twelve weeks producing a non-obese, hyperinsulinemic prediabetic state [7, 105, 111, 253, 314]. This modification was associated with almost a 50% reduction in dietary Pi. In the present study, the salient features of this model were confirmed in the cohort of rats fed HC diet with 0.375 mg/Kcal Pi, particularly hyperinsulinemia and an increased fat:lean ratio indicative of adipose tissue expansion and potential inflammation. Significantly, the insulin spike following simple and refined sugar intake triggered increased peripheral Pi uptake in a manner independent of the status of insulin resistance further reducing its availability [365]. Moreover, fructose intake, in particular, was shown to reduce serum and intra-cellular phosphate levels [366].

Importantly, a considerable body of research demonstrated the beneficial metabolic impact of Pi. Prior findings from our group showed that Pi supplementation reduced post-prandial blood glucose and insulin levels [367], decreased body weight, body mass



index and waist circumference [368], increased post-prandial energy expenditure [369], and preserved the exercise-induced elevation in total energy expenditure potentially by inhibition of energy compensation [370]. Furthermore, other investigators showed that, besides reducing blood glucose, insulin, and lipid levels, phosphate supplementation reduced body fat accumulation, especially in visceral adipose [371, 372].

In this context, increased adipose tissue UCP1 expression was consistently reported in different high-fat diet fed animals models [373]. Of relevance, UCP1 activity is stimulated by long chain fatty acids increasing in abundance following this kind of diet [374]. UCP1-mediated uncoupling was suggested to be an energy wasting mechanism to allow sufficient protein intake, especially that this effect was simulated with a diet containing low-quality protein in comparison to another diet containing the phosphate-rich casein [375]. Significantly, while our rat model lacked systemic inflammation [7, 111, 314], these rats had localized PVAT inflammation that coincided with increased UCP1 expression and adipocyte hypertrophy resulting in increased hypoxia and inflammation, which were not seen in WAT [7]. In the present study, the same results were recapitulated in the HC: 0.375 Pi diet. No increases in UCP1 or HIF1- $\alpha$  expression or in proinflammatory IL-1 $\beta$  level were seen in representative visceral WAT or BAT depots, despite an increase in adipocyte size. This observation confirms the previous suggestion that the growing oxygen demand due to increased UCP1 expression [376-378] possibly underlies the selective vulnerability of PVAT to hypoxia and inflammation at this early stage. Furthermore, the lack of detectable changes in serum levels of leptin and adiponectin, despite an increased fat:lean ratio, supports the notion that the functional and structural deterioration observed in this rat model result from a local paracrine effect of PVAT inflammation rather than a remote effect due to wider

involvement of other adipose depots similar to that observed in late stages of obesity and diabetes [111].

Pi supplementation in rats feeding HC diet, particularly at the 1.5 mg/Kcal dose, reduced serum insulin and lipid levels, as well as adipocyte size. This occurred with a parallel reduction in PVAT UCP1 and HIF1- $\alpha$  expression levels with a consequent decrease in IL-1 $\beta$ . The amelioration of the PVAT inflammatory status was also demonstrated by a restoration of the macrophage polarization state observed in control rats. Even though Pi supplementation did not result in statistically significant changes in calorie intake, body weight, or overall adiposity as measured by fat:lean ratio, a significant restoration of metabolic efficiency was achieved in rats receiving Pi supplementation in HC diet. The reduction of metabolic efficiency seen in rats fed HC:0.375 could be attributed to increased mitochondrial uncoupling resulting from increased UCP1 expression, hence the dissipation of excess dietary energy as heat. Indeed, increased UCP1 expression and activity was shown to be recruited in adipose tissue for diet induced thermogenesis and was associated with an increased oxygen consumption [379]. As such, the restoration of metabolic efficiency in Pi supplemented rats might be accounted for by the reduction in UCP1 expression and activity. In this regard, the ability of Pi to reduce mitochondrial uncoupling and energy dissipation via the inhibition of UCP1 has been recently shown [380]. Whereas Pi mediated changes in calorie intake and body weight were below the threshold of statistical significance, the intra-animal normalization involved in the calculation of metabolic efficiency for each rat in different groups might have accentuated these differences, which are inherently limited given the relatively small size of PVAT being the depot where UCP1 expression is upregulated.

Importantly, while previous studies suggested that Pi supplementation induced a preferential increase in lipid use as an energy source evident by a reduced respiratory quotient without a decrease in oxygen consumption [372] this appeared to be mediated via coupled mitochondrial respiration. Indeed, low serum Pi levels were shown to reduce mitochondrial ATP production [381], while extra-mitochondrial Pi was shown to induce a balanced activation of the electron transport chain enhancing mitochondrial coupling and ATP production [382]. As such, given the known difference in rates of mitochondrial oxygen consumption between coupled and uncoupled mitochondrial respiration [383], it becomes plausible that the Pi-induced shift either through inhibition of UCP1, activation of coupled electron transport, or both, underlies the observed alleviation of PVAT hypoxia and inflammation. The increased efficiency of respiration relieving the metabolic stress triggering energy dissipation could explain the observed normalization of UCP1 expression in PVAT from animals receiving phosphate supplementation.

As for the triglyceride levels, while increased serum levels could be tied to increased calorie intake, adipose tissue inflammation was shown to contribute to increased triglyceride levels by a variety of mechanisms including increased insulin resistance [384]. As such, it might be plausible that Pi supplementation could normalize serum triglyceride levels through the amelioration of PVAT inflammation and normalization of insulin levels. Indeed, a lowering effect on serum lipids was observed for Pi supplementation before [371, 372]. However, a potential caveat for this explanation would be the relatively limited impact of a small adipose depot like PVAT on systemic levels of triglycerides. As such, it might be necessary to invoke additional

explanations including the overall improvement of metabolism and energy expenditure previously reported for Pi supplementation.

Yet, the results of the *in vivo* treatment experiments are insufficient to support a direct effect of Pi on PVAT inflammation particularly that Pi interferes with the function of many pathways with impact on endocrine function and inflammation. In this context, increased Pi intake was found to impact calcium homeostasis and decrease serum calcium by affecting parathyroid hormone (PTH) levels [385], however this has been reported when very high Pi intake levels were coupled with reduced calcium intake [386]. Similarly, serum Pi alterations could affect magnesium levels either through renal excretion or via PTH activation [387]. Indeed not only had PTH been implicated in a cross-talk with IL-1 $\beta$  for bone resorption and metabolism [388], PTH was shown to induce inflammatory IL-6 expression in osteoblastic cells [389]. However, the lack of detectable differences in Pi serum levels among groups (apart from a limited reduction in HC: 1.5 group at 12 weeks) neither at eight weeks of feeding nor at 12 weeks of feeding, as well as the absence of changes in serum calcium and magnesium levels argue against changes in PTH-dependent functions. Thus, it remains unlikely that PTH would drive PVAT inflammatory changes, especially when more relevant mediators such as insulin were clearly elevated.

Moreover, the results of the *in vitro* cell culture experiments support a direct role of Pi supplementation on PVAT inflammation. Whereas HIF-1 $\alpha$  and IL-1 $\beta$  expression levels increased in the stressed adipocytes exposed to monocytes as observed in the PVAT of prediabetic rats receiving HC: 0.375, such increases were attenuated in adipocytes exposed to a parallel increase in Pi concentration. However, direct effects might not only be relevant to the proposed effect on hypoxia. Interestingly, recent

investigation proposed the calcium sensing receptor (CaSR) as a mediator of adipose tissue dysfunction whereby the activation of this receptor was associated with pro-inflammatory cytokine production [390, 391]. On the other hand, other studies showed that selective CaSR knockout in visceral adipose tissue did not alter high-fat diet induced adipose inflammation and vascular dysfunction arguing against its role in this context [392]. Significantly, emerging data suggested that increasing Pi concentration appeared to inhibit CaSR activity by non-competitive antagonism [393]. However, no appreciable inhibition of CaSR was observed at physiological serum levels of Pi, rather a 2.5-fold increase was required to achieve this inhibitory effect. As such, the contribution of this mechanism in the context of our present findings showing no increase in serum phosphate remains unlikely.

Under such circumstances, rats receiving Pi supplemented HC-diet showed mitigated cardiovascular consequences of PVAT inflammation. As observed previously, HC: 0.375 Pi feeding was associated with increased vascular reactivity, decreased rate of ventricular contractility, and blunted parasympathetic baroreflex sensitivity, which were tied to increased paracrine IL-1 $\beta$  production from the inflamed PVAT [7, 314]. Pi supplementation, particularly at the 1.5 mg/Kcal dose ameliorated the observed cardiovascular and parasympathetic functional impairment. Moreover, heart mid-section and aortic tissues from rats receiving Pi supplemented HC diet showed reduced signs of focal ischemia and decreased medial thickness upon H&E staining, respectively. As well, fibrosis and oxidative stress were also decreased. Furthermore, our previous work showed that the prediabetic state induced in these rats by HC feeding increased cerebrovascular tone triggering an increase in brain oxidative stress and neuroinflammation [253]. Pi supplementation normalized cerebrovascular tone in

response to a range of intra-vascular pressure values and reduced signs of brainstem neuroinflammation and oxidative stress. Cardiac autonomic neuropathy is a major cardiovascular risk factor in prediabetes and is known to emerge from a disproportionate sympathetic activation due to hyperinsulinemia [106]. Yet, it could also be argued that the observed autonomic insult is a consequence of increased brainstem oxidative stress and inflammation [394]. In either case, Pi supplementation appear to reverse hyperinsulinemia and increased cerebrovascular tone leading to brainstem oxidative stress.

From a different perspective, the ability of Pi administration to improve insulin sensitivity [395] and reduce insulin levels [367] could be invoked to explain the observed effect of Pi supplementation on PVAT. Indeed, hyperinsulinemia was proposed as a possible instigator of adipose inflammation via insulin-induced adipocyte hypertrophy [38]. Nevertheless, the insulin lowering effect of Pi cannot rule out other mechanisms discussed above. This could be inferred from the observations in rats receiving a two-week treatment protocol of 1.5 mg/Kcal Pi supplemented diet after being fed HC: 0.375 Pi diet for 10 weeks. Whereas the relatively short duration of exposure to Pi supplementation was not sufficient to trigger changes in serum insulin level and adipocyte size, together with a lack of reversal of cumulative metabolic efficiency, this two-week regimen improved PVAT hypoxia and inflammation, as well as the functional, histological and molecular manifestations of autonomic and cardiovascular deterioration. These findings suggest that Pi produced a direct insulin-independent PVAT effect potentially reducing hypoxia by UCP1 inhibition and promotion of coupled mitochondrial respiration. On the other hand, Pi deficiency on its own could not explain the observed PVAT and cardiovascular phenotype. A low Pi

control diet evoked neither PVAT inflammation nor cardiovascular deterioration, apart from a reduced rate of ventricular contraction. Such a finding is expected since a diet with standard composition would not be anticipated to upregulate UCP1. Alternatively, the present findings propose that a dual insult with increased availability of fatty acids and reduced Pi would be required to facilitate an increased PVAT UCP1 activity, and thus augment oxygen consumption, hypoxia and inflammation.

The effect of low Pi control diet on the rate of ventricular contraction could be viewed in terms of data showing that increased serum Pi levels were tied to ventricular diastolic dysfunction in uremic patients [396]. Another study found that even slightly elevated serum Pi levels, while still within the normal range, might be associated with adverse cardiac outcomes [397]. While no difference was detected in the serum Pi level between NC and low Pi diet fed groups, our results show a trend towards an increased serum Pi level, which might be analogous to these observations.

Despite the availability of information describing the molecular mechanism of Pi in this context and the favorable outcomes of Pi supplementation in early metabolic dysfunction, its recommendation for clinical investigation will be hampered by the perceived adverse effects. Literature shows a biphasic relationship for the impact of serum phosphate level. Whereas lower serum phosphate levels correlated with metabolic impairment leading to increased cardiovascular risk, higher levels were also associated with cardiovascular disease [398]. Moreover, fluctuations in serum phosphate concentrations triggered changes in calcium levels as well as those of the parathyroid hormone [395]. Importantly, studies showed that high serum phosphate levels or an excessive intake of phosphate were linked to cardiovascular and renal damage [399, 400]. Studies reporting adverse effects of increased Pi intake show clear

signs of deposition of calcium phosphate in the kidneys [386]. Indeed, increased Pi intake was associated with tubular necrosis and renal calcification in rats albeit at intake levels that are 3-4 fold higher than the highest concentration used in the present study [328]. As well, osteogenic changes including increased RUNX2 expression and vascular calcification were observed in rats fed a high Pi, however this occurred only in nephrectomized rats receiving more than twice as much Pi as in our highest dietary composition leading to profound changes in serum Pi and calcium not observed in the present study [401]. Nonetheless, histological examination revealed normal renal glomerular and tubular structure in the kidneys in rats of all groups. Importantly, silver staining showed a total lack of calcium deposits in the kidneys in all groups. In parallel, histological examination of aortic tissue in our different rat groups did not show any sign of structural disruption. Additionally, the vasculature remained fully responsive to vasopressor/vasodilator challenges as observed in the hemodynamic experiments potentially ruling out vascular stiffness secondary to Pi-triggered increases in fibroblast growth factor 23 expression [402]. As such, careful examination of the impact of serum phosphate on oxygen consumption and adipose respiration rates in humans must be undertaken prior to the recommendation of a Pi dose for supplementation for the purposes suggested in the present study. Moreover, such a recommendation for Pi intake must be decided within a more holistic process taking the overall patient profile, including serum electrolyte, parathyroid hormone, and insulin levels, as well kidney function status.

In conclusion, the present study proposes a novel role for Pi supplementation in curbing PVAT inflammation occurring in early metabolic dysfunction triggered by intake of diets with a diluted Pi content. Pi normalization relieves PVAT hypoxia and



mitigates the detrimental cardiac autonomic and vascular consequences. The combined metabolic and cardiovascular impact highlights a potential role for Pi in the amelioration of the emergence of the early cardiometabolic complications of increased calorie intake.

#### **D. Conclusions and Future Directions**

Non-obese prediabetic phenotype was observed in male rats in response to twelve and twenty-four weeks of HC feeding, characterized by hyperinsulinemia, euglycemia, insulin resistance and increased adiposity without a significant increase in total body weight. This early stage of prediabetes was associated with alarming metabolic and cardiovascular impairment, which were provoked by an interplay between hyperinsulinemia and sympathetic overflow which in turn triggered PVAT dysfunction. In male rats, PVAT dysfunction in our model was consistently presented as hypertrophied pool with impaired MT function and UCP1 upregulation, leading to a state of metabolic inefficiency and accelerated hypoxia that triggers inevitable inflammatory cascade fueling cardiovascular dysfunction. Thus, inhibiting UCP1 in PVAT seemed a reasonable target to interrupt the hypoxia machinery. Achieving this with inorganic phosphate seemed promising, as it was recognized as UCP1 inhibitor[280]. Indeed, clinical trials from our group showed positive metabolic effect of Pi supplementation[298, 301, 302, 369, 403]. Pi supplementation inhibited UCP1 and corrected PVAT dysfunction associated with HC-induced prediabetic phenotype, in addition to the subsequent cardiometabolic derangements. Despite the important impact of Pi supplementation in our model, the opposite was not observed, as phosphate

deficiency in the diet *per se* was not enough to provoke these metabolic derangements as observed in NC and low phosphate arm. Yet, in the presence of HC low phosphate was found to be detrimental and exacerbated the pathological effect. On the other hand, HC-fed premenopausal female rats seemed to be resilient to the prediabetic metabolic phenotype and its related cardiometabolic derangements. This seemed to be mediated by estrogen, as bilateral ovariectomy in rats exaggerated the impact of HC feeding, and they developed an obese prediabetic phenotype, with PVAT and cardiovascular dysfunction. Indeed, exogenous estrogen appeared to restore the cardiometabolic derangements induced by HC feeding and prevent obesity and prediabetes induced by HC feeding in ovariectomized females. Estrogen in our model, seemed to reduce sympathetic overflow, increase insulin sensitivity, and degrade HIF1- $\alpha$  finally leading to a disruption of the hypoxia machinery and its repercussions.

In our non-obese prediabetic rat model, therapeutic fasting was implemented as a possible intervention to modulate insulin resistance and sympathetic overactivation. Indeed, after twelve weeks of fasting and despite having free access to HC diet during the feeding hours, TF was able to reverse prediabetes, PVAT dysfunction and improve cardiovascular function in male rats. The same protective outcome was observed in HC-fed ovariectomized females. This opens the door for a wide range of possibilities as TF ameliorated cardiometabolic impairment in the presence of HC feeding, and in the absence of endogenous estrogen. Specifically, another study involving IF in a calorie restriction protocol showed a shift in AT macrophages to the M2 polarization that was mediated by Sirtuin-1 (SIRT1) activity [247]. SIRT1 is a nutrient sensitive histone deacetylase that is thought to mediate the beneficial metabolic effects of fasting and calorie restriction including improved serum glucose and lipid levels, increased insulin

sensitivity and reduced body weight [248, 249]. Interestingly, mild SIRT1 overexpression protected against HFD-induced inflammation by reducing NF- $\kappa$ B activation and pro-inflammatory cytokine production [250]. Pertinent to the inflammatory context in AT, SIRT1 activation was shown to mitigate hypoxic cell damage through the augmentation of autophagic flux that was mediated by AMPK activation [251]. Indeed, IF was found to augment AMPK phosphorylation [252]. Significantly, not only has our work shown a reduced AMPK activity in cardiovascular impairment associated with early metabolic dysfunction involving PVAT inflammation[404], our results also demonstrated autophagy suppression as a possible contributor to the observed phenotype [111, 405]. Moreover, a lack of AMPK activity was implicated in AC hypertrophy [254]. As such, IF-mediated SIRT1 activation could offer a mechanistic link for the observed positive changes in AT remodeling. One of our future targets is to further study the mechanism of which TF induce its effect in a sex dependent manner and probably find more precise and targeted interventions, of which gut microbiome can play a major role, since diet induced dysbiosis was linked to sympathetic activation [347].

On the same note, LPS migration into the circulation has been suggested to be a contributing factor to the onset of AT inflammation, insulin resistance, obesity, and diabetes [406-408]. Interestingly, HFD consumption had a similar effect as LPS subcutaneous infusion on elevating serum LPS and promoting AT inflammation in male mice [406]. Significantly, HFD-fed TLR4 knockout mice did not have increased proinflammatory cytokines in the isolated epididymal AT depot, whereas wild-type mice were hyperinsulinemic and exhibited a proinflammatory response in the epididymal WAT manifested by increased TNF $\alpha$ , IL-1 $\beta$ , and IL-6, and macrophage

infiltration [409]. Moreover, TLR4 knockout male mice had an increased insulin sensitivity in subcutaneous and epididymal WAT even in presence of HFD feeding [410]. LPS activates TLR4 on target tissues including AT and macrophages triggering proinflammatory cascade and activating NF- $\kappa$ B. AT overactivation and hypertrophied expansion due to dysbiosis. In parallel, LPS induced neuroinflammation triggers sympathetic firing. The resultant sympathetic overactivation and insulin resistance, which are expected to be higher in males, will lead to early inflammation and negative remodeling of PVAT precipitating a wide range of subclinical cardiovascular insults [120, 125, 126, 139, 222, 343, 411]. Since estrogen holds a protective effect against hypoxia in AT, possibly estrogen will block dysbiosis-mediated dysfunction cardiovascular dysfunction by interfering with PVAT inflammation. Hence, dysbiosis can add an extra layer to diet induced sex-dependent cardiovascular dysfunction.

## REFERENCES

1. WHO, *Cardiovascular diseases (CVDs) fact sheet*. World Health Organization, 2017.
2. Anand, S., C. Bradshaw, and D. Prabhakaran, *Prevention and management of CVD in LMICs: why do ethnicity, culture, and context matter?* BMC medicine, 2020. **18**(1): p. 7.
3. Raghavan, S., et al., *Diabetes Mellitus–Related All-Cause and Cardiovascular Mortality in a National Cohort of Adults*. Journal of the American Heart Association, 2019. **8**(4): p. e011295.
4. Richardson, V.R., K.A. Smith, and A.M. Carter, *Adipose tissue inflammation: Feeding the development of type 2 diabetes mellitus*. Immunobiology, 2013. **218**(12): p. 1497-1504.
5. Weir, G.C. and S. Bonner-Weir, *Five stages of evolving beta-cell dysfunction during progression to diabetes*. Diabetes, 2004. **53**(suppl 3): p. S16-S21.
6. Al-Assi, O., et al., *Cardiac autonomic neuropathy as a result of mild hypercaloric challenge in absence of signs of diabetes: modulation by antidiabetic drugs*. Oxidative medicine and cellular longevity, 2018. **2018**.
7. Elkhatib, M.A.W., et al., *Amelioration of perivascular adipose inflammation reverses vascular dysfunction in a model of nonobese prediabetic metabolic challenge: potential role of antidiabetic drugs*. Transl Res, 2019. **214**: p. 121-143.
8. Hostalek, U., *Global epidemiology of prediabetes-present and future perspectives*. Clinical diabetes and endocrinology, 2019. **5**(1): p. 1-5.
9. Maffetone, P.B. and P.B. Laursen, *Revisiting the global overfat pandemic*. Frontiers in Public Health, 2020. **8**.
10. Hamdy, O., S. Porramatikul, and E. Al-Ozairi, *Metabolic obesity: the paradox between visceral and subcutaneous fat*. Current diabetes reviews, 2006. **2**(4): p. 367-373.
11. Berg, A.H. and P.E. Scherer, *Adipose tissue, inflammation, and cardiovascular disease*. Circulation research, 2005. **96**(9): p. 939-949.
12. Shah, A., N. Mehta, and M.P. Reilly, *Adipose inflammation, insulin resistance, and cardiovascular disease*. Journal of Parenteral and Enteral Nutrition, 2008. **32**(6): p. 638-644.
13. Segalla, L., S. Chirumbolo, and A. Sbarbati, *Dermal white adipose tissue: much more than a metabolic, lipid-storage organ?* Tissue and Cell, 2021: p. 101583.
14. Dragoo, J., et al., *The essential roles of human adipose tissue: Metabolic, thermoregulatory, cellular, and paracrine effects*. Journal of Cartilage & Joint Preservation, 2021: p. 100023.
15. Chusyd, D.E., et al., *Relationships between rodent white adipose fat pads and human white adipose fat depots*. Frontiers in nutrition, 2016. **3**: p. 10.
16. Foster, D.O. and M.L. Frydman, *Brown adipose tissue: the dominant site of nonshivering thermogenesis in the rat*, in *Effectors of thermogenesis*. 1978, Springer. p. 147-151.

17. Rui\*, L., *Brown and Beige Adipose Tissues in Health and Disease*, in *Comprehensive Physiology*. 2017. p. 1281-1306.
18. Fedorenko, A., P.V. Lishko, and Y. Kirichok, *Mechanism of fatty-acid-dependent UCP1 uncoupling in brown fat mitochondria*. *Cell*, 2012. **151**(2): p. 400-413.
19. Klingenberg, M., et al., *Structure–function relationship in UCP1*. *International Journal of Obesity*, 1999. **23**(6): p. S24-S29.
20. Agabiti-Rosei, C., et al., *Modulation of vascular reactivity by perivascular adipose tissue (PVAT)*. *Current hypertension reports*, 2018. **20**(5): p. 44.
21. Qi, X.-Y., et al., *Perivascular adipose tissue (PVAT) in atherosclerosis: a double-edged sword*. *Cardiovascular diabetology*, 2018. **17**(1): p. 1-20.
22. Hildebrand, S., J. Stümer, and A. Pfeifer, *PVAT and its relation to brown, beige, and white adipose tissue in development and function*. *Frontiers in physiology*, 2018. **9**: p. 70.
23. Nishimura, S., I. Manabe, and R. Nagai, *Adipose tissue inflammation in obesity and metabolic syndrome*. *Discovery medicine*, 2009.
24. Sun, K., C.M. Kusminski, and P.E. Scherer, *Adipose tissue remodeling and obesity*. *The Journal of clinical investigation*, 2011. **121**(6): p. 2094-2101.
25. Chait, A. and L.J. den Hartigh, *Adipose tissue distribution, inflammation and its metabolic consequences, including diabetes and cardiovascular disease*. *Frontiers in cardiovascular medicine*, 2020. **7**: p. 22.
26. Bays, H., et al., *Adiposopathy: treating pathogenic adipose tissue to reduce cardiovascular disease risk*. *Current treatment options in cardiovascular medicine*, 2007. **9**(4): p. 259-271.
27. Klötting, N. and M. Blüher, *Adipocyte dysfunction, inflammation and metabolic syndrome*. *Reviews in Endocrine and Metabolic Disorders*, 2014. **15**(4): p. 277- 287.
28. Dwaib, H.S., et al., *Modulatory Effect of Intermittent Fasting on Adipose Tissue Inflammation: Amelioration of Cardiovascular Dysfunction in Early Metabolic Impairment*. *Frontiers in Pharmacology*, 2021. **12**: p. 451.
29. Choe, S.S., et al., *Adipose tissue remodeling: its role in energy metabolism and metabolic disorders*. *Frontiers in endocrinology*, 2016. **7**: p. 30.
30. Bays, H.E., *Adiposopathy: is “sick fat” a cardiovascular disease?* *Journal of the American College of Cardiology*, 2011. **57**(25): p. 2461-2473.
31. Bays, H.E., et al., *Pathogenic potential of adipose tissue and metabolic consequences of adipocyte hypertrophy and increased visceral adiposity*. *Expert review of cardiovascular therapy*, 2008. **6**(3): p. 343-368.
32. Gustafson, B. and U. Smith, *Regulation of white adipogenesis and its relation to ectopic fat accumulation and cardiovascular risk*. *Atherosclerosis*, 2015. **241**(1): p. 27-35.
33. Friesen, M., et al., *Adipocyte insulin receptor activity maintains adipose tissue mass and lifespan*. *Biochemical and biophysical research communications*, 2016. **476**(4): p. 487-492.
34. Goossens, G.H. and E.E. Blaak, *Adipose tissue dysfunction and impaired metabolic health in human obesity: a matter of oxygen?* *Frontiers in endocrinology*, 2015. **6**: p. 55.

35. Rausch, M., et al., *Obesity in C57BL/6J mice is characterized by adipose tissue hypoxia and cytotoxic T-cell infiltration*. International journal of obesity, 2008. **32**(3): p. 451-463.
36. Ye, J., et al., *Hypoxia is a potential risk factor for chronic inflammation and adiponectin reduction in adipose tissue of ob/ob and dietary obese mice*. American Journal of Physiology-Endocrinology and Metabolism, 2007. **293**(4): p. E1118-E1128.
37. Lempesis, I.G., et al., *Oxygenation of adipose tissue: A human perspective*. Acta Physiologica, 2020. **228**(1): p. e13298.
38. Pedersen, D.J., et al., *A major role of insulin in promoting obesity-associated adipose tissue inflammation*. Mol Metab, 2015. **4**(7): p. 507-18.
39. Trayhurn, P., *Hypoxia and Adipose Tissue Function and Dysfunction in Obesity*. Physiological Reviews, 2013. **93**(1): p. 1-21.
40. He, Q., et al., *Regulation of HIF-1 $\alpha$  activity in adipose tissue by obesity-associated factors: adipogenesis, insulin, and hypoxia*. American Journal of Physiology- Endocrinology and Metabolism, 2011. **300**(5): p. E877-E885.
41. Rius, J., et al., *NF-kappaB links innate immunity to the hypoxic response through transcriptional regulation of HIF-1alpha*. Nature, 2008. **453**(7196): p. 807-11.
42. van Uden, P., N.S. Kenneth, and S. Rocha, *Regulation of hypoxia-inducible factor- 1alpha by NF-kappaB*. Biochem J, 2008. **412**(3): p. 477-84.
43. Dzhaliilova, D.S., et al., *Dependence of the severity of the systemic inflammatory response on resistance to hypoxia in male Wistar rats*. J Inflamm Res, 2019. **12**: p. 73-86.
44. Jeong, H.-J., et al., *Hypoxia-induced IL-6 production is associated with activation of MAP kinase, HIF-1, and NF- $\kappa$ B on HEI-OC1 cells*. Hearing Research, 2005. **207**(1): p. 59-67.
45. Fitzgibbons, T.P. and M.P. Czech, *Epicardial and Perivascular Adipose Tissues and Their Influence on Cardiovascular Disease: Basic Mechanisms and Clinical Associations*. J Am Heart Assoc, 2014. **3**(2).
46. Saxton, S.N., et al., *Mechanistic links between obesity, diabetes, and blood pressure: role of perivascular adipose tissue*. Physiological reviews, 2019. **99**(4): p. 1701-1763.
47. AlZaim, I., et al., *Adipose Tissue Immunomodulation: A Novel Therapeutic Approach in Cardiovascular and Metabolic Diseases*. Frontiers in Cardiovascular Medicine, 2020. **7**(277).
48. Thapa, B. and K. Lee, *Metabolic influence on macrophage polarization and pathogenesis*. BMB reports, 2019. **52**(6): p. 360.
49. Caslin, H.L., et al., *Adipose tissue macrophages: Unique polarization and bioenergetics in obesity*. Immunological Reviews, 2020. **295**(1): p. 101-113.
50. Morris, D.L., K. Singer, and C.N. Lumeng, *Adipose tissue macrophages: phenotypic plasticity and diversity in lean and obese states*. Current opinion in clinical nutrition and metabolic care, 2011. **14**(4): p. 341.
51. Chylikova, J., et al., *M1/M2 macrophage polarization in human obese adipose tissue*. Biomed Pap Med Fac Univ Palacky Olomouc Czech Repub, 2018. **162**(2): p. 79-82.

52. Kralova Lesna, I., et al., *Characterisation and comparison of adipose tissue macrophages from human subcutaneous, visceral and perivascular adipose tissue*. Journal of Translational Medicine, 2016. **14**(1): p. 208.
53. Lumeng, C.N., et al., *Phenotypic switching of adipose tissue macrophages with obesity is generated by spatiotemporal differences in macrophage subtypes*. Diabetes, 2008. **57**(12): p. 3239-3246.
54. Lumeng, C.N., J.L. Bodzin, and A.R. Saltiel, *Obesity induces a phenotypic switch in adipose tissue macrophage polarization*. J Clin Invest, 2007. **117**(1): p. 175-84.
55. Wensveen, F.M., et al., *The "Big Bang" in obese fat: Events initiating obesity-induced adipose tissue inflammation*. Eur J Immunol, 2015. **45**(9): p. 2446-56.
56. Cinti, S., et al., *Adipocyte death defines macrophage localization and function in adipose tissue of obese mice and humans*. Journal of lipid research, 2005. **46**(11): p. 2347-2355.
57. Weisberg, S.P., et al., *Obesity is associated with macrophage accumulation in adipose tissue*. The Journal of clinical investigation, 2003. **112**(12): p. 1796-1808.
58. Sartipy, P. and D.J. Loskutoff, *Monocyte chemoattractant protein 1 in obesity and insulin resistance*. Proceedings of the National Academy of Sciences, 2003. **100**(12): p. 7265-7270.
59. Xu, H., et al., *Chronic inflammation in fat plays a crucial role in the development of obesity-related insulin resistance*. The Journal of clinical investigation, 2003. **112**(12): p. 1821-1830.
60. Charrière, G., et al., *Preadipocyte conversion to macrophage Evidence of plasticity*. Journal of Biological Chemistry, 2003. **278**(11): p. 9850-9855.
61. Suganami, T., J. Nishida, and Y. Ogawa, *A paracrine loop between adipocytes and macrophages aggravates inflammatory changes: role of free fatty acids and tumor necrosis factor  $\alpha$* . Arteriosclerosis, thrombosis, and vascular biology, 2005. **25**(10): p. 2062-2068.
62. Ye, J., *Regulation of PPAR $\gamma$  function by TNF- $\alpha$* . Biochemical and biophysical research communications, 2008. **374**(3): p. 405-408.
63. Suzawa, M., et al., *Cytokines suppress adipogenesis and PPAR- $\gamma$  function through the TAK1/TAB1/NIK cascade*. Nature Cell Biology, 2014. **16**(11).
64. Ren, T., et al., *Metformin reduces lipolysis in primary rat adipocytes stimulated by tumor necrosis factor- $\alpha$  or isoproterenol*. Journal of Molecular Endocrinology, 2006. **37**(1): p. 175-183.
65. Fujisaka, S., et al., *Telmisartan improves insulin resistance and modulates adipose tissue macrophage polarization in high-fat-fed mice*. Endocrinology, 2011. **152**(5): p. 1789-1799.
66. Uysal, K.T., et al., *Protection from obesity-induced insulin resistance in mice lacking TNF- $\alpha$  function*. Nature, 1997. **389**(6651): p. 610-4.
67. Cawthorn, W.P. and J.K. Sethi, *TNF- $\alpha$  and adipocyte biology*. FEBS letters, 2008. **582**(1): p. 117-131.
68. Ruan, H., et al., *Profiling gene transcription in vivo reveals adipose tissue as an immediate target of tumor necrosis factor- $\alpha$ : implications for insulin resistance*. Diabetes, 2002. **51**(11): p. 3176-3188.



69. Stephens, J.M., J. Lee, and P.F. Pilch, *Tumor necrosis factor- $\alpha$ -induced insulin resistance in 3T3-L1 adipocytes is accompanied by a loss of insulin receptor substrate-1 and GLUT4 expression without a loss of insulin receptor-mediated signal transduction*. Journal of Biological Chemistry, 1997. **272**(2): p. 971-976.
70. Engelman, J.A., et al., *Tumor necrosis factor  $\alpha$ -mediated insulin resistance, but not dedifferentiation, is abrogated by MEK1/2 inhibitors in 3T3-L1 adipocytes*. Molecular endocrinology, 2000. **14**(10): p. 1557-1569.
71. Steinberg, G.R., et al., *Tumor necrosis factor  $\alpha$ -induced skeletal muscle insulin resistance involves suppression of AMP-kinase signaling*. Cell metabolism, 2006. **4**(6): p. 465-474.
72. Chan, K.L., et al., *Palmitoleate reverses high fat-induced proinflammatory macrophage polarization via AMP-activated protein kinase (AMPK)*. Journal of Biological Chemistry, 2015. **290**(27): p. 16979-16988.
73. AlZaim, I., et al., *Adipose Tissue Immunomodulation: A Novel Therapeutic Approach in Cardiovascular and Metabolic Diseases*. Frontiers in Cardiovascular Medicine, 2020. **7**: p. 277.
74. Liu, J., et al., *Genetic deficiency and pharmacological stabilization of mast cells reduce diet-induced obesity and diabetes in mice*. Nature Medicine, 2009. **15**(8): p. 940-945.
75. Xue, B., et al., *Transcriptional synergy and the regulation of Ucp1 during brown adipocyte induction in white fat depots*. Mol Cell Biol, 2005. **25**(18): p. 8311-22.
76. Cannon, B. and J. Nedergaard, *What ignites UCP1?* Cell metabolism, 2017. **26**(5): p. 697-698.
77. Coman, O.A., et al., *Beta 3 adrenergic receptors: molecular, histological, functional and pharmacological approaches*. Rom J Morphol Embryol, 2009. **50**(2): p. 169-79.
78. Nedergaard, J., et al., *Life without UCPI: mitochondrial, cellular and organismal characteristics of the UCPI-ablated mice*. Biochemical Society Transactions, 2001. **29**(6): p. 756-763.
79. Ricquier, D. and F. BOUILLAUD, *The uncoupling protein homologues: UCP1, UCP2, UCP3, StUCP and AtUCP*. Biochemical Journal, 2000. **345**(2): p. 161-179.
80. Nedergaard, J. and B. Cannon, *The browning of white adipose tissue: some burning issues*. Cell metabolism, 2014. **20**(3): p. 396-407.
81. Liu, B., et al., *Intermittent fasting increases energy expenditure and promotes adipose tissue browning in mice*. Nutrition, 2019. **66**: p. 38-43.
82. Sakamoto, T., et al., *Inflammation induced by RAW macrophages suppresses UCP1 mRNA induction via ERK activation in 10T1/2 adipocytes*. American Journal of Physiology-Cell Physiology, 2013. **304**(8): p. C729-C738.
83. Nøhr, M.K., et al., *Inflammation downregulates UCP1 expression in brown adipocytes potentially via SIRT1 and DBC1 interaction*. International journal of molecular sciences, 2017. **18**(5): p. 1006.
84. Bonet, M.L., J. Mercader, and A. Palou, *A nutritional perspective on UCP1-dependent thermogenesis*. Biochimie, 2017. **134**: p. 99-117.

85. García-Ruiz, E., et al., *The intake of high-fat diets induces the acquisition of brown adipocyte gene expression features in white adipose tissue*. International Journal of Obesity, 2015. **39**(11): p. 1619-1629.
86. Rahman, S. and R. Islam, *Mammalian Sirt1: insights on its biological functions*. Cell Communication and Signaling, 2011. **9**(1): p. 11.
87. Gerhart-Hines, Z., et al., *Metabolic control of muscle mitochondrial function and fatty acid oxidation through SIRT1/PGC-1a*. EMBO J, 1913. **26**.
88. Winn, N.C., et al., *Loss of UCP1 exacerbates Western diet-induced glycemic dysregulation independent of changes in body weight in female mice*. American Journal of Physiology-Regulatory, Integrative and Comparative Physiology, 2017. **312**(1): p. R74-R84.
89. Festuccia, W.T., et al., *Basal adrenergic tone is required for maximal stimulation of rat brown adipose tissue UCP1 expression by chronic PPAR- $\gamma$  activation*. American Journal of Physiology-Regulatory, Integrative and Comparative Physiology, 2010. **299**(1): p. R159-R167.
90. Balfour, J.A.B. and G.L. Plosker, *Rosiglitazone*. Drugs, 1999. **57**(6): p. 921-930.
91. Petrovic, N., et al., *Thermogenically competent nonadrenergic recruitment in brown preadipocytes by a PPAR $\gamma$  agonist*. American journal of physiology- endocrinology and metabolism, 2008. **295**(2): p. E287-E296.
92. Anderson, E.A., et al., *Hyperinsulinemia produces both sympathetic neural activation and vasodilation in normal humans*. The Journal of clinical investigation, 1991. **87**(6): p. 2246-2252.
93. Thorp, A.A. and M.P. Schlaich, *Relevance of Sympathetic Nervous System Activation in Obesity and Metabolic Syndrome*. J Diabetes Res, 2015. **2015**: p. 341583.
94. Pisani, D.F., et al., *Mitochondrial fission is associated with UCP1 activity in human brite/beige adipocytes*. Molecular metabolism, 2018. **7**: p. 35-44.
95. Velazquez-Villegas, L.A., et al., *TGR5 signalling promotes mitochondrial fission and beige remodelling of white adipose tissue*. Nature Communications, 2018. **9**(1): p. 245.
96. Wikstrom, J.D., et al., *Hormone-induced mitochondrial fission is utilized by brown adipocytes as an amplification pathway for energy expenditure*. Embo j, 2014. **33**(5): p. 418-36.
97. Li, A., et al., *Metformin and resveratrol inhibit Drp1-mediated mitochondrial fission and prevent ER stress-associated NLRP3 inflammasome activation in the adipose tissue of diabetic mice*. Molecular and Cellular Endocrinology, 2016. **434**: p. 36-47.
98. Mottillo, E.P., et al., *Lack of Adipocyte AMPK Exacerbates Insulin Resistance and Hepatic Steatosis through Brown and Beige Adipose Tissue Function*. Cell Metab, 2016. **24**(1): p. 118-29.
99. Wu, L., et al., *AMP-activated protein kinase (AMPK) regulates energy metabolism through modulating thermogenesis in adipose tissue*. Frontiers in physiology, 2018. **9**: p. 122.

100. Pollard, A.E., et al., *AMPK activation protects against diet induced obesity through Ucp1-independent thermogenesis in subcutaneous white adipose tissue*. *Nat Metab*, 2019. **1**(3): p. 340-349.
101. Hirata, Y., et al., *Coronary atherosclerosis is associated with macrophage polarization in epicardial adipose tissue*. *Journal of the American College of Cardiology*, 2011. **58**(3): p. 248-255.
102. Eiras, S., et al., *Extension of coronary artery disease is associated with increased IL-6 and decreased adiponectin gene expression in epicardial adipose tissue*. *Cytokine*, 2008. **43**(2): p. 174-80.
103. Salgado-Somoza, A., et al., *Proteomic analysis of epicardial and subcutaneous adipose tissue reveals differences in proteins involved in oxidative stress*. *Am J Physiol Heart Circ Physiol*, 2010. **299**(1): p. H202-9.
104. Apovian, C.M., et al., *Adipose macrophage infiltration is associated with insulin resistance and vascular endothelial dysfunction in obese subjects*. *Arteriosclerosis, thrombosis, and vascular biology*, 2008. **28**(9): p. 1654-1659.
105. Alaaeddine, R., et al., *Impaired Endothelium-Dependent Hyperpolarization Underlies Endothelial Dysfunction during Early Metabolic Challenge: Increased ROS Generation and Possible Interference with NO Function*. *J Pharmacol Exp Ther*, 2019. **371**(3): p. 567-582.
106. Bakkar, N.Z., et al., *Cardiac Autonomic Neuropathy: A Progressive Consequence of Chronic Low-Grade Inflammation in Type 2 Diabetes and Related Metabolic Disorders*. *Int J Mol Sci*, 2020. **21**(23).
107. Serhiyenko, V.A. and A.A. Serhiyenko, *Cardiac autonomic neuropathy: risk factors, diagnosis and treatment*. *World journal of diabetes*, 2018. **9**(1): p. 1.
108. Vinik, A.I., T. Erbas, and C.M. Casellini, *Diabetic cardiac autonomic neuropathy, inflammation and cardiovascular disease*. *Journal of diabetes investigation*, 2013. **4**(1): p. 4-18.
109. Williams, S.M., et al., *Cardiac autonomic neuropathy in obesity, the metabolic syndrome and prediabetes: a narrative review*. *Diabetes Therapy*, 2019: p. 1-27.
110. Gonzalez, M.A. and A.P. Selwyn, *Endothelial function, inflammation, and prognosis in cardiovascular disease*. *The American journal of medicine*, 2003. **115**(8): p. 99-106.
111. Bakkar, N.Z., et al., *Worsening baroreflex sensitivity on progression to type 2 diabetes: localized vs. systemic inflammation and role of antidiabetic therapy*. *Am J Physiol Endocrinol Metab*, 2020. **319**(5): p. E835-e851.
112. Steyers, C.M. and F.J. Miller, *Endothelial dysfunction in chronic inflammatory diseases*. *International journal of molecular sciences*, 2014. **15**(7): p. 11324- 11349.
113. Sena, C.M., A.M. Pereira, and R. Seiça, *Endothelial dysfunction—a major mediator of diabetic vascular disease*. *Biochimica et Biophysica Acta (BBA)- Molecular Basis of Disease*, 2013. **1832**(12): p. 2216-2231.
114. Endemann, D.H. and E.L. Schiffrin, *Endothelial dysfunction*. *Journal of the American Society of Nephrology*, 2004. **15**(8): p. 1983-1992.
115. Cai, H. and D.G. Harrison, *Endothelial dysfunction in cardiovascular diseases: the role of oxidant stress*. *Circulation research*, 2000. **87**(10): p.

840-844.

116. Alaaeddine, R., et al., *Endothelial Dysfunction as a result of Hypercaloric Intake: Underlying Mechanism in Absence of Hyperglycemia*. The FASEB Journal, 2018. **32**(1\_supplement): p. 837.2-837.2.
117. van den Oever, I.A., et al., *Endothelial dysfunction, inflammation, and apoptosis in diabetes mellitus*. Mediators of inflammation, 2010. **2010**.
118. Muniyappa, R. and J.R. Sowers, *Role of insulin resistance in endothelial dysfunction*. Reviews in Endocrine and Metabolic Disorders, 2013. **14**(1): p. 5-12.
119. Akoumianakis, I., A. Tarun, and C. Antoniades, *Perivascular adipose tissue as a regulator of vascular disease pathogenesis: identifying novel therapeutic targets*. British journal of pharmacology, 2017. **174**(20): p. 3411-3424.
120. Akoumianakis, I., A. Tarun, and C. Antoniades, *Perivascular adipose tissue as a regulator of vascular disease pathogenesis: identifying novel therapeutic targets*. Br J Pharmacol, 2017. **174**(20): p. 3411-3424.
121. Azul, L., et al., *Increased inflammation, oxidative stress and a reduction in antioxidant defense enzymes in perivascular adipose tissue contribute to vascular dysfunction in type 2 diabetes*. Free Radic Biol Med, 2019.
122. Almagrouk, T.A., et al., *High fat diet attenuates the anticontractile activity of aortic PVAT via a mechanism involving AMPK and reduced adiponectin secretion*. Frontiers in physiology, 2018. **9**: p. 51.
123. Omar, A., et al., *Proinflammatory phenotype of perivascular adipocytes*. Arteriosclerosis, thrombosis, and vascular biology, 2014. **34**(8): p. 1631-1636.
124. Gollasch, M., *Adipose-vascular coupling and potential therapeutics*. Annual Review of Pharmacology and Toxicology, 2017. **57**: p. 417-436.
125. Bulloch, J.M. and C.J. Daly, *Autonomic nerves and perivascular fat: interactive mechanisms*. Pharmacol Ther, 2014. **143**(1): p. 61-73.
126. Alaaeddine, R.A., et al., *Impaired cross-talk between NO and hyperpolarization in myoendothelial feedback: A novel therapeutic target in early endothelial dysfunction of metabolic disease*. Current opinion in pharmacology, 2019. **45**: p. 33-41.
127. Thanassoulis, G., et al., *Periaortic Adipose Tissue and Aortic Dimensions in the Framingham Heart Study*. Journal of the American Heart Association, 2012. **1**(6): p. e000885.
128. Wang, J., et al., *Exercise improves endothelial function associated with alleviated inflammation and oxidative stress of perivascular adipose tissue in type 2 diabetic mice*. Oxidative Medicine and Cellular Longevity, 2020. **2020**.
129. Lehman, S.J., et al., *Peri-aortic fat, cardiovascular disease risk factors, and aortic calcification: the Framingham Heart Study*. Atherosclerosis, 2010. **210**(2): p. 656- 661.
130. Britton, K.A., et al., *Prevalence, Distribution, and Risk Factor Correlates of High Thoracic Periaortic Fat in the Framingham Heart Study*. Journal of the American Heart Association, 2012. **1**(6): p. e004200.
131. Ren, L., et al., *Perivascular adipose tissue modulates carotid plaque formation induced by disturbed flow in mice*. Journal of vascular surgery, 2019. **70**(3): p. 927-936. e4.

132. Soltis, E.E. and L.A. Cassis, *Influence of perivascular adipose tissue on rat aortic smooth muscle responsiveness*. Clin Exp Hypertens A, 1991. **13**(2): p. 277-96.
133. Lohn, M., et al., *Periadventitial fat releases a vascular relaxing factor*. Faseb j, 2002. **16**(9): p. 1057-63.
134. Ouchi, N., et al., *Adipokines in inflammation and metabolic disease*. Nature reviews immunology, 2011. **11**(2): p. 85.
135. Sung, B., et al., *Modulation of PPAR in aging, inflammation, and calorie restriction*. The Journals of Gerontology Series A: Biological Sciences and Medical Sciences, 2004. **59**(10): p. B997-B1006.
136. Chang, L., et al., *Loss of perivascular adipose tissue on peroxisome proliferator-activated receptor- $\gamma$  deletion in smooth muscle cells impairs intravascular thermoregulation and enhances atherosclerosis*. Circulation, 2012. **126**(9): p. 1067-1078.
137. Rafeh, R., et al., *Targeting perivascular and epicardial adipose tissue inflammation: therapeutic opportunities for cardiovascular disease*. Clin Sci (Lond), 2020. **134**(7): p. 827-851.
138. Manka, D., et al., *Transplanted perivascular adipose tissue accelerates injury-induced neointimal hyperplasia: role of monocyte chemoattractant protein-1*. Arteriosclerosis, thrombosis, and vascular biology, 2014. **34**(8): p. 1723-1730.
139. Britton, K. and C. Fox, *Perivascular adipose tissue and vascular disease*. Clinical lipidology, 2011. **6**(1): p. 79-91.
140. Greenstein, A.S., et al., *Local inflammation and hypoxia abolish the protective anticontractile properties of perivascular fat in obese patients*. Circulation, 2009. **119**(12): p. 1661-70.
141. Horimatsu, T., et al., *Remote Effects of Transplanted Perivascular Adipose Tissue on Endothelial Function and Atherosclerosis*. Cardiovascular drugs and therapy, 2018. **32**(5): p. 503-510.
142. Chatterjee, T.K., et al., *Proinflammatory phenotype of perivascular adipocytes: influence of high-fat feeding*. Circ Res, 2009. **104**(4): p. 541-9.
143. Sacks, H.S., et al., *Adult epicardial fat exhibits beige features*. J Clin Endocrinol Metab, 2013. **98**(9): p. E1448-55.
144. Gaborit, B., et al., *Human epicardial adipose tissue has a specific transcriptomic signature depending on its anatomical peri-atrial, peri-ventricular, or peri-coronary location*. Cardiovasc Res, 2015. **108**(1): p. 62-73.
145. de Jong, J.M., et al., *The  $\beta$ 3-adrenergic receptor is dispensable for browning of adipose tissues*. American Journal of Physiology-Endocrinology And Metabolism, 2017. **312**(6): p. E508-E518.
146. Kong, L.-R., et al., *Decrease of perivascular adipose tissue browning is associated with vascular dysfunction in spontaneous hypertensive rats during aging*. Frontiers in physiology, 2018. **9**: p. 400.
147. Lefranc, C., et al., *MR (Mineralocorticoid Receptor) Induces Adipose Tissue Senescence and Mitochondrial Dysfunction Leading to Vascular Dysfunction in Obesity*. Hypertension, 2019. **73**(2): p. 458-468.

148. Colafella, K.M.M. and K.M. Denton, *Sex-specific differences in hypertension and associated cardiovascular disease*. Nature Reviews Nephrology, 2018. **14**(3): p. 185-201.
149. Chella Krishnan, K., M. Mehrabian, and A.J. Lusis, *Sex differences in metabolism and cardiometabolic disorders*. Curr Opin Lipidol, 2018. **29**(5): p. 404-410.
150. Kim, S.H. and G. Reaven, *Sex differences in insulin resistance and cardiovascular disease risk*. The Journal of Clinical Endocrinology & Metabolism, 2013. **98**(11): p. E1716-E1721.
151. El Akoum, S., et al., *Nature of fatty acids in high fat diets differentially delineates obesity-linked metabolic syndrome components in male and female C57BL/6J mice*. Diabetology & metabolic syndrome, 2011. **3**(1): p. 1-11.
152. Lew, J., et al., *Sex-based differences in cardiometabolic biomarkers*. Circulation, 2017. **135**(6): p. 544-555.
153. Meyer, M.R. and M. Barton, *Role of Perivascular Adipose Tissue for Sex Differences in Coronary Artery Disease and Spontaneous Coronary Artery Dissection (SCAD)*. Endocrine and Metabolic Science, 2021. **2**: p. 100068.
154. Durand, J.L., et al., *Gender differences in adiponectin modulation of cardiac remodeling in mice deficient in endothelial nitric oxide synthase*. Journal of cellular biochemistry, 2012. **113**(10): p. 3276-3287.
155. Schorr, M., et al., *Sex differences in body composition and association with cardiometabolic risk*. Biology of sex differences, 2018. **9**(1): p. 1-10.
156. Chang, E., M. Varghese, and K. Singer, *Gender and sex differences in adipose tissue*. Current diabetes reports, 2018. **18**(9): p. 69.
157. Bradley, D., et al., *Adipocyte DIO2 Expression Increases in Human Obesity but Is Not Related to Systemic Insulin Sensitivity*. Journal of diabetes research, 2018. **2018**.
158. Rogers, N.H., et al., *Estradiol stimulates Akt, AMP-activated protein kinase (AMPK) and TBC1D1/4, but not glucose uptake in rat soleus*. Biochemical and biophysical research communications, 2009. **382**(4): p. 646-650.
159. Riedel, K., et al., *Estrogen determines sex differences in adrenergic vessel tone by regulation of endothelial  $\beta$ -adrenoceptor expression*. American Journal of Physiology-Heart and Circulatory Physiology, 2019. **317**(2): p. H243-H254.
160. Lemieux, S., et al., *Sex differences in the relation of visceral adipose tissue accumulation to total body fatness*. The American journal of clinical nutrition, 1993. **58**(4): p. 463-467.
161. Thanassoulis, G., et al., *Prevalence, distribution, and risk factor correlates of high pericardial and intrathoracic fat depots in the Framingham heart study*. Circulation: Cardiovascular Imaging, 2010. **3**(5): p. 559-566.
162. Nguyen, T.T., et al., *Postprandial leg and splanchnic fatty acid metabolism in nonobese men and women*. American Journal of Physiology-Endocrinology And Metabolism, 1996. **271**(6): p. E965-E972.
163. Romanski, S.A., R.M. Nelson, and M.D. Jensen, *Meal fatty acid uptake in adipose tissue: gender effects in nonobese humans*. American Journal of Physiology- Endocrinology And Metabolism, 2000. **279**(2): p. E455-E462.

164. Fried, S.K. and J.G. Kral, *Sex differences in regional distribution of fat cell size and lipoprotein lipase activity in morbidly obese patients*. International journal of obesity, 1987. **11**(2): p. 129-140.
165. Elbers, J., et al., *Effects of sex steroid hormones on regional fat depots as assessed by magnetic resonance imaging in transsexuals*. American Journal of Physiology- Endocrinology And Metabolism, 1999. **276**(2): p. E317-E325.
166. Kohlgruber, A. and L. Lynch, *Adipose tissue inflammation in the pathogenesis of type 2 diabetes*. Curr Diab Rep, 2015. **15**(11): p. 92.
167. Mauvais-Jarvis, F., D.J. Clegg, and A.L. Hevener, *The role of estrogens in control of energy balance and glucose homeostasis*. Endocrine reviews, 2013. **34**(3): p. 309-338.
168. Masding, M.G., et al., *Premenopausal advantages in postprandial lipid metabolism are lost in women with type 2 diabetes*. Diabetes Care, 2003. **26**(12): p. 3243-3249.
169. Wallen, W.J., M.P. Belanger, and C. Wittnich, *Sex hormones and the selective estrogen receptor modulator tamoxifen modulate weekly body weights and food intakes in adolescent and adult rats*. The Journal of nutrition, 2001. **131**(9): p. 2351-2357.
170. Jones, M.E., et al., *Aromatase-deficient (ArKO) mice have a phenotype of increased adiposity*. Proceedings of the National Academy of Sciences, 2000. **97**(23): p. 12735-12740.
171. Kristensen, K., et al., *Hormone replacement therapy affects body composition and leptin differently in obese and non-obese postmenopausal women*. Journal of endocrinology, 1999. **163**(1): p. 55-62.
172. Davis, K.E., et al., *The sexually dimorphic role of adipose and adipocyte estrogen receptors in modulating adipose tissue expansion, inflammation, and fibrosis*. Molecular metabolism, 2013. **2**(3): p. 227-242.
173. Pfeilschifter, J., et al., *Changes in proinflammatory cytokine activity after menopause*. Endocrine reviews, 2002. **23**(1): p. 90-119.
174. Rogers, N.H., et al., *Reduced energy expenditure and increased inflammation are early events in the development of ovariectomy-induced obesity*. Endocrinology, 2009. **150**(5): p. 2161-2168.
175. Camporez, J.P., et al., *Anti-inflammatory effects of oestrogen mediate the sexual dimorphic response to lipid-induced insulin resistance*. The Journal of physiology, 2019. **597**(15): p. 3885-3903.
176. Vasconcelos, R.P., et al., *Sex differences in subcutaneous adipose tissue redox homeostasis and inflammation markers in control and high-fat diet fed rats*. Applied physiology, nutrition, and metabolism, 2019. **44**(7): p. 720-726.
177. Navia, B., et al., *Interleukin-6 deletion in mice driven by a P 2-C re-ERT 2 prevents against high-fat diet-induced gain weight and adiposity in female mice*. Acta Physiologica, 2014. **211**(4): p. 585-596.
178. Moran, A., et al., *Changes in insulin resistance and cardiovascular risk during adolescence: establishment of differential risk in males and females*. Circulation, 2008. **117**(18): p. 2361-8.



179. Nuutila, P., et al., *Gender and insulin sensitivity in the heart and in skeletal muscles. Studies using positron emission tomography*. Diabetes, 1995. **44**(1): p. 31-6.
180. Goossens, G.H., J.W. Jocken, and E.E. Blaak, *Sexual dimorphism in cardiometabolic health: the role of adipose tissue, muscle and liver*. Nature Reviews Endocrinology, 2020: p. 1-20.
181. Kulakosky, P., et al., *Response element sequence modulates estrogen receptor alpha and beta affinity and activity*. Journal of Molecular Endocrinology, 2002. **29**(1): p. 137-152.
182. Joyner, J.M., L.J. Hutley, and D.P. Cameron, *Estrogen receptors in human preadipocytes*. Endocrine, 2001. **15**(2): p. 225-230.
183. Geary, N., et al., *Deficits in E2-dependent control of feeding, weight gain, and cholecystokinin satiation in ER- $\alpha$  null mice*. Endocrinology, 2001. **142**(11): p. 4751-4757.
184. Heine, P., et al., *Increased adipose tissue in male and female estrogen receptor-  $\alpha$  knockout mice*. Proceedings of the National Academy of Sciences, 2000. **97**(23): p. 12729-12734.
185. Smith, E.P., et al., *Estrogen resistance caused by a mutation in the estrogen- receptor gene in a man*. New England Journal of Medicine, 1994. **331**(16): p. 1056-1061.
186. Roesch, D.M., *Effects of selective estrogen receptor agonists on food intake and body weight gain in rats*. Physiology & behavior, 2006. **87**(1): p. 39-44.
187. Santollo, J., M.D. Wiley, and L.A. Eckel, *Acute activation of ER $\alpha$  decreases food intake, meal size, and body weight in ovariectomized rats*. American Journal of Physiology-Regulatory, Integrative and Comparative Physiology, 2007. **293**(6): p. R2194-R2201.
188. Yepuru, M., et al., *Estrogen receptor- $\beta$ -selective ligands alleviate high-fat diet- and ovariectomy-induced obesity in mice*. Journal of Biological Chemistry, 2010. **285**(41): p. 31292-31303.
189. Wahrenberg, H., F. Lönnqvist, and P. Arner, *Mechanisms underlying regional differences in lipolysis in human adipose tissue*. The Journal of clinical investigation, 1989. **84**(2): p. 458-467.
190. Rydén, M., H. Gao, and P. Arner, *Influence of aging and menstrual status on subcutaneous fat cell lipolysis*. The Journal of Clinical Endocrinology & Metabolism, 2020. **105**(4): p. e955-e962.
191. Pedersen, S.B., et al., *Estrogen controls lipolysis by up-regulating  $\alpha$ 2A-adrenergic receptors directly in human adipose tissue through the estrogen receptor  $\alpha$ . Implications for the female fat distribution*. The Journal of Clinical Endocrinology & Metabolism, 2004. **89**(4): p. 1869-1878.
192. Jensen, M.D., et al., *Effects of epinephrine on regional free fatty acid and energy metabolism in men and women*. American Journal of Physiology-Endocrinology And Metabolism, 1996. **270**(2): p. E259-E264.
193. Shadid, S., C. Koutsari, and M.D. Jensen, *Direct free fatty acid uptake into human adipocytes in vivo: relation to body fat distribution*. Diabetes, 2007. **56**(5): p. 1369-1375.

194. Nookaew, I., et al., *Adipose tissue resting energy expenditure and expression of genes involved in mitochondrial function are higher in women than in men*. The Journal of Clinical Endocrinology & Metabolism, 2013. **98**(2): p. E370-E378.
195. Rodriguez, A., et al., *Opposite actions of testosterone and progesterone on UCP1 mRNA expression in cultured brown adipocytes*. Cellular and Molecular Life Sciences CMLS, 2002. **59**(10): p. 1714-1723.
196. Quevedo, S., et al., *Sex-associated differences in cold-induced UCP1 synthesis in rodent brown adipose tissue*. Pflügers Archiv, 1998. **436**(5): p. 689-695.
197. Winn, N.C., et al., *Loss of UCP1 exacerbates Western diet-induced glycemic dysregulation independent of changes in body weight in female mice*. Am J Physiol Regul Integr Comp Physiol, 2017. **312**(1): p. R74-R84.
198. Nadal-Casellas, A., et al., *Sex-dependent differences in rat brown adipose tissue mitochondrial biogenesis and insulin signaling parameters in response to an obesogenic diet*. Molecular and cellular biochemistry, 2013. **373**(1): p. 125-135.
199. Rodriguez-Cuenca, S., et al., *Sex-dependent thermogenesis, differences in mitochondrial morphology and function, and adrenergic response in brown adipose tissue*. Journal of Biological Chemistry, 2002. **277**(45): p. 42958-42963.
200. Rodríguez, A.M., et al., *Sex-dependent dietary obesity, induction of UCPs, and leptin expression in rat adipose tissues*. Obesity research, 2001. **9**(9): p. 579-588.
201. Peixoto, T., et al., *Nicotine exposure during breastfeeding reduces sympathetic activity in brown adipose tissue and increases in white adipose tissue in adult rats: sex-related differences*. Food and Chemical Toxicology, 2020. **140**: p. 111328.
202. Kim, S.-N., et al., *Sex differences in sympathetic innervation and browning of white adipose tissue of mice*. Biology of sex differences, 2016. **7**(1): p. 1-13.
203. Norheim, F., et al., *Gene-by-sex interactions in mitochondrial functions and cardio-metabolic traits*. Cell metabolism, 2019. **29**(4): p. 932-949. e4.
204. Keuper, M., et al., *Preadipocytes of obese humans display gender-specific bioenergetic responses to glucose and insulin*. Molecular metabolism, 2019. **20**: p. 28-37.
205. Fatima, L., et al., *Estrogen receptor 1 (ESR1) regulates VEGFA in adipose tissue*. Scientific reports, 2017. **7**(1): p. 1-14.
206. George, A.L., et al., *Hypoxia and estrogen are functionally equivalent in breast cancer-endothelial cell interdependence*. Molecular cancer, 2012. **11**(1): p. 1-12.
207. Rudnicki, M., et al., *Female mice have higher angiogenesis in perigonadal adipose tissue than males in response to high-fat diet*. Frontiers in physiology, 2018. **9**: p. 1452.
208. Keuper, M. and M. Jastroch, *The good and the BAT of metabolic sex differences in thermogenic human adipose tissue*. Molecular and Cellular Endocrinology, 2021: p. 111337.
209. Dobner, J., et al., *Fat-enriched rather than high-fructose diets promote whitening of adipose tissue in a sex-dependent manner*. The Journal of nutritional biochemistry, 2017. **49**: p. 22-29.

210. Cooney, M., et al., *HDL cholesterol protects against cardiovascular disease in both genders, at all ages and at all levels of risk*. *Atherosclerosis*, 2009. **206**(2): p. 611-616.
211. Ahmad, A.A., M.D. Randall, and R.E. Roberts, *Sex differences in the regulation of porcine coronary artery tone by perivascular adipose tissue: a role of adiponectin?* *British journal of pharmacology*, 2017. **174**(16): p. 2773-2783.
212. Taylor, L.E. and J.C. Sullivan, *Sex differences in obesity-induced hypertension and vascular dysfunction: a protective role for estrogen in adipose tissue inflammation?* *American Journal of Physiology-Regulatory, Integrative and Comparative Physiology*, 2016. **311**(4): p. R714-R720.
213. Watts, S.W., et al., *Male and Female High Fat Fed Dahl SS rats are largely protected from vascular dysfunctions: PVAT contributions reveal sex differences*. *American Journal of Physiology-Heart and Circulatory Physiology*, 2021.
214. Ahmad, A.A., M.D. Randall, and R.E. Roberts, *Sex differences in the role of phospholipase A2-dependent arachidonic acid pathway in the perivascular adipose tissue function in pigs*. *The Journal of physiology*, 2017. **595**(21): p. 6623- 6634.
215. Zaborska, K., et al., *Loss of anti-contractile effect of perivascular adipose tissue in offspring of obese rats*. *International Journal of Obesity*, 2016. **40**(8): p. 1205- 1214.
216. Zaborska, K.E., et al., *The role of O-GlcNAcylation in perivascular adipose tissue dysfunction of offspring of high-fat diet-fed rats*. *Journal of vascular research*, 2017. **54**(2): p. 79-91.
217. Victorio, J.A., et al., *Effects of High-Fat and High-Fat/High-Sucrose Diet-Induced Obesity on PVAT Modulation of Vascular Function in Male and Female Mice*. *Frontiers in Pharmacology*, 2021: p. 2252.
218. Contreras, G.A., et al., *The distribution and adipogenic potential of perivascular adipose tissue adipocyte progenitors is dependent on sexual dimorphism and vessel location*. *Physiological reports*, 2016. **4**(19): p. e12993.
219. Sasoh, T., et al., *Different effects of high-fat and high-sucrose diets on the physiology of perivascular adipose tissues of the thoracic and abdominal aorta*. *Adipocyte*, 2021.
220. Badran, M., et al., *Gestational intermittent hypoxia induces endothelial dysfunction, reduces perivascular adiponectin and causes epigenetic changes in adult male offspring*. *The Journal of physiology*, 2019. **597**(22): p. 5349-5364.
221. Kumar, R.K., et al., *Naïve, regulatory, activated, and memory immune cells Co- exist in PVATs that are comparable in density to non-PVAT fats in health*. *Frontiers in physiology*, 2020. **11**: p. 58.
222. Khatib, M.A.-W., et al., *Mild hyper-caloric intake is associated with perivascular adipose inflammation and vascular dysfunction: modulation by antidiabetic drugs*. *The FASEB Journal*, 2018. **32**(1\_supplement): p. 569.11-569.11.
223. Maddie, N. and M.A.A. Carrillo-sepulveda. *Loss Of The Brown-Like Phenotype Of Aortic PVAT Is Associated With Mitochondrial Dysfunction In Obesity-Induced Endothelial Dysfunction In Female Rats*. in *HYPERTENSION*. 2020. LIPPINCOTT WILLIAMS & WILKINS TWO COMMERCE SQ, 2001 MARKET ST, PHILADELPHIA ....

224. Maddie, N.M., D. Persand, and M.A. Carrillo-Sepulveda, *BCL6 is Upregulated in Perivascular Adipose Tissue (PVAT) in Western Diet-Induced Obesity-Related Hypertension in Female Rats*. The FASEB Journal, 2020. **34**(S1): p. 1-1.
225. Rodríguez, E., et al., *Sexual dimorphism in the adrenergic control of rat brown adipose tissue response to overfeeding*. Pflügers Archiv, 2001. **442**(3): p. 396-403.
226. Patterson, R.E., et al., *Intermittent fasting and human metabolic health*. Journal of the Academy of Nutrition and Dietetics, 2015. **115**(8): p. 1203-1212.
227. Antoni, R., et al., *Effects of intermittent fasting on glucose and lipid metabolism*. Proceedings of the Nutrition Society, 2017. **76**(3): p. 361-368.
228. St-Onge, M.-P., et al., *Meal timing and frequency: implications for cardiovascular disease prevention: a scientific statement from the American Heart Association*. Circulation, 2017. **135**(9): p. e96-e121.
229. Liu, B., et al., *Intermittent Fasting Improves Glucose Tolerance and Promotes Adipose Tissue Remodeling in Male Mice Fed a High-Fat Diet*. Endocrinology, 2018. **160**(1): p. 169-180.
230. Kivela, R. and K. Alitalo, *White adipose tissue coloring by intermittent fasting*. Cell Res, 2017. **27**(11): p. 1300-1301.
231. de Souza Marinho, T., et al., *Browning of the subcutaneous adipocytes in diet- induced obese mouse submitted to intermittent fasting*. Molecular and Cellular Endocrinology, 2020: p. 110872.
232. Aksungar, F.B., et al., *Comparison of intermittent fasting versus caloric restriction in obese subjects: A two year follow-up*. The journal of nutrition, health & aging, 2017. **21**(6): p. 681-685.
233. Kim, K.-H., et al., *Intermittent fasting promotes adipose thermogenesis and metabolic homeostasis via VEGF-mediated alternative activation of macrophage*. Cell Research, 2017. **27**(11): p. 1309-1326.
234. Tang, H.-N., et al., *Plasticity of adipose tissue in response to fasting and refeeding in male mice*. Nutrition & metabolism, 2017. **14**(1): p. 3.
235. Varady, K.A., C.S. Hudak, and M.K. Hellerstein, *Modified alternate-day fasting and cardioprotection: relation to adipose tissue dynamics and dietary fat intake*. Metabolism, 2009. **58**(6): p. 803-811.
236. Varady, K., et al., *Effects of modified alternate-day fasting regimens on adipocyte size, triglyceride metabolism, and plasma adiponectin levels in mice*. Journal of lipid research, 2007. **48**(10): p. 2212-2219.
237. Varady, K.A., et al., *Improvements in body fat distribution and circulating adiponectin by alternate-day fasting versus calorie restriction*. The Journal of nutritional biochemistry, 2010. **21**(3): p. 188-195.
238. Dwaib, H.S., et al., *Therapeutic fasting mitigates metabolic and cardiovascular dysfunction in a prediabetic rat model: Possible role of adipose inflammation*. The FASEB Journal, 2020. **34**(S1): p. 1-1.
239. Bhutani, S., et al., *Alternate day fasting and endurance exercise combine to reduce body weight and favorably alter plasma lipids in obese humans*. Obesity (Silver Spring), 2013. **21**(7): p. 1370-9.
240. Harvie, M.N., et al., *The effects of intermittent or continuous energy restriction on weight loss and metabolic disease risk markers: a randomized trial in young*

- overweight women. *International journal of obesity* (2005), 2011. **35**(5): p. 714-727.
241. Tinsley, G.M. and P.M. La Bounty, *Effects of intermittent fasting on body composition and clinical health markers in humans*. *Nutrition Reviews*, 2015. **73**(10): p. 661-674.
  242. Wang, X., et al., *Effects of intermittent fasting diets on plasma concentrations of inflammatory biomarkers: A systematic review and meta-analysis of randomized controlled trials*. *Nutrition*, 2020. **79-80**: p. 110974.
  243. Kacimi, S., et al., *Intermittent fasting during Ramadan attenuates proinflammatory cytokines and immune cells in healthy subjects*. *Nutrition research*, 2012. **32**(12): p. 947-955.
  244. Klempel, M.C., et al., *Intermittent fasting combined with calorie restriction is effective for weight loss and cardio-protection in obese women*. *Nutrition journal*, 2012. **11**(1): p. 98.
  245. Patterson, R.E. and D.D. Sears, *Metabolic effects of intermittent fasting*. *Annual review of nutrition*, 2017. **37**.
  246. Liu, B., et al., *Markers of adipose tissue inflammation are transiently elevated during intermittent fasting in women who are overweight or obese*. *Obes Res Clin Pract*, 2019. **13**(4): p. 408-415.
  247. Fabbiano, S., et al., *Caloric restriction leads to browning of white adipose tissue through type 2 immune signaling*. *Cell metabolism*, 2016. **24**(3): p. 434-446.
  248. Bordone, L., et al., *SIRT1 transgenic mice show phenotypes resembling calorie restriction*. *Aging Cell*, 2007. **6**(6): p. 759-67.
  249. Schenk, S., et al., *Sirt1 enhances skeletal muscle insulin sensitivity in mice during caloric restriction*. *J Clin Invest*, 2011. **121**(11): p. 4281-8.
  250. Pfluger, P.T., et al., *Sirt1 protects against high-fat diet-induced metabolic damage*. *Proceedings of the National Academy of Sciences*, 2008. **105**(28): p. 9793-9798.
  251. Luo, G., et al., *Sirt1 promotes autophagy and inhibits apoptosis to protect cardiomyocytes from hypoxic stress*. *Int J Mol Med*, 2019. **43**(5): p. 2033-2043.
  252. Kajita, K., et al., *Effect of fasting on PPAR $\gamma$  and AMPK activity in adipocytes*. *Diabetes research and clinical practice*, 2008. **81**(2): p. 144-149.
  253. Fakh, W., et al., *Dysfunctional cerebrovascular tone contributes to cognitive impairment in a non-obese rat model of prediabetic challenge: Role of suppression of autophagy and modulation by anti-diabetic drugs*. *Biochemical Pharmacology*, 2020: p. 114041.
  254. Villena, J.A., et al., *Induced adiposity and adipocyte hypertrophy in mice lacking the AMP-activated protein kinase-alpha2 subunit*. *Diabetes*, 2004. **53**(9): p. 2242- 9.
  255. Pedersen, S.B., et al., *Low Sirt1 expression, which is upregulated by fasting, in human adipose tissue from obese women*. *Int J Obes (Lond)*, 2008. **32**(8): p. 1250- 5.
  256. Madkour, M.I., et al., *Ramadan diurnal intermittent fasting modulates SOD2, TFAM, Nrf2, and sirtuins (SIRT1, SIRT3) gene expressions in subjects with*

- overweight and obesity*. *diabetes research and clinical practice*, 2019. **155**: p. 107801.
257. Kivelä, R. and K. Alitalo, *White adipose tissue coloring by intermittent fasting*. *Cell research*, 2017. **27**(11): p. 1300.
258. Weir, H.J., et al., *Dietary restriction and AMPK increase lifespan via mitochondrial network and peroxisome remodeling*. *Cell metabolism*, 2017. **26**(6): p. 884-896. e5.
259. Barnosky, A.R., et al., *Intermittent fasting vs daily calorie restriction for type 2 diabetes prevention: a review of human findings*. *Translational Research*, 2014. **164**(4): p. 302-311.
260. Lettieri-Barbato, D., E. Giovannetti, and K. Aquilano, *Effects of dietary restriction on adipose mass and biomarkers of healthy aging in human*. *Aging (Albany NY)*, 2016. **8**(12): p. 3341.
261. Erdem, Y., et al., *The effect of intermittent fasting on blood pressure variability in patients with newly diagnosed hypertension or prehypertension*. *Journal of the American Society of Hypertension*, 2018. **12**(1): p. 42-49.
262. Lotfi, S., et al., *CNS activation, reaction time, blood pressure and heart rate variation during ramadan intermittent fasting and exercise*. *World J Sports Sci*, 2010. **3**(1): p. 37-43.
263. Wan, R., S. Camandola, and M.P. Mattson, *Intermittent fasting and dietary supplementation with 2-deoxy-D-glucose improve functional and metabolic cardiovascular risk factors in rats*. *The FASEB Journal*, 2003. **17**(9): p. 1133-1134.
264. Mager, D.E., et al., *Caloric restriction and intermittent fasting alter spectral measures of heart rate and blood pressure variability in rats*. *The FASEB Journal*, 2006. **20**(6): p. 631-637.
265. Cansel, M., et al., *The effects of Ramadan fasting on heart rate variability in healthy individuals: a prospective study*. *Anatolian Journal of Cardiology/Anadolu Kardiyoloji Dergisi*, 2014. **14**(5).
266. Esmaeilzadeh, F. and P. Van De Borne, *Does intermittent fasting improve microvascular endothelial function in healthy middle-aged subjects?* *Biology and Medicine*, 2016. **8**(6): p. 1.
267. Razzak, R., et al., *Assessment of enhanced endothelium-dependent vasodilation by intermittent fasting in Wistar albino rats*. *Indian J Physiol Pharmacol*, 2011. **55**(4): p. 336-42.
268. Malinowski, B., et al., *Intermittent fasting in cardiovascular disorders—An overview*. *Nutrients*, 2019. **11**(3): p. 673.
269. Fann, D.Y.-W., et al., *Positive effects of intermittent fasting in ischemic stroke*. *Experimental gerontology*, 2017. **89**: p. 93-102.
270. Bussey, C.E., et al., *Obesity-related perivascular adipose tissue damage is reversed by sustained weight loss in the rat*. *Arteriosclerosis, Thrombosis, and Vascular Biology*, 2016. **36**(7): p. 1377-1385.
271. Boucher, J.M., et al., *Pathological conversion of mouse perivascular adipose tissue by notch activation*. *Arteriosclerosis, thrombosis, and vascular biology*, 2020. **40**(9): p. 2227-2243.

272. Zuo, L., et al., *Comparison of high-protein, intermittent fasting low-calorie diet and heart healthy diet for vascular health of the obese*. *Frontiers in physiology*, 2016. **7**: p. 350.
273. Wilson, R.A., et al., *Intermittent fasting and high-intensity exercise elicit sexual- dimorphic and tissue-specific adaptations in diet-induced obese mice*. *Nutrients*, 2020. **12**(6): p. 1764.
274. Lin, S., et al., *Does the weight loss efficacy of alternate day fasting differ according to sex and menopausal status?* *Nutrition, Metabolism and Cardiovascular Diseases*, 2021. **31**(2): p. 641-649.
275. Chung, H., et al., *Time-restricted feeding improves insulin resistance and hepatic steatosis in a mouse model of postmenopausal obesity*. *Metabolism*, 2016. **65**(12): p. 1743-1754.
276. Valle, A., et al., *Sex-related differences in energy balance in response to caloric restriction*. *American Journal of Physiology-Endocrinology and Metabolism*, 2005. **289**(1): p. E15-E22.
277. Bakkar, N.-M.Z., et al., *Worsening baroreflex sensitivity on progression to type 2 diabetes: localized vs. systemic inflammation and role of antidiabetic therapy*. *American Journal of Physiology-Endocrinology and Metabolism*, 2020. **319**(5): p. E835-E851.
278. Alaaeddine, R., et al., *Impaired endothelium-dependent hyperpolarization underlies endothelial dysfunction during early metabolic challenge: Increased ROS generation and possible interference with NO function*. *Journal of Pharmacology and Experimental Therapeutics*, 2019. **371**(3): p. 567-582.
279. Anunciado-Koza, R., et al., *Inactivation of UCP1 and the glycerol phosphate cycle synergistically increases energy expenditure to resist diet-induced obesity*. *Journal of Biological Chemistry*, 2008. **283**(41): p. 27688-27697.
280. Macher, G., et al., *Inhibition of mitochondrial UCP1 and UCP3 by purine nucleotides and phosphate*. *Biochimica et Biophysica Acta (BBA)-Biomembranes*, 2018. **1860**(3): p. 664-672.
281. Nedergaard, J., et al., *UCP1: the only protein able to mediate adaptive non- shivering thermogenesis and metabolic inefficiency*. *Biochimica et Biophysica Acta (BBA)-Bioenergetics*, 2001. **1504**(1): p. 82-106.
282. Boden, G., *Obesity and free fatty acids*. *Endocrinology and metabolism clinics of North America*, 2008. **37**(3): p. 635-646.
283. León, J.B., C.M. Sullivan, and A.R. Sehgal, *The prevalence of phosphorus- containing food additives in top-selling foods in grocery stores*. *Journal of Renal Nutrition*, 2013. **23**(4): p. 265-270. e2.
284. Erem, S. and M.S. Razzaque, *Dietary phosphate toxicity: An emerging global health concern*. *Histochemistry and cell biology*, 2018. **150**(6): p. 711-719.
285. Dudley, F. and C. Blackburn, *Extraskeletal calcification complicating oral neutral- phosphate therapy*. *The Lancet*, 1970. **296**(7674): p. 628-630.
286. Schwarz, S., et al., *Association of disorders in mineral metabolism with progression of chronic kidney disease*. *Clinical Journal of the American Society of Nephrology*, 2006. **1**(4): p. 825-831.

287. Olanbiwonnu, T. and R.M. Holden, *Inorganic phosphate as a potential risk factor for chronic disease*. CMAJ, 2018. **190**(26): p. E784-E785.
288. Scialla, J.J. and M. Wolf, *Roles of phosphate and fibroblast growth factor 23 in cardiovascular disease*. Nature Reviews Nephrology, 2014. **10**(5): p. 268.
289. Foley, R.N., *Phosphate levels and cardiovascular disease in the general population*. Clinical Journal of the American Society of Nephrology, 2009. **4**(6): p. 1136-1139.
290. Park, W., et al., *Serum phosphate levels and the risk of cardiovascular disease and metabolic syndrome: a double-edged sword*. Diabetes research and clinical practice, 2009. **83**(1): p. 119-125.
291. McClelland, R., et al., *Accelerated ageing and renal dysfunction links lower socioeconomic status and dietary phosphate intake*. Aging (Albany NY), 2016. **8**(5): p. 1135.
292. Yamamoto, K.T., et al., *Dietary phosphorus is associated with greater left ventricular mass*. Kidney international, 2013. **83**(4): p. 707-714.
293. Cheungpasitporn, W., et al., *Admission serum phosphate levels predict hospital mortality*. Hospital Practice, 2018. **46**(3): p. 121-127.
294. Stevens, K.K., et al., *Deleterious effects of phosphate on vascular and endothelial function via disruption to the nitric oxide pathway*. Nephrology Dialysis Transplantation, 2017. **32**(10): p. 1617-1627.
295. Tsai, W.-C., et al., *Effects of lower versus higher phosphate diets on fibroblast growth factor-23 levels in patients with chronic kidney disease: a systematic review and meta-analysis*. Nephrology Dialysis Transplantation, 2018. **33**(11): p. 1977-1983.
296. Six, I., et al., *Effects of phosphate on vascular function under normal conditions and influence of the uraemic state*. Cardiovascular research, 2012. **96**(1): p. 130- 139.
297. Rubio-Aliaga, I., *Phosphate and kidney healthy aging*. Kidney and Blood Pressure Research, 2020. **45**(5): p. 1-10.
298. Ayoub, J., et al., *Effect of phosphorus supplementation on weight gain and waist circumference of overweight/obese adults: a randomized clinical trial*. Nutrition & diabetes, 2015. **5**(12): p. e189-e189.
299. Imi, Y., et al., *High phosphate diet suppresses lipogenesis in white adipose tissue*. Journal of Clinical Biochemistry and Nutrition, 2018. **63**(3): p. 181-191.
300. Hazim, J., et al., *Phosphorus supplement alters postprandial lipemia of healthy male subjects: a pilot cross-over trial*. Lipids in health and disease, 2014. **13**(1): p. 109.
301. Khattab, M., et al., *Phosphorus ingestion improves oral glucose tolerance of healthy male subjects: a crossover experiment*. Nutrition journal, 2015. **14**(1): p. 1-8.
302. Khattab, M., et al., *Effect of phosphorus on the oral glucose tolerance test*. Proceedings of the Nutrition Society, 2011. **70**(OCE3).
303. Tanaka, S., et al., *Dietary phosphate restriction induces hepatic lipid accumulation through dysregulation of cholesterol metabolism in mice*. Nutrition Research, 2013. **33**(7): p. 586-593.



304. Obeid, O., *Low phosphorus status might contribute to the onset of obesity*. Obesity reviews, 2013. **14**(8): p. 659-664.
305. Shimodaira, M., S. Okaniwa, and T. Nakayama, *Reduced Serum Phosphorus Levels Were Associated with Metabolic Syndrome in Men But Not in Women: A Cross- Sectional Study among the Japanese Population*. Annals of Nutrition and Metabolism, 2017. **71**(3-4): p. 150-156.
306. Voelkl, J., et al., *Inflammation: a putative link between phosphate metabolism and cardiovascular disease*. Clinical Science, 2021. **135**(1): p. 201-227.
307. Peacock, M., *Phosphate metabolism in health and disease*. Calcified tissue international, 2021. **108**(1): p. 3-15.
308. Li, S., et al., *Diabetes mellitus and cause-specific mortality: a population-based study*. Diabetes & metabolism journal, 2019. **43**(3): p. 319-341.
309. Leinonen, E.S., et al., *Low-grade inflammation, endothelial activation and carotid intima-media thickness in type 2 diabetes*. Journal of internal medicine, 2004. **256**(2): p. 119-127.
310. Cani, P.D., et al., *Metabolic endotoxemia initiates obesity and insulin resistance*. Diabetes, 2007. **56**(7): p. 1761-1772.
311. Shimizu, I., et al., *Adipose tissue inflammation in diabetes and heart failure*. Microbes and Infection, 2013. **15**(1): p. 11-17.
312. National Research Council Committee for the Update of the Guide for the, C. and A. Use of Laboratory, *The National Academies Collection: Reports funded by National Institutes of Health*, in *Guide for the Care and Use of Laboratory Animals*, th, Editor. 2011, National Academies Press (US) National Academy of Sciences.: Washington (DC).
313. Reeves, P.G., F.H. Nielsen, and G.C. Fahey, Jr., *AIN-93 purified diets for laboratory rodents: final report of the American Institute of Nutrition ad hoc writing committee on the reformulation of the AIN-76A rodent diet*. J Nutr, 1993. **123**(11): p. 1939-51.
314. Al-Assi, O., et al., *Cardiac Autonomic Neuropathy as a Result of Mild Hypercaloric Challenge in Absence of Signs of Diabetes: Modulation by Antidiabetic Drugs*. 2018. **2018**: p. 9389784.
315. Hammoud, S.H., et al., *Peri-renal adipose inflammation contributes to renal dysfunction in a non-obese prediabetic rat model: Role of anti-diabetic drugs*. Biochem Pharmacol, 2021. **186**: p. 114491.
316. El-Yazbi, A.F., K.S. Abd-Elrahman, and A. Moreno-Dominguez, *PKC-mediated cerebral vasoconstriction: Role of myosin light chain phosphorylation versus actin cytoskeleton reorganization*. Biochem Pharmacol, 2015. **95**(4): p. 263-78.
317. El-Gowell, H.M., et al., *Role of NADPHox/Rho-kinase signaling in the cyclosporine-NSAIDs interactions on blood pressure and baroreflexes in female rats*. Life sciences, 2017. **185**: p. 15-22.
318. Fishbein, M.C., *Reperfusion injury*. Clin Cardiol, 1990. **13**(3): p. 213-7.
319. Hammoud, S.H., et al., *Peri-renal adipose inflammation contributes to renal dysfunction in a non-obese prediabetic rat model: Role of anti-diabetic drugs*. Biochemical Pharmacology, 2021. **186**: p. 114491.

320. Wong, T.-Y., et al., *Detection and characterization of mineralo-organic nanoparticles in human kidneys*. Scientific reports, 2015. **5**(1): p. 1-13.
321. El-Yazbi, A.F., et al., *Pressure-dependent contribution of Rho kinase-mediated calcium sensitization in serotonin-evoked vasoconstriction of rat cerebral arteries*. J Physiol, 2010. **588**(Pt 10): p. 1747-62.
322. Cho, K.W., D.L. Morris, and C.N. Lumeng, *Flow Cytometry Analyses of Adipose Tissue Macrophages*. Methods Enzymol, 2014. **537**: p. 297-314.
323. Rubio-Navarro, A., et al., *Phenotypic Characterization of Macrophages from Rat Kidney by Flow Cytometry*. J Vis Exp, 2016(116).
324. Fink, T. and V. Zachar, *Adipogenic differentiation of human mesenchymal stem cells*, in *Mesenchymal stem cell assays and applications*. 2011, Springer. p. 243- 251.
325. Dwaib, H.S.A., Ghina; AlZaim, Ibrahim; Rafeh, Rim; Mroueh, Ali; Mougharbil, Nahed; Ragi, Marie-Elizabeth; Refaat, Marwan ; Obeid, Omar ; and El-Yazbi, Ahmed F. , *Phosphorus Supplementation Mitigates Perivascular Adipose Inflammation Induced Cardiovascular Consequences in Early Metabolic Impairment* Journal of American Heart Association 2021.
326. Morris, D.L., K. Singer, and C.N. Lumeng, *Adipose tissue macrophages: phenotypic plasticity and diversity in lean and obese states*. Current opinion in clinical nutrition and metabolic care, 2011. **14**(4): p. 341-346.
327. Kazak, L., et al., *Ablation of adipocyte creatine transport impairs thermogenesis and causes diet-induced obesity*. Nature metabolism, 2019. **1**(3): p. 360-370.
328. Chang, A.R. and C. Anderson, *Dietary Phosphorus Intake and the Kidney*. Annual review of nutrition, 2017. **37**: p. 321-346.
329. Palmer, B.F. and D.J. Clegg, *The sexual dimorphism of obesity*. Molecular and cellular endocrinology, 2015. **402**: p. 113-119.
330. Kim, J.H., H.T. Cho, and Y.J. Kim, *The role of estrogen in adipose tissue metabolism: insights into glucose homeostasis regulation*. Endocrine journal, 2014: p. EJ14-0262.
331. Dubey, R.K. and E.K. Jackson, *Estrogen-induced cardiorenal protection: potential cellular, biochemical, and molecular mechanisms*. American Journal of Physiology-Renal Physiology, 2001. **280**(3): p. F365-F388.
332. Suzuki, M., et al., *Role of estradiol and testosterone in Ucp1 expression in brown/beige adipocytes*. Cell biochemistry and function, 2018. **36**(8): p. 450-456.
333. Velickovic, K., et al., *Expression and subcellular localization of estrogen receptors  $\alpha$  and  $\beta$  in human fetal brown adipose tissue*. The Journal of Clinical Endocrinology & Metabolism, 2014. **99**(1): p. 151-159.
334. Santos, R.S., et al., *Activation of estrogen receptor alpha induces beiging of adipocytes*. Molecular metabolism, 2018. **18**: p. 51-59.
335. Porter, J.W., et al., *Age, Sex, and Depot-Specific Differences in Adipose-Tissue Estrogen Receptors in Individuals with Obesity*. Obesity, 2020. **28**(9): p. 1698- 1707.
336. Frank, A.P., B.F. Palmer, and D.J. Clegg, *Do estrogens enhance activation of brown and beiging of adipose tissues?* Physiology & behavior, 2018. **187**: p. 24- 31.

337. MacCannell, A.D., et al., *Sexual dimorphism in adipose tissue mitochondrial function and metabolic flexibility in obesity*. International Journal of Obesity, 2021: p. 1-9.
338. Hoffmann, C., et al., *Response of mitochondrial respiration in adipose tissue and muscle to 8 weeks of endurance exercise in obese subjects*. The Journal of Clinical Endocrinology & Metabolism, 2020. **105**(11): p. e4023-e4037.
339. Xu, J., et al., *Estrogen improved metabolic syndrome through down-regulation of VEGF and HIF-1 $\alpha$  to inhibit hypoxia of periaortic and intra-abdominal fat in ovariectomized female rats*. Molecular biology reports, 2012. **39**(8): p. 8177- 8185.
340. Kim, M., et al., *ER $\alpha$  upregulates Phd3 to ameliorate HIF-1 induced fibrosis and inflammation in adipose tissue*. Molecular metabolism, 2014. **3**(6): p. 642-651.
341. Elkhatib, M.A., et al., *Amelioration of perivascular adipose inflammation reverses vascular dysfunction in a model of nonobese prediabetic metabolic challenge: potential role of antidiabetic drugs*. Translational Research, 2019. **214**: p. 121- 143.
342. Moreira-Pais, A., et al., *Sex differences on adipose tissue remodeling: from molecular mechanisms to therapeutic interventions*. Journal of Molecular Medicine, 2020. **98**(4): p. 483-493.
343. Bakkar, N.-M.Z., et al., *Cardiac Autonomic Neuropathy: A Progressive Consequence of Chronic Low-Grade Inflammation in Type 2 Diabetes and Related Metabolic Disorders*. International Journal of Molecular Sciences, 2020. **21**(23): p. 9005.
344. Amengual-Cladera, E., et al., *Sex differences in the effect of high-fat diet feeding on rat white adipose tissue mitochondrial function and insulin sensitivity*. Metabolism, 2012. **61**(8): p. 1108-1117.
345. Heilbronn, L.K. and L.V. Campbell, *Adipose tissue macrophages, low grade inflammation and insulin resistance in human obesity*. Current pharmaceutical design, 2008. **14**(12): p. 1225-1230.
346. Muraki, K., S. Okuya, and Y. Tanizawa, *Estrogen receptor  $\alpha$  regulates insulin sensitivity through IRS-1 tyrosine phosphorylation in mature 3T3-L1 adipocytes*. Endocrine journal, 2006: p. 0609250044-0609250044.
347. Dwaib, H.S., et al., *Sex Differences in Cardiovascular Impact of Early Metabolic Impairment: Interplay between Dysbiosis and Adipose Inflammation*. Molecular Pharmacology, 2021.
348. Zhang, C., et al., *Structural resilience of the gut microbiota in adult mice under high-fat dietary perturbations*. The ISME journal, 2012. **6**(10): p. 1848-1857.
349. Murphy, E.A., K.T. Velazquez, and K.M. Herbert, *Influence of high-fat-diet on gut microbiota: a driving force for chronic disease risk*. Current opinion in clinical nutrition and metabolic care, 2015. **18**(5): p. 515.
350. Hildebrandt, M.A., et al., *High-fat diet determines the composition of the murine gut microbiome independently of obesity*. Gastroenterology, 2009. **137**(5): p. 1716-1724. e2.
351. Gabel, K., et al., *Effect of time restricted feeding on the gut microbiome in adults with obesity: A pilot study*. Nutrition and health, 2020. **26**(2): p. 79-85.

352. Jamshed, H., et al., *Early time-restricted feeding improves 24-hour glucose levels and affects markers of the circadian clock, aging, and autophagy in humans*. *Nutrients*, 2019. **11**(6): p. 1234.
353. Parkar, S.G., A. Kalsbeek, and J.F. Cheeseman, *Potential role for the gut microbiota in modulating host circadian rhythms and metabolic health*. *Microorganisms*, 2019. **7**(2): p. 41.
354. Brownell, K.D. and L.R. Cohen, *Adherence to dietary regimens 1: An overview of research*. *Behavioral Medicine*, 1995. **20**(4): p. 149-154.
355. Bennett, E., S.A. Peters, and M. Woodward, *Sex differences in macronutrient intake and adherence to dietary recommendations: findings from the UK Biobank*. *BMJ open*, 2018. **8**(4): p. e020017.
356. Dokken, B.B., *The Pathophysiology of Cardiovascular Disease and Diabetes: Beyond Blood Pressure and Lipids*. *Diabetes Spectrum*, 2008. **21**(3): p. 160-165.
357. Zinman, B., et al., *Empagliflozin, Cardiovascular Outcomes, and Mortality in Type 2 Diabetes*. *New England Journal of Medicine*, 2015. **373**(22): p. 2117-2128.
358. Marso, S.P., et al., *Liraglutide and Cardiovascular Outcomes in Type 2 Diabetes*. *New England Journal of Medicine*, 2016. **375**(4): p. 311-322.
359. Mahaffey Kenneth, W., et al., *Canagliflozin for Primary and Secondary Prevention of Cardiovascular Events*. *Circulation*, 2018. **137**(4): p. 323-334.
360. Shah, A., N. Mehta, and M.P. Reilly, *Adipose inflammation, insulin resistance, and cardiovascular disease*. *JPEN J Parenter Enteral Nutr*, 2008. **32**(6): p. 638-44.
361. Wang, Z. and T. Nakayama, *Inflammation, a Link between Obesity and Cardiovascular Disease*. *Mediators of Inflammation*, 2010. **2010**: p. 535918.
362. Christensen, R.H., et al., *Epicardial adipose tissue: an emerging biomarker of cardiovascular complications in type 2 diabetes?* *Ther Adv Endocrinol Metab*, 2020. **11**: p. 2042018820928824.
363. Valensi, P., *Hypertension, single sugars and fatty acids*. *J Hum Hypertens*, 2005. **19 Suppl 3**: p. S5-9.
364. Gibson, S.A., *Dietary sugars intake and micronutrient adequacy: a systematic review of the evidence*. *Nutrition Research Reviews*, 2007. **20**(2): p. 121-131.
365. Nguyen, T.Q., et al., *Comparison of insulin action on glucose versus potassium uptake in humans*. *Clin J Am Soc Nephrol*, 2011. **6**(7): p. 1533-9.
366. Karczmar, G.S., et al., *Regulation of hepatic inorganic phosphate and ATP in response to fructose loading: an in vivo 31P-NMR study*. *Biochim Biophys Acta*, 1989. **1012**(2): p. 121-7.
367. Khattab, M., et al., *Phosphorus ingestion improves oral glucose tolerance of healthy male subjects: a crossover experiment*. *Nutr J*, 2015. **14**: p. 112.
368. Ayoub, J.J., et al., *Effect of phosphorus supplementation on weight gain and waist circumference of overweight/obese adults: a randomized clinical trial*. *Nutr Diabetes*, 2015. **5**(12): p. e189.
369. Assaad, M., C. El Mallah, and O. Obeid, *Phosphorus ingestion with a high-carbohydrate meal increased the postprandial energy expenditure of obese and lean individuals*. *Nutrition*, 2019. **57**: p. 59-62.

370. Sawaya, S.W., et al., *Daily energy expenditure in rats following structured exercise training is affected by dietary phosphorus content*. Br J Nutr, 2020: p. 1- 11.
371. Imi, Y., et al., *High phosphate diet suppresses lipogenesis in white adipose tissue*. J Clin Biochem Nutr, 2018. **63**(3): p. 181-191.
372. Abuduli, M., et al., *Effects of dietary phosphate on glucose and lipid metabolism*. American Journal of Physiology-Endocrinology and Metabolism, 2016. **310**(7): p. E526-E538.
373. Fromme, T. and M. Klingenspor, *Uncoupling protein 1 expression and high-fat diets*. Am J Physiol Regul Integr Comp Physiol, 2011. **300**(1): p. R1-8.
374. Fedorenko, A., P.V. Lishko, and Y. Kirichok, *Mechanism of fatty-acid-dependent UCP1 uncoupling in brown fat mitochondria*. Cell, 2012. **151**(2): p. 400-13.
375. Torre-Villalvazo, I., et al., *Soy protein ameliorates metabolic abnormalities in liver and adipose tissue of rats fed a high fat diet*. J Nutr, 2008. **138**(3): p. 462-8.
376. Shabalina, I.G., et al., *UCP1 in brite/beige adipose tissue mitochondria is functionally thermogenic*. Cell Rep, 2013. **5**(5): p. 1196-203.
377. Vijgen, G.H.E.J., et al., *Increased Oxygen Consumption in Human Adipose Tissue From the “Brown Adipose Tissue” Region*. The Journal of Clinical Endocrinology & Metabolism, 2013. **98**(7): p. E1230-E1234.
378. Schneider, K., et al., *Increased Energy Expenditure, Ucp1 Expression, and Resistance to Diet-induced Obesity in Mice Lacking Nuclear Factor-Erythroid-2- related Transcription Factor-2 (Nrf2)*. Journal of Biological Chemistry, 2016. **291**(14): p. 7754-7766.
379. Luijten, I.H.N., et al., *In the absence of UCP1-mediated diet-induced thermogenesis, obesity is augmented even in the obesity-resistant 129S mouse strain*. American Journal of Physiology-Endocrinology and Metabolism, 2019. **316**(5): p. E729-E740.
380. Macher, G., et al., *Inhibition of mitochondrial UCP1 and UCP3 by purine nucleotides and phosphate*. Biochimica et biophysica acta. Biomembranes, 2018. **1860**(3): p. 664-672.
381. Pesta, D.H., et al., *Hypophosphatemia promotes lower rates of muscle ATP synthesis*. Faseb j, 2016. **30**(10): p. 3378-3387.
382. Bose, S., et al., *Metabolic network control of oxidative phosphorylation: multiple roles of inorganic phosphate*. J Biol Chem, 2003. **278**(40): p. 39155-65.
383. Ramsay, R.R., *Electron carriers and energy conservation in mitochondrial respiration*. ChemTexts, 2019. **5**(2): p. 9.
384. van de Woestijne, A.P., et al., *Adipose tissue dysfunction and hypertriglyceridemia: mechanisms and management*. Obes Rev, 2011. **12**(10): p. 829-40.
385. Vorland, C.J., et al., *Effects of Excessive Dietary Phosphorus Intake on Bone Health*. Current osteoporosis reports, 2017. **15**(5): p. 473-482.
386. Katsumata, S., et al., *Effects of Dietary Calcium Supplementation on Bone Metabolism, Kidney Mineral Concentrations, and Kidney Function in Rats Fed a High-Phosphorus Diet*. Journal of Nutritional Science and Vitaminology, 2015. **61**(2): p. 195-200.

387. Abbas Raza, S. and M.K. Drezner, 33 - *Phosphorus and Magnesium*, in *The Bone and Mineral Manual (Second Edition)*, M. Kleerekoper, E.S. Siris, and M. McClung, Editors. 2005, Academic Press: Burlington. p. 165-172.
388. Lee, Y.-M., et al., *IL-1 plays an important role in the bone metabolism under physiological conditions*. *International Immunology*, 2010. **22**(10): p. 805-816.
389. Nagy, Z., J. Radeff, and P.H. Stern, *Stimulation of Interleukin-6 Promoter by Parathyroid Hormone, Tumor Necrosis Factor  $\alpha$ , and Interleukin-1 $\beta$  in UMR-106 Osteoblastic Cells Is Inhibited by Protein Kinase C Antagonists*. *Journal of Bone and Mineral Research*, 2001. **16**(7): p. 1220-1227.
390. Bravo-Sagua, R., et al., *Calcium Sensing Receptor as a Novel Mediator of Adipose Tissue Dysfunction: Mechanisms and Potential Clinical Implications*. *Frontiers in physiology*, 2016. **7**: p. 395-395.
391. Mattar, P., et al., *Calcium-Sensing Receptor in Adipose Tissue: Possible Association with Obesity-Related Elevated Autophagy*. *International journal of molecular sciences*, 2020. **21**(20): p. 7617.
392. Sundararaman, S.S., et al., *Adipocyte calcium sensing receptor is not involved in visceral adipose tissue inflammation or atherosclerosis development in hyperlipidemic Apoe<sup>-/-</sup> mice*. *Scientific Reports*, 2021. **11**(1): p. 10409.
393. Centeno, P.P., et al., *Phosphate acts directly on the calcium-sensing receptor to stimulate parathyroid hormone secretion*. *Nature Communications*, 2019. **10**(1): p. 4693.
394. Cruz, J.C., et al., *Reactive Oxygen Species in the Paraventricular Nucleus of the Hypothalamus Alter Sympathetic Activity During Metabolic Syndrome*. *Frontiers in Physiology*, 2015. **6**: p. 384.
395. Nowicki, M., et al., *Changes in plasma phosphate levels influence insulin sensitivity under euglycemic conditions*. *J Clin Endocrinol Metab*, 1996. **81**(1): p. 156-9.
396. Galetta, F., et al., *Left ventricular function and calcium phosphate plasma levels in uraemic patients*. *J Intern Med*, 2005. **258**(4): p. 378-84.
397. Tonelli, M., et al., *Relation Between Serum Phosphate Level and Cardiovascular Event Rate in People With Coronary Disease*. *Circulation*, 2005. **112**(17): p. 2627- 2633.
398. Park, W., et al., *Serum phosphate levels and the risk of cardiovascular disease and metabolic syndrome: a double-edged sword*. *Diabetes Res Clin Pract*, 2009. **83**(1): p. 119-25.
399. Matsuzaki, H., et al., *High phosphorus diet rapidly induces nephrocalcinosis and proximal tubular injury in rats*. *J Nutr Sci Vitaminol (Tokyo)*, 1997. **43**(6): p. 627- 41.
400. Lau, W.L., et al., *Direct effects of phosphate on vascular cell function*. *Adv Chronic Kidney Dis*, 2011. **18**(2): p. 105-12.
401. Gracioli, F.G., et al., *Phosphorus overload and PTH induce aortic expression of Runx2 in experimental uraemia*. *Nephrology Dialysis Transplantation*, 2008. **24**(5): p. 1416-1421.
402. Mirza, M.A., et al., *Circulating fibroblast growth factor-23 is associated with vascular dysfunction in the community*. *Atherosclerosis*, 2009. **205**(2): p. 385-90.

403. Obeid, O., S. Dimachkie, and S. Hlais, *Increased phosphorus content of preload suppresses ad libitum energy intake at subsequent meal*. International Journal of Obesity, 2010. **34**(9): p. 1446-1448.
404. Al-Assi, O., et al., *Cardiac Autonomic Neuropathy as a Result of Mild Hypercaloric Challenge in Absence of Signs of Diabetes: Modulation by Antidiabetic Drugs*. Oxid Med Cell Longev, 2018. **2018**: p. 9389784.
405. Fakih, W., et al., *Dysfunctional cerebrovascular tone contributes to cognitive impairment in a non-obese rat model of prediabetic challenge: Role of suppression of autophagy and modulation by anti-diabetic drugs*. Biochemical Pharmacology, 2020. **178**: p. 114041.
406. Cani, P.D., et al., *Metabolic endotoxemia initiates obesity and insulin resistance*. Diabetes, 2007. **56**(7): p. 1761-72.
407. Cani, P.D., et al., *Changes in gut microbiota control metabolic endotoxemia-induced inflammation in high-fat diet-induced obesity and diabetes in mice*. Diabetes, 2008. **57**(6): p. 1470-81.
408. Hersoug, L.G., P. Møller, and S. Loft, *Gut microbiota-derived lipopolysaccharide uptake and trafficking to adipose tissue: implications for inflammation and obesity*. Obesity Reviews, 2016. **17**(4): p. 297-312.
409. Kim, K.-A., et al., *High fat diet-induced gut microbiota exacerbates inflammation and obesity in mice via the TLR4 signaling pathway*. PloS one, 2012. **7**(10): p. e47713.
410. Poggi, M., et al., *C3H/HeJ mice carrying a toll-like receptor 4 mutation are protected against the development of insulin resistance in white adipose tissue in response to a high-fat diet*. Diabetologia, 2007. **50**(6): p. 1267-76.
411. Greenstein, A.S., et al., *Local inflammation and hypoxia abolish the protective anticontractile properties of perivascular fat in obese patients*. Circulation, 2009. **119**(12): p. 1661.